WA School of Mines: Minerals, Energy and Chemical Engineering

Study on the Rheology of Drilling Fluid and Its Impact on Drilling Operation

Yiwen Wang

This thesis is presented for the Degree of
Master of Philosophy (Petroleum Engineering)
of
Curtin University

October 2019

Declaration

To the best of my knowledge and belief this thesis contains no material previously published by any other person except where due acknowledgement has been made.

This thesis contains no material which has been accepted for the award of any other degree or diploma in any university.

Signature: Yiwen Wang

Date: 20 October, 2019

Acknowledgements

I would first like to express my deepest gratitude to my thesis advisor and research supervisor, Dr Masood Mostofi, who provides me infinite encouragement and inspiration throughout my study and life. I appreciate his persistent guidance and help me to embark the research journey. His personality and passion for work will influence and motivate me to make constant progress in my future work.

Having this opportunity, I would like to thank Dr Dimple Quyn for her valuable advice and discussions throughout the process of thesis writing, which had a great influence on this graduation thesis.

I would like to acknowledge the Australian Federal Government for the financial support of Australian Postgraduate Awards (APA) during the whole period of my study at Curtin University.

I am grateful to everyone in our Drilling Mechanics Group. The completion of this thesis work was impossible without the support of all of them. I am glad to be among of this research team.

Finally, special thanks to my lovely parents, Jianlin Wang and Yan Zhang, for their endless love and support during my life.

Contents

List of Figures

List of Tables

Abstract

Optimisation and automation are becoming an integral part of drilling workflow in which, drilling operation is predicted under different scenarios. In these predictions, fluid rheology is an important component. Indeed the accuracy and effectiveness of drilling prediction and optimisation can be significantly improved by including more realistic characteristics of fluid rheology. The measurement and characterisation of fluid rheology in the open literature and in the field are simplifications.

An objective of this thesis was to study the fluid rheology in more depth using different fluid rheology methods including rotational, extensional and hydraulic viscometers. Amongst these measurements, the Marsh Funnel viscosity test can indicate changes in fluid properties, with basic measurements taken at atmospheric condition. The Ofite 900 and Brookfield viscometers have advantages in measuring fluid rheology but have limitations in measuring suspensions with cuttings. The Haake Mars viscometer, with a concentric cylinder sensor system, provides rheological measurement over a wide range of shear rates under thermal and pressure controlled experimental conditions, but it cannot measure suspension with particles of high volume concentration and large size. The straight pipe viscometer can be used for flowing fluid rheology measurement in the presence of solid particles.

In the second part of the thesis, a series of experiments was conducted to ascertain the synergic interaction of low-end viscosifiers to enhance drilling fluid properties. In addition to laboratory studies, a series of field applications was undertaken using RoXplorer drilling rig to compare the efficiency of Ctrol^{TM} and CTrolX^{TM} with two commercial drilling fluid systems.

Furthermore, rheological experiments were performed to investigate the effect of fine particles on the rheology of mono-dispersed suspensions. It was found that a key factor affecting viscosity of mono-dispersed suspension is the volume fraction of particles in suspension. The particle size effect is minimum at medium and high shear rate regions.

Chapter 1. Introduction

1.1. Background

Drilling fluid can be considered the lifeblood of drilling operation as it provides several different functions in the drilling industry, such as cutting evacuation from the drill bit face and well, cutting suspension and transportation, controlling formation fluid flowing into the borehole, stabilising and cleaning the borehole, and sealing permeable formations [1].

Therefore, the properties of drilling fluids, such as fluid density [2], viscosity [3] and the ability to control fluid loss and filtration [4], are critical parameters that require optimisation. The density of mud is vital for well control [5], and chemical composition significantly influences borehole stability [6]. Mud rheology has a considerable impact on suspending and carrying drilling cuttings, optimizing wellbore hydrodynamic pressure, and efficient cleaning of borehole.

In drilling operation, the drilling fluid is exposed to a wide range of shear rates during one cycle of circulation, from the low-end shear rate when pumping is stopped, to the high–end shear rate when drilling [1]. The range of shear rates also depends on area open to flow: the high-end and low-end shear rates may be experienced in different sections of the drilling string/wellbore. The shear rate of drilling fluid in laminar flow cannot be measured directly but can be calculated through the Mooney-Rabinowitsch equation [7].

$$\dot{\gamma} = \frac{8U}{D} \qquad (1.1)$$

where $\dot{\gamma}$ is shear rate, U is the average velocity of the fluid and D is the diameter of the fluid flowing area. The quantity (8U/D) or the equivalent form in this equation, also known as the flow characteristics, provides a basic estimation of the shear rate of drilling fluid during mud circulation. In this project, a case of vertical well drilling is experimentally simulated to demonstrate the wide range of shear rates for mud circulation, [Figure 1] with key vertical well drilling information is listed in Table 1. From Table 1, the calculated shear rate ranges from 0.1 1/s while the fluids are being lost into borehole formations along the fracture planes, to approximately 10^3 1/s when the drilling fluid injecting out of bit nozzle, or being at the bit/rock interface. It is important to measure and monitor the fluid rheology along all these shear rate ranges, in order to effectively design the drilling fluid.
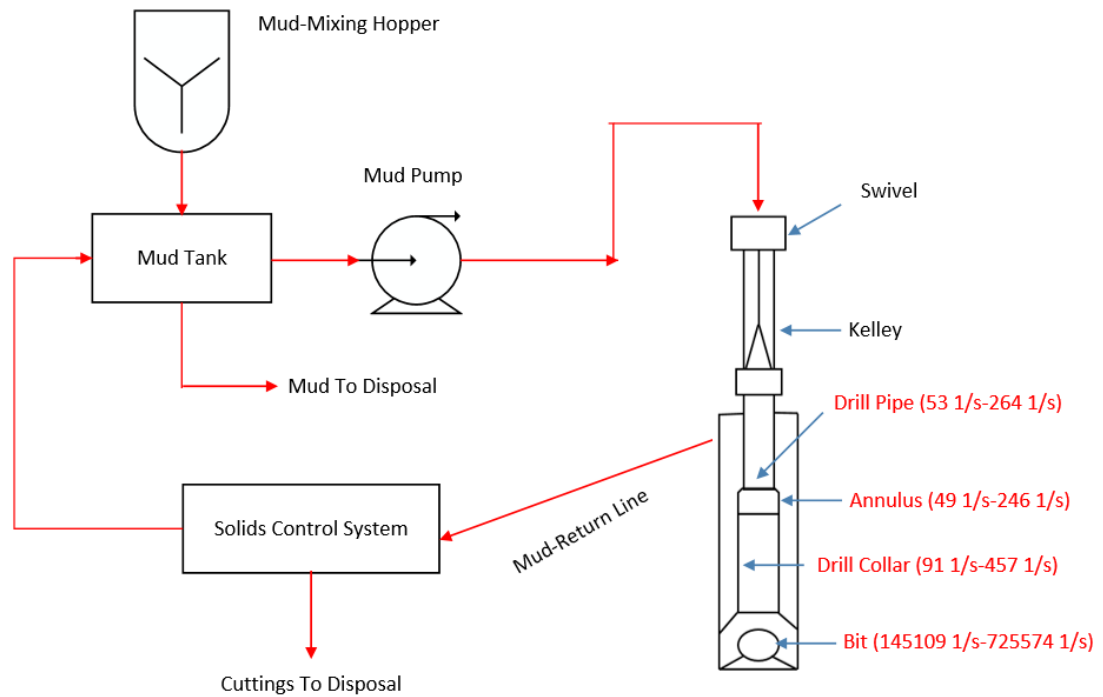
Figure 1: Schematic of the drilling fluid circulation system.

Table 1: Drilling parameters of vertical well.

Vertical Drilling Parameters

Hole Size	Depth	Mud Weight	PV	YP
8.5 inch	2,000 ft	9.2 lb/gal	13 CP	10 lb/100 ft²
Drill Pipe	**Drill Pipe ID**	**Drill Collar**	**Drill Collar ID**	**Drill Collar Length**
5 inch	4.2 inch	6.75 inch	3.5 inch	800 ft
Bit Nozzle ID	**Flow Rate Range**	**Max Pressure**		
0.3 inch	100 - 500 gpm	4500 psi		

Shear Rate Through (1/s) :

Drill Pipe	53 - 264
Annulus (Average)	49 -246
Drill Collar	91 - 457
Borehole Formation	/
Bit Nozzle	145109 - 725547
Mud Tank	/

However, the oil and gas industry standard implements relatively simplified characterization of rheology. Currently, the laboratory 10-speed viscometer (600, 300, 200, 100, 60, 30, 6, 3, 2 and 1 rpm) is used to measure the rheology of drilling mud. The rheological readings of this viscometer at 600 rpm and 300 rpm are then applied to calculate mud plastic viscosity and yield point, and used to describe the flow behaviour of drilling fluid. The drilling fluids are assumed to behave with similar flow characteristic when their Θ_{300} and Θ_{600} values similar. Furthermore the classical rotary viscometer Ofite or Fanne used in the drilling field cannot measure mud rheology at very low shear rates which are below 0.1 1/s; therefore, low-shear-rate measurement is ignored but it is very crucial for operation. Due to this deficiency in rheology measurement for drilling operations, this research will aim to fill the gaps in drilling fluid characterization across a wide shear rate range.

1.2. Objective

This thesis aims to obtain a better understanding of the rheology of polymer drilling fluid solutions over an extensive range of shear rates that exceeds the range typically measured in the drilling fluid industry. The experiments are performed with and without cuttings, to explore the solid impact on fluid rheology. The experimental study of fluid rheology will be obtained from three different rheology measurement techniques using the Ofite 900, the Haake Mars and a straight pipe viscometer. These advanced and detailed measurements of fluid viscosity will be used in conjunction with engineering models developed for specific drilling processes, and the accurate measurement of fluid rheology using current models in characterising the drilling processes will be investigated. Examples of these processes are fluid flowing in straight pipes, solid suspension and solid removal.

The specific objectives of this thesis are as follows:

1) To quantify the impact of different fluid viscosifiers on the fluid rheology, and in particular investigate how viscosity will be affected at a wide range of shear rates. Synergistic experiments with different polymers will be investigated to pave the way for the development of the preventative drilling fluid Ctrol^{TM} and the remedial drilling fluid CTrolX^{TM} for particular drilling application.

2) To investigate and study the cuttings size and concentration effects on the drilling fluid viscosity. Different sizes of cuttings were prepared for the experiment, ranging from 1 wt. % to 10 wt. %, which can simulate actual well downhole conditions.

3) To predict the fluid friction loss under various conditions such as fluid rheology, flow rate. The investigations will be carried out using straight pipe viscometer with 0.5 inch diameter.

1.3. Significance

This research attempts to better characterise fluid rheology at a wide range of shear rates, i.e. the fluid behaviour when the fluid is under low shear rate in the range of 0.01-0.1 1/s (e.g. in the case of fluid loss) or high shear rates in the range of 2,000-6,000 1/s (e.g. in the case of fluid processing in a centrifuge or hydrocyclone). In particular, this research investigates the low-end rheology of different polymer combinations and facilitates the development of two drilling fluid systems Ctrol^{TM} and CTrolX^{TM} for fluid loss control. This research presents a novel approach to determine fluid rheological parameters in real-time by using pipe viscometer, with elimination of the efforts to apply traditional rheology measurement.

1.4. Organization of thesis

This thesis comprises a total of five chapters. Chapter 1 introduces the background of current research and an overview of proposed topic. The research objective, the significance of this work as well as thesis structure are presented.

In Chapter 2, the literature review of drilling fluid rheology and its impact on drilling operation are presented. The vital role of mud rheology in drilling industry is highlighted in this chapter, illustrating a comprehensive summary of rheology which includes flow behaviour models, viscosity measurement techniques, cutting effect, low-end rheology, drilling fluid synergy and fluid hydraulics.

Chapter 3 describes experimental setup for cutting effect tests and straight pipe viscometer measurement. Detailed specification of measurement apparatus and procedures are presented. The method of preparing the test fluid and solid particles is elaborated.

In Chapter 4, the benchmark experiments with Marsh Funnel, rotational, extensional and capillary viscometers are provided. Different viscosity modified additives including bentonite, natural and synthetic polymers are compared to study the interaction of additives in modifying the low-end rheology of fluid. Experiments are performed to investigate cutting effect on the full range rheology of polymer.

And finally, the summary of findings of this research is presented in Chapter 5 followed by recommendation for future research in this area.

Chapter 2. Literature review

In this chapter, a summary of previous work in the area of fluid rheology from different engineering disciplines are reviewed. The chapter covers fluid rheological models and different viscosity measurement techniques, and reviews previous work related to the influence of particle cuttings on fluid rheology. In terms of fluid rheology measurement techniques, both API and capillary viscometer techniques are discussed in details. A summary of previous experimental studied on the synergy of polymers are also discussed at the end of this chapter.

2.1. Drilling fluid rheology

Drilling fluid rheology plays an important role in cutting transportation and drilling hydraulics. Due to the significance of fluid rheology in drilling operation, it has been the focus of extensive research in petroleum engineering. However, there is considerable and relevant research into fluid rheology in other disciplines such as such as food processing, chemical engineering and mechanical engineering. "Rheology" is an area of science concerned with deformation and flow of materials, which embraces viscosity, elasticity and plasticity. The term was first invented by Eugene C. Bingham at Lafayette College in 1920 [7]. Although the study of fluid rheology covers an immense range of engineering applications, it is especially vital for optimization of drilling fluids and cementing slurries in terms of both fluid hydraulics and flow behaviour of solid suspended in fluids.

Fluids can be classified to Newtonian and Non-Newtonian fluids, based on the relationship between shear stress and shear rate,

$$\tau = \mu \times \dot{\gamma} \tag{2.1}$$

where τ is shear stress, μ is viscosity and $\dot{\gamma}$ is shear rate [7]. In SI units, shear stress is in Pa, shear rate in 1/s and viscosity in Pa.s.

Newton's Law of Viscosity describes the simplest fluid flow behaviour: fluid viscosity is measured as the ratio between shear stress and shear rate under constant pressure and temperature [7]. Newtonian fluids start to flow when an infinitely small amount of shear stress is initiated, and the shear stress increases linearly with shear rate. Many common liquids, such as water, oil, air, gasoline and glycerine behave like a Newtonian fluid. However, fluid characterization is far more complex and this relationship can be influenced by the timeframe at which the shear rate is applied. No real fluids fit this mathematical description perfectly.

For non-Newtonian fluids, there is no constant of proportionality between shear rate and shear stress, i.e., the viscosity varies with shear rate and time. In the case of variation of viscosity with shear rate, fluids are classified as shear-thinning and shear-thickening fluids, [Figure 2] [7]. The term "shear- thinning" refers to fluids exhibiting lower viscosities at higher shear rates. The shear-thinning property is very desirable in drilling, when lower viscosity (at higher shear rate) reduces circulating pressure, while higher viscosity is essential when circulation is stopped to suspend drill cuttings in the well annulus, or to control the fluids loss into permeable/fractured formations.

In contrast, there are fluids which have higher viscosities with increasing of shear rate, which are called "shear-thickening" fluids. Examples of these fluids are corn starch-water mixtures or suspensions with a high concentration of solid particles. These fluids do not have a particular application in drilling operation.
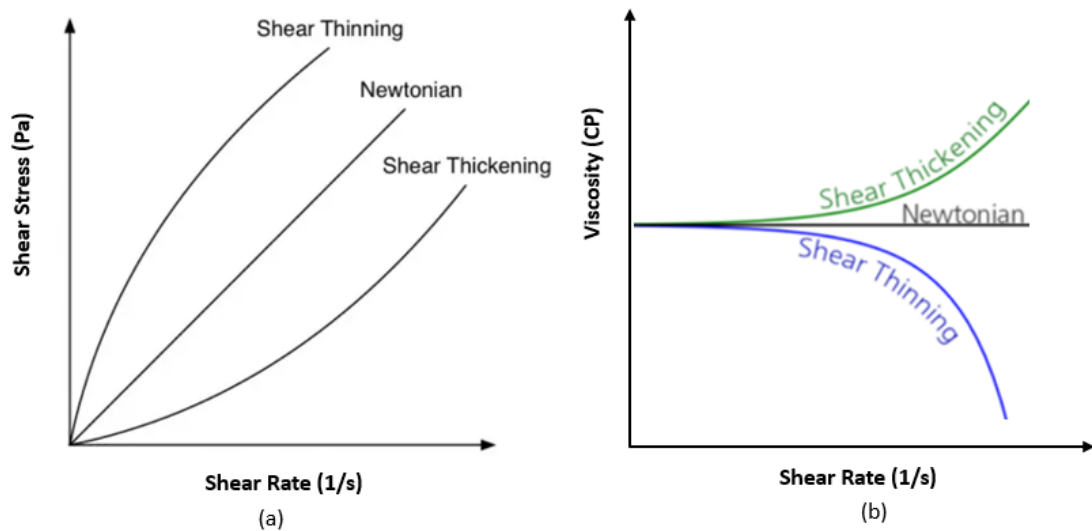
Figure 2: Newtonian fluid, shear thinning and shear thickening of Non-Newtonian fluids: (a) variation of shear stress with shear rate, (b) variation of viscosity with shear rate [7].

Most drilling muds are shear-thinning thixotropic fluids; "thixotropy" means that the fluids take time to establish equilibrium for the applied shear rate [Figure 3] [8]. This time-dependent fluid characteristic can be quantified with a thixotropic loop test. As will be explained later, loop tests can be performed to quantify the extent of thixotropic behaviour.
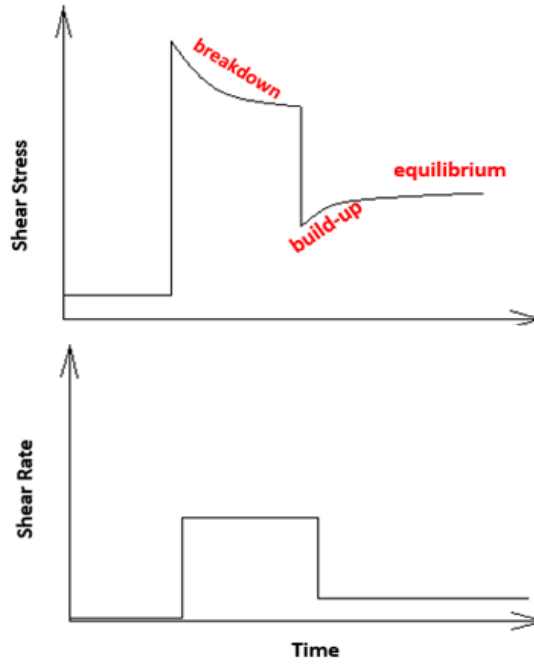
Figure 3: Thixotropic behaviour of Non-Newtonian fluids: the variation of shear stress and shear rate with time [7].

2.2. Rheological models

Rheological models are mathematical correlations of shear stress with shear rate. Typical rheological models used in the drilling industry to simulate and characterise fluid dynamics are listed in Table 2. Not all fluids conform precisely to a single model over the entire range of shear rates but a combination of models may be applied.

Table 2: Typical rheological models [7].

Drilling Model	Equations	
Bingham Model	$\tau = \tau_p + \mu_P \times \dot{\gamma}$	K: Consistency index
Power Law Model	$\tau = k\dot{\gamma}^n$	n: Power index
Herschel-Bulkley Model	$\tau = \tau_p + k\dot{\gamma}^n$	τ_p: Yield point
Cross Model	$\frac{\eta - \eta_\infty}{\eta_0 - \eta_\infty} = 1 + \sigma \times \dot{\gamma}^2$	η: Apparent viscosity η_0: η at $\dot{\gamma} \rightarrow 0$
Carreu Model	$\frac{\eta - \eta_\infty}{\eta_0 - \eta_\infty} = 1 + \sigma \times \dot{\gamma}^n$	η_∞: η at $\dot{\gamma} \rightarrow \infty$
Casson Model	$\sqrt{\tau} = \sqrt{\tau_p} + \sqrt{\eta_\infty \dot{\gamma}}$	σ: Relaxation time

The variation of fluid viscosity with shear rate for polymers can be characterised by three stages [9]. In the first stage, polymers behave like Newtonian fluids at very low shear rates. The fluids exhibit shear-thinning property at medium shear rates in the second stage and at higher shear rates, stage three shows that polymers have constant infinite shear viscosity, [Figure 4].
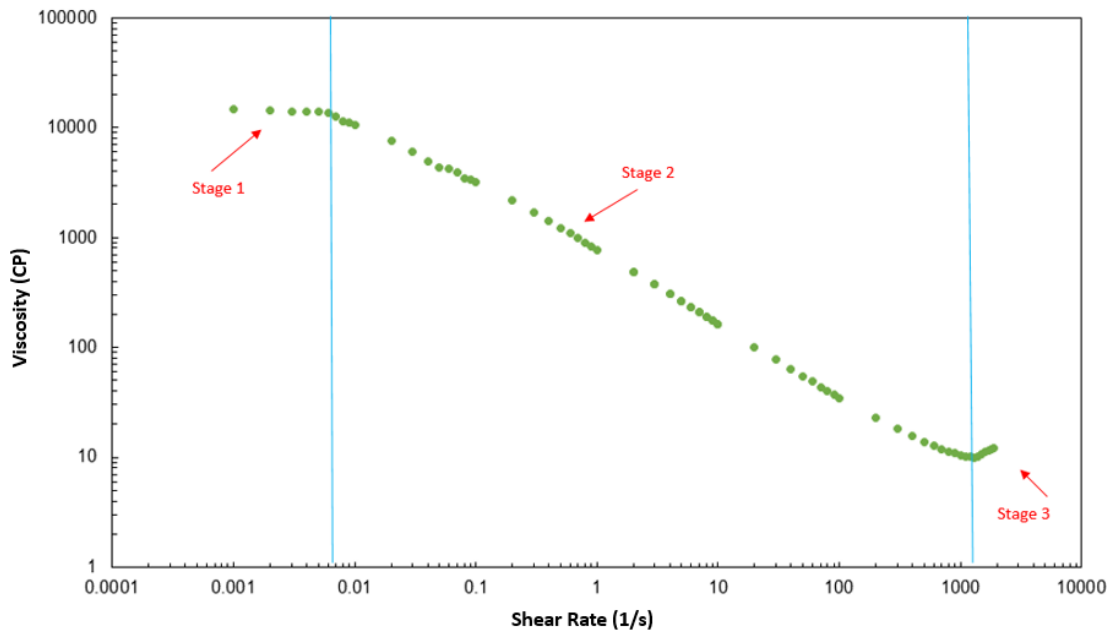
Figure 4: Demonstration of zero shear and infinite shear viscosity for a polymer [9].

The selection of a correct rheological model depends on the application of the model at the specific shear rate. The Bingham plastic model [10] is a two-parameter model that is widely used in the drilling industry to describe mud viscosity. However, it does not accurately represent mud flow behaviour at low or at high shear rate. The power law rheological model [10] provides a better rheological prediction at low shear rates condition but has the disadvantage at predicting the viscosity at the high shear rate region. The three-parameter Herschel-Bulkley model (also known as yield power law) [11] accurately predicts mud behaviours across a wider range of shear rates.

To cover the entire range of shear rate, four-parameter Casson and Carreu models [12] can be used, however, the complexity in mathematic analysis increases with the number of parameters in a given model. Furthermore, a model that covers the entire range of shear rates would not necessarily lead to very accurate estimation over a specific shear rate range. For example, the medium to high range of shear rate is important for an engineering application (for example fluid flow in drill string and annulus), the yield power law model may provide a better estimation of the pressure drop than four-parameter models which are capable of covering the full range of shear rate [9].

2.3. Rheological measurement methods

2.3.1. Marsh Funnel measurement

The rheology of a fluid can be measured using a Marsh Funnel (flow through constriction), a rotary viscometer, an extensional viscometer, and a pipe viscometer [7]. The simplest measurement of drilling fluid viscosity is using a Marsh Funnel, [Figure 5]. The Marsh Funnel time is often referred to as Marsh Funnel viscosity. It is not a true viscosity but serves as a qualitative measurement of fluid viscosity [13]. Prior to measurement, the Marsh Funnel should be clean and dry. The funnel is held erect with a finger over the outlet tube while the fresh slurry sample is poured into the funnel through the screen until the slurry level reaches the bottom of the screen. Then, the finger is quickly removed from the outlet tube and the flow of mud is timed simultaneously. The Marsh Funnel time is recorded as the elapsed time required for one quart (946ml) of slurry to flow out a full funnel into a graduated mud cup [1].

Figure 5: Marsh Funnel viscosity measurement.

Accurate and simple techniques for measurement of fluid rheological properties are important for field drilling operation. The Marsh Funnel viscosity measurement is simple, and provides the drilling engineer with only one parameter (drainage time) to characterise the average viscosity of drilling fluid. However, this measurement cannot be used directly for engineering analysis of drilling fluid, and also is sensitive to operator use. Limited attempts have been performed before regarding the Marsh Funnel measurement of non-Newtonian fluid, i.e., there could be examples of fluids with the same Marsh Funnel viscosities but drastically different fluid rheology.

2.3.2. Rotary viscometer measurement

In addition to Marsh Funnel measurement, drilling fluid viscosity is often measured using the API rotary viscometer. In a rotary viscometer, the fluid is placed between a sleeve (rotor) and a solid cone (bob), [Figure 6]. During rheology measurement, the viscous drag force exerted by the fluid creates a torque on the bob, and a transducer measures the bob angular displacement [14]. The dimensions of the bob and rotor of different API rotary Ofite 900 viscometers are listed in Table 3.
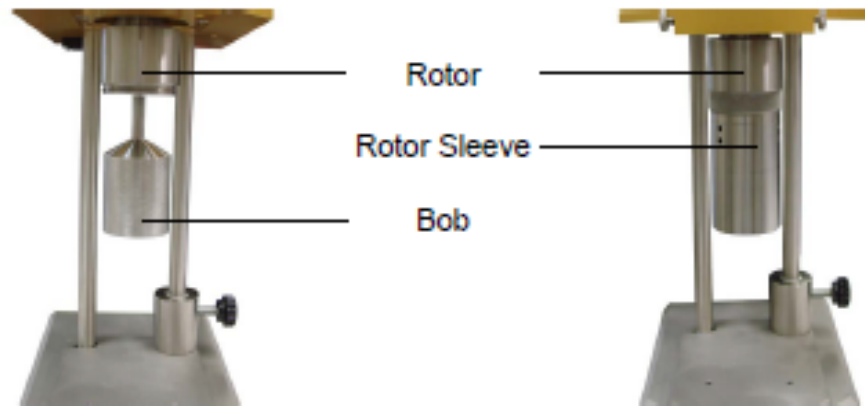
Figure 6: API rotary viscometer Ofite 900 [7].

Table 3: The diameter of different Ofite 900 rotor-bob arrangement [7].

Rotor - Bob	R1B1	R1B2	R1B3	R1B4	R1B5
Rotor Radius (cm)	1.8415	1.8415	1.8415	1.8415	1.8415
Bob Radius (cm)	1.7245	1.2276	0.8622	0.8622	1.5987
Bob Height (cm)	3.8	3.8	3.8	1.9	3.8
Shear Gap (cm)	0.1170	0.6139	0.9793	0.9793	0.2428
R Ratio (Bob Radius/Rotor Radius)	0.9365	0.6660	0.4680	0.4680	0.8681
Shear Rate Constant K_R (sec^{-1} per RPM)	1.7023	0.3770	0.2682	0.2682	0.8603

The angular velocity and dial reading of an Ofite 900 viscometer can be converted to corresponding shear rate and viscosity, by multiplying by an appropriate factor based on the dimensions of the rotor and bob. The shear rate can be converted to 1/s by multiplying the shear rate in RPM by a factor of 1.7023 for a R1B1 bob. Shear stress can be converted to lb$_f$/100ft^2, Dyes/cm^2 and Pa by multiplying the dial reading by a factor of 1.067, 5.11 and 0.511 respectively for a R1B1 bob.

Based on API standard practice 13D [15], the readings are commonly measured at 600, 300, 6 and 3 rpm, while the Ofite 900 can also operate at 200, 100, 60, 30, 20, 10, 2 and 1 rpm. The

digital API rotary viscometers have more flexibility. The shear rate range of the Ofite 900 viscometer can be from 0.01 1/s to 1700 1/s when controlled by a programmed computer.

In addition to the API rotary viscometer, there are other rotary viscometers designed to measure fluid properties in the lab. Two examples are the Brookfield and the HAAKE Mars viscometers, [Figure 7].

(a)   (b)

Figure 7: Examples of other rotary viscometers: (a) Brookfield viscometer, (b) Haake Mars viscometer [7].

The Brookfield viscometer [16] is a rheology testing machine that provides both controlled shear rate and controlled shear stress measurements and a variety of flow characterization tools including ramp, loop and single point testings using specific spindles, [Figure 8][16]. The application of the Brookfield viscosity measurement is mostly relevant for quality control and benchmarking of additives and products.

Figure 8: Different spindle sets of Brookfield viscometer [16].

The Haake Mars viscometer [17] provides rheology measurement over a wide range of shear rates. The equipment can be equipped with different sensors for rotary viscometry. The application of each sensor is different, [Figure 9].
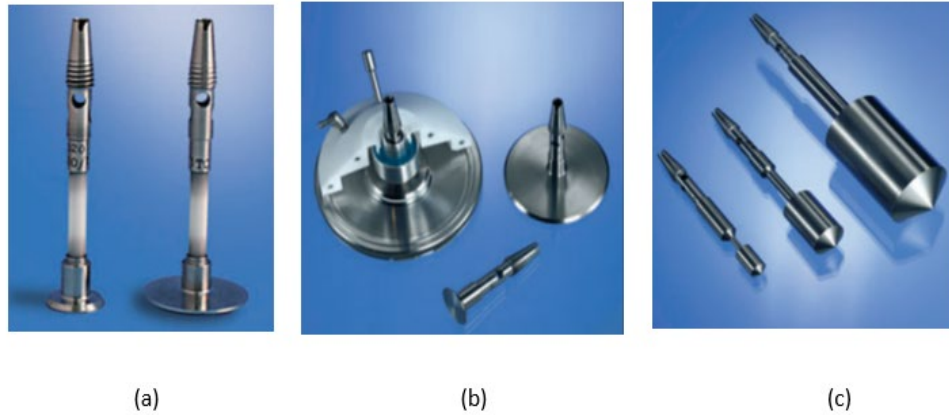
A cylinder sensor comprises of a rotor and a stator, which is similar to an Ofite 900 viscometer. This sensor is suitable for polymer dispersion measurement. A cone-plate sensor, which consists of a low angle cone set above the flat plate, is predominately used for measurement of high viscosity in fluids. Either the cone or the plate can rotate while the other part is held stationary. The cone radius and cone angle are important aspects of the sensor. Testing using this sensor is limited when coarse particles and fibre strings are used. Moreover, if a cone/plate sensor system is insufficiently filled or the sensor gap empties during the measurement, significant measurement errors can result. A plate-plate sensor is similar to the cone-plate sensor but both plates are flat, and used on high viscosity solutions. The radius of the plate and the distance between the stationary and movable plate is fixed for each sensor. The parallel plate geometry enables the top plate to rotate while bottom plate remains stationary. Fluids with solid particles can be measured using this sensor only if the sensor gap is at least three times larger than the particle size.

2.3.3. Pipe viscometer measurement

A pipe viscometer, which is also known as capillary viscometer, is another instrument used for fluid rheology measurement. Straight pipe viscometers provide better reliable and accurate measurement compared with other viscometers, especially at higher shear rates. It can measure the rheology of flowing fluids with solid cuttings and represent well downhole conditions.

The schematic of a pipe viscometer is shown in Figure 10 [18]. The test fluid is circulated through the pipeline with inner diameter D under pressure using a pump, and the friction pressure drop (ΔP) across test section length ΔL and the flow rate (Q) are measured and recorded by the Data Acquisition System (DAQ). The flow rate can be converted to actual shear rate while pressure drop can be converted to actual shear stress, using the relationships between parameters given below. The pipe viscometer is mostly used to measure the fluid rheology at steady shear rates, i.e., it is not used to measure thixotropic properties.
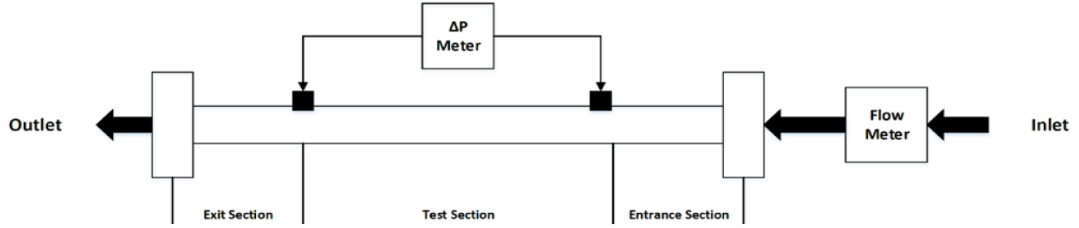
Figure 10: Pipeline viscometer system [18].

To obtain reliable and accurate rheology measurement, the pipe viscometer should have a sufficiently long entrance and exit section to ensure the fully developed flow condition is established within the test section. Collins and Schowalter [19] proposed a correlation to estimate the entrance length of the pipe X_D for power law fluids as shown below,

$$X_D = (-0.126n + 0.1752)D \cdot Re \tag{2.2}$$

where n, D and Re are the fluid behaviour index, pipe inner diameter and the Reynold number. The pipe wall shear rate $\dot{\gamma}_w$ and shear stress τ_w are defined as [20],

$$\dot{\gamma}_w = \left(\frac{3N+1}{4N}\right)\frac{8u}{D} \tag{2.3}$$

where u is the mean velocity, which is directly proportional to flow rate and inversely proportional to the cross-section area of the pipe. $\frac{8u}{D}$ is termed as nominal Newtonian shear rate. N is the generalized flow behaviour index, which is expressed as below,

$$N = \frac{d(\ln \tau_w)}{d\left(\ln \frac{8u}{D}\right)} \qquad (2.4)$$

where τ_w is the shear stress at pipe wall surface and applies to both Newtonian and non-Newtonian fluids,

$$\tau_w = \frac{D}{4} \times \frac{\Delta P}{\Delta L} \qquad (2.5)$$

Results from pipe viscometer tests [18] presented in Figure 11 show the plot of the average wall shear stress as a function of nominal Newtonian shear rate for a test fluid, and this flow curve can be used to screen out measurements that fall outside the laminar flow regime. The wall shear stress increases sharply as the nominal shear rate increases in this area (the right-side region of blue dashed line). In general, the wall shear stress in terms of nominal shear rate can be also re-written as follows,

$$\tau_w = K' \left(\frac{8u}{D}\right)^N \qquad (2.6)$$

where K' is the generalized consistency index, which is a function of nominal Newtonian shear rate. If plotting the curve of τ_w versus $\frac{8u}{D}$ forms the straight line, then the fluid flowing in the pipeline is a Power-Law fluid. If the fluid is Newtonian fluid, N=1 and then equation (2.3) reduces to:

$$\dot{\gamma}_w = \frac{8u}{D} \qquad (2.7)$$
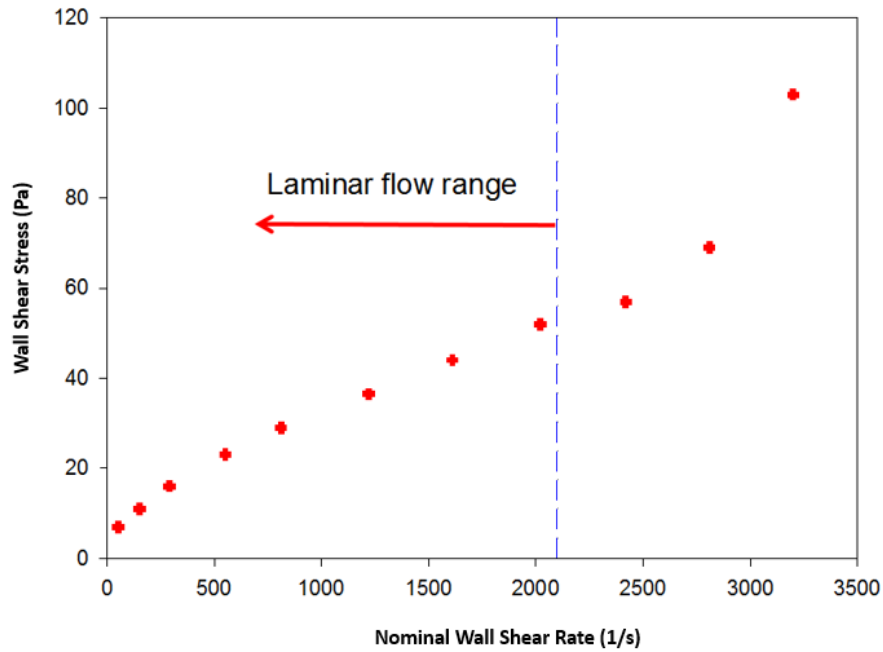
Figure 11: Wall shear stress versus nominal wall shear rate [18].

Fluid rheological properties can be calculated using the pipe viscometer and the resulting information can be used for prediction of pressure losses using different rheological models, [Table 4]. In drilling operation, it is known that mud pump pressure is important as it supplies sufficient pressure to circulate drilling fluids through the annulus. The mud pump pressure is partly used to overcome friction as the mud flows along the drilling string and annulus, and the remaining pressure drop is due to mud from the bit nozzle. The total mud pressure drop that occurs due to circulation is termed as Stand Pipe Pressure (SPP). This SPP is a key parameter during drilling operation as it determines the optimization of pump flow rate to remove the drilling cuttings as well as proper pump power selection. Better monitoring and prediction of SSP will eliminate well downhole problems. For example, relatively high SPP indicates that an increasing mud density or viscosity would decrease pump efficiency and lead to potential well control hazards. Relatively low SPP could be caused by loose or broken joints of the drilling string. Thus, a pipe viscometer will help drilling engineer to predict pressure drop of mud circulation and better prevent well control hazards.

Table 4: Predicted straight pipe friction loss of a certain fluid with different rheological models [21].

Flow rate (lit/min)	Measured SPP (bar)	Predicted SPP (bar)			
		Newton	Bingham plastic	Power law	Herschel-Bulkley
1640	46.6	493.24	47.14	45.32	45.95
2460	103.3	1027.99	102.34	94.92	96.49
3270	176.3	1721.75	176.6	160.25	163.15

2.4. Rheology measurement conditions

While fluid properties are measured at atmospheric condition, in reality the fluid is exposed to elevated temperature and pressure during drilling operations. In the drilling string the fluid is free of solids, but in the annulus, the fluid carries cuttings to surface, and therefore, the presence of cuttings in the drilling fluid can influence fluid rheology. It is therefore important to measure the fluid rheology at elevated temperature and pressure, and also at different solid concentrations.

A review of the literature showed that the viscosity of water-based drilling fluid is very dependent on the temperature and pressure [22]. High temperature and high pressure have a significant impact on the fluid rheology, as shown by the variations of shear stress with shear rate, at varying temperature or varying pressure, [Figure 12]. However, there is little research on the rheological properties of drilling fluids over wide range of shear rates at very high pressures/temperatures, which needs more investigation in the further study.
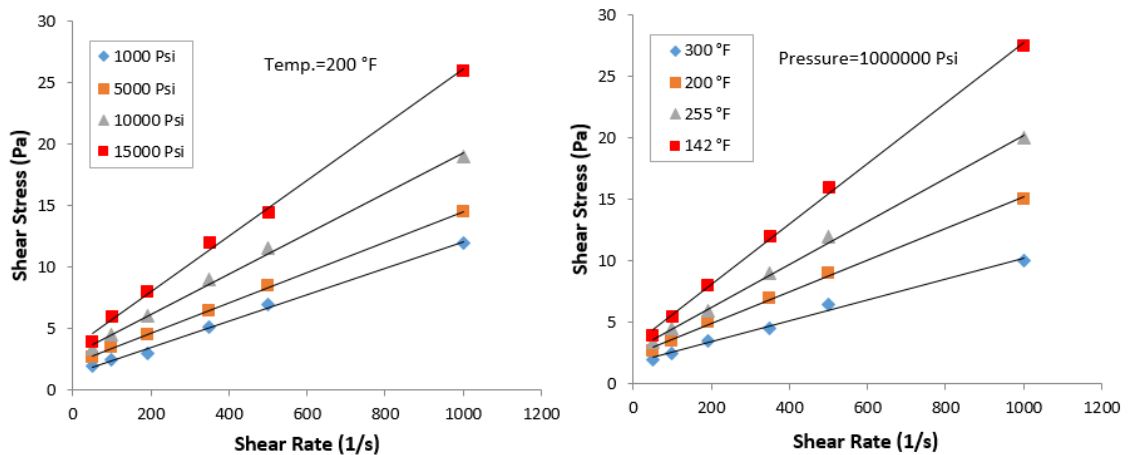
Figure 12: Effect of temperature and pressure on rheology of a certain fluid [22].

2.5. Influence of particles on drilling fluid rheology

The process of transporting rock cuttings from the drill bit through the annulus to the surface is called cuttings transportation. The main factors affecting cutting transportation is the mud rheology, borehole geometry and drilling fluid flow rate [23]. While the rheology of drilling fluid is controlled by the composition of drilling fluid and wellbore temperature profile, the solid particles in mud also have an impact on the drilling fluid rheology. The presence of solid particles in the drilling fluid is associated with two factors: (a) the transportation of solid particles in the annulus, which is associated with a wide range of solid particles and relative high concentration of particles, and (b) the accumulated concentration of low-density solid particles that cannot be removed from the drilling fluid [1].

25

The insoluble mud solids can be divided into two categories: high-gravity and low-gravity solids. The concentration of high-gravity solids is minimized by the solid-control equipments (from shale shaker to desander cone and the decanting centrifuge) after processing of the drilling fluid at the surface. However, some solids are dispersed as fine particles, which cannot be efficiently removed. As a result, the mud viscosity will be altered after re-circulation of drilling fluid due to accumulation of low gravity solids. In this case, the drilling fluid must be diluted with fresh mud containing no solid particles. However, the adding of zero solid fresh mud will increase the mud cost dramatically and might affect the drilling fluid rheology, which in turn affects the pumping efficiency. Currently, there are limited studies and experiments with fine particles effect on rheology, which is ignored but it is very crucial for operation.

2.5.1. Solid particles in drilling fluid

Different types of solid particles found in drilling fluids include soluble material such as Potassium Chloride (KCL) and insoluble fine/coarse drill cuttings and additives such as barite, calcium carbonate or hematite.

The concentration of solid particles can be quantified using total solid content and total suspended solid concentration. Total solid content is the percentage of the total solid in drilling mud, which refers to soluble and insoluble solid content in the mud system. The total suspended solid concentration is the weight fraction of the dry-weight of suspended particles that are not dissolved in the suspending fluid.

The particle dispersion of suspensions can be divided into mono-dispersion and poly-dispersion. Mono-dispersion refers to the particles of uniform size in a dispersed phase while poly-dispersion, also known as disorder dispersion, refers to the particles of varied sizes in a dispersed phase, [Figure 13] [24]. In the drilling industry, the coarse particles slightly influence the bulk fluids viscosity but the fine cuttings are assumed to have significant impact on slurry rheology, as shown in Figure 14.

Furthermore, cuttings transportation in drilling operation, becomes one of major factors affecting drilling time and quality of well operation, which leads to pressure drop in circulating flow [1].This phenomenon brings challenge for the drilling engineer to determine how the cuttings affect pressure drop along the well annulus. Meanwhile, the accumulation of fine cutting particles will increase drilling fluid density and finally affect equivalent drilling circulating density, creating higher risk for well control procedures.
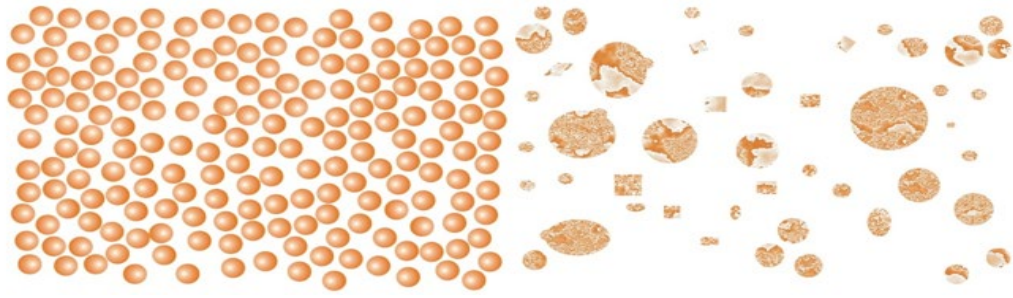
Figure 13: Monodisperse and poly-disperse suspensions with particles [24].
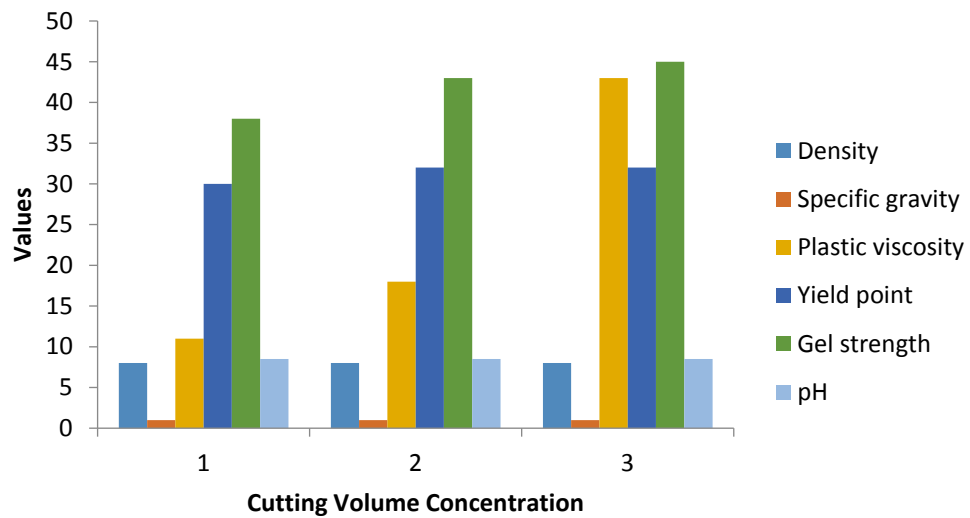
Figure 14: Properties of drilling fluids with different volume concentration of cuttings within same size [25].

2.5.2. Suspensions in drilling fluid

There has been extensive research focusing on characterising the impact of insoluble solids on the drilling fluid rheology during medium and high shear rate regions [26]. Adding solid particles to liquids changes the optical and physical properties of fluid. As the particles are insoluble, the fluid is a two-phase/multi-phase mixture.

This two-phase/multi-phase mixture can form two types of systems depending on the settling velocity of the particles. If the particles are suspended in the fluid and in a relatively long period of time the particles will not settle, i.e. the particle settling velocity is regarded as zero, the mixture is called as a suspension. Otherwise the mixture is unstable and usually referred as slurry when the particle settling velocity is large enough.

Mud viscosity is difficult to measure in an unstable particle fast-settling system. The viscosity of the suspending fluid is often not sufficiently high to suspend coarse drilling particles, and as a result, the solid particles settle during rheology measurement, leading to inaccurate measurements. For a suspension, the particles are generally fine or the suspending fluid has to

be viscous. To estimate whether the mixture is a suspension or not, it is necessary to predict the particle settling velocity based on the properties of the fluid and particle such as the particle size and fluid rheology. For a Newtonian fluid, Stokes's law is used to calculate the particle velocity for the laminar regime. But for the turbulent regime, the correlation of the particle drag coefficient and Reynolds number is needed.

A low particle volume fraction might induce shear-thinning behaviour whereas high particle volume fraction might result in shear-thickening [27]. Furthermore, in most suspensions, the particle size distribution, particle shape and particle surface charge may alter the fluid rheology as well, leading to more complex rheological behaviour in suspensions.

To avoid this source of error, this study will focus only on the stable suspensions in which the particles are mono-sized and suspended by the viscous suspending fluid, so that the particles will not settle down during measurements [28].

2.5.3. Effect of solid particles on fluid rheology

Here, a review of previous work studying the effect of solid particles on the fluid rheology is summarized.

In various engineering disciplines, the relative viscosity η_r, which is the ratio between the apparent viscosity of the suspension η_{app} and the viscosity of the suspending fluid η_0, is used to quantify the fluid resistance to flow against shear rate [29].

$$\eta_r = \frac{\eta_{app}}{\eta_0} \tag{2.8}$$

Research by Rutgers et al [27] has addressed the parameters that affect the relative viscosity of suspension fluids: (1) the volume fraction of the solid particles, (2) the type of suspended particles and their shape and size, (3) the particle size distribution and (4) the shear rate variation.

2.5.3.1. Effect of particle concentration on suspension viscosity

Previous research from Watanabe et al [30] showed that the suspension apparent viscosity increases with the presence of solid particles. This study suggests that the apparent viscosity increases with increasing solid concentration. This phenomenon is attributed to the enhanced particle-particle interactions in the fluid, as shown in Figure 15. This contact between particles increases particle frictional interaction, thereby increasing the apparent viscosity of suspensions.
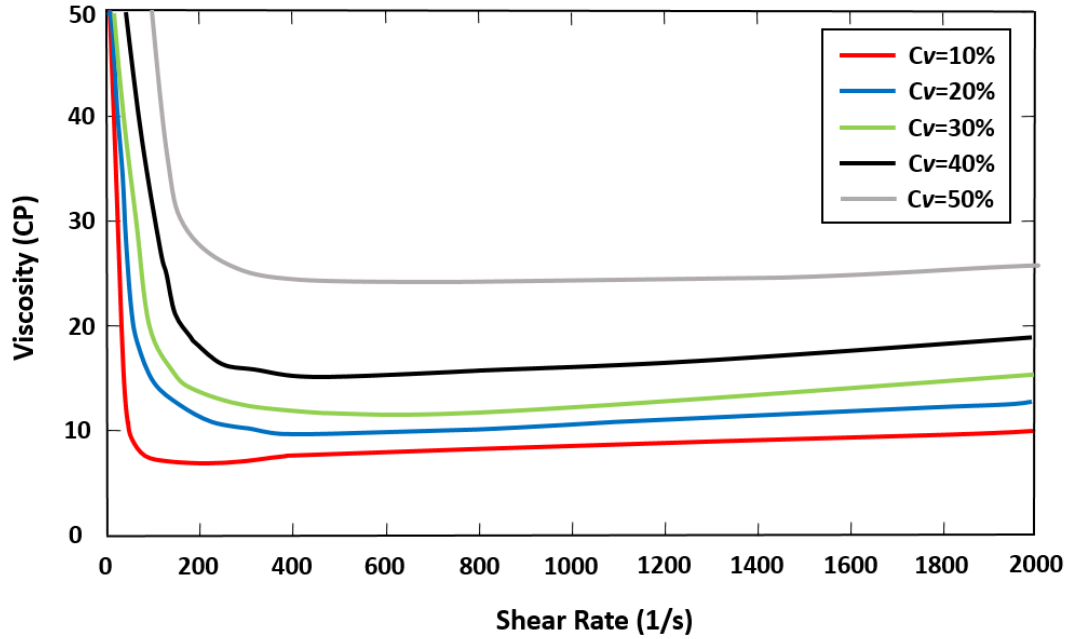
Figure 15: The impact of increasing particles concentration on the apparent viscosity of suspension [31].

2.5.3.2. Effect of particle size on suspension viscosity

Previous research confirmed that the size of cuttings heavily influences the increase in the viscosity of suspension fluid[31]. Kawatra and Eisele [31] observed that the reduction of particle size results in an increase in slurry viscosity at constant solid concentration, [Figure 16]. This trend was explained by the increase in particle surface area: by decreasing the size of cuttings the surface area increases, and therefore the contacting surface area of particles binding up with fluid molecules increases and leads to the increasing effective solid concentration.
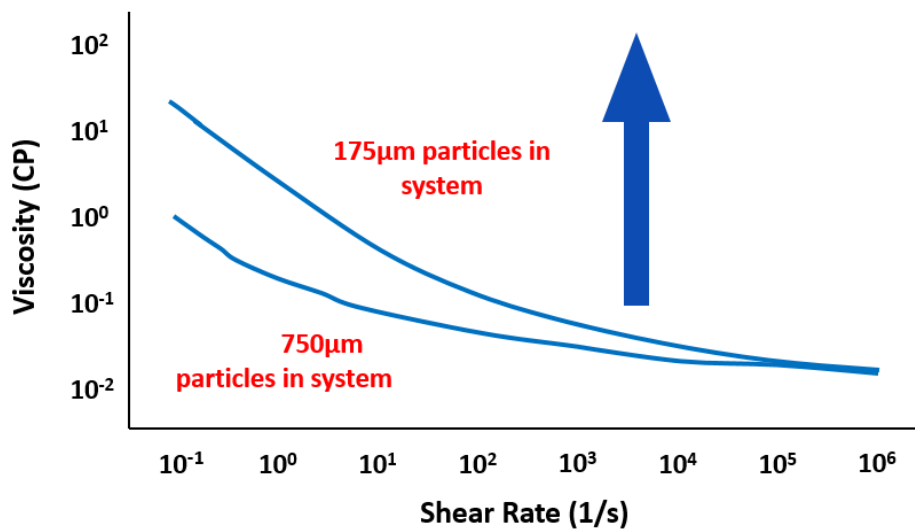
Figure 16: The impact of particles size on the apparent viscosity of silica sand based suspension [31].

In contrast, the other research from Clark [31] showed the viscosity of suspension fluid increases with the size of solid particles, as shown in Figure 17. This variation of viscosity was attributed to the inertial effect resulting in additional energy dissipation, which increases the viscosity of the suspension fluid.
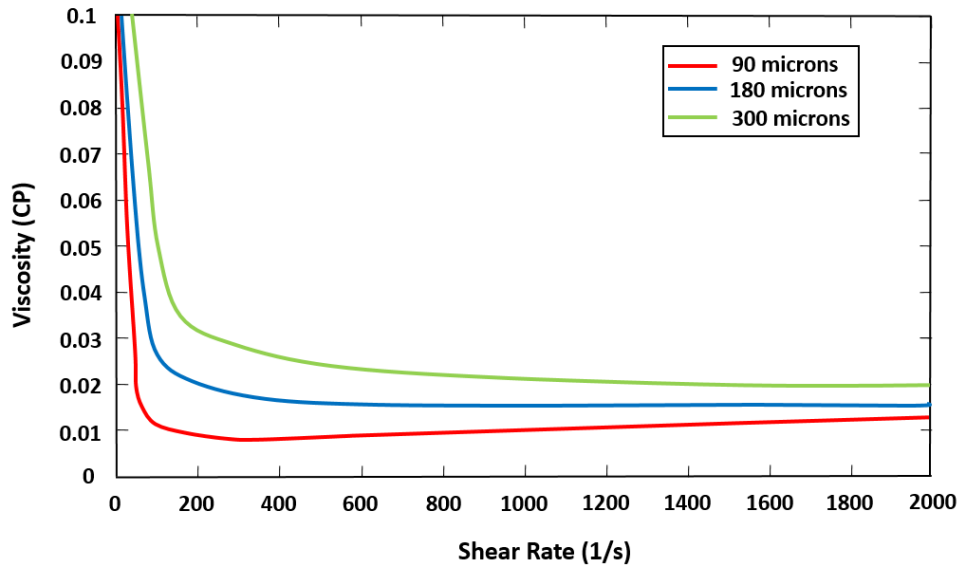
Figure 17: The increase of suspension apparent viscosity by increasing particles size [31].

One explanation of this apparent contradiction is related to the effect of particle size on the fluid viscosity - the microscopic structures of the suspended particles with different sizes are very different. As shown Figure 18 in research conducted by S Mueller et al [32], the initial state of the particle in suspension is characterized by the average size and fractal dimension of the primary particles. Particles can easily form aggregates in low shear velocity conditions with decreasing solid particles size, which results in the strongly entangled networks of immobile particles. When the sample is sheared at medium or high shear rate, the flocculent networks are broken up and the distance separating the fine particles increases and lowering the attraction of particles.
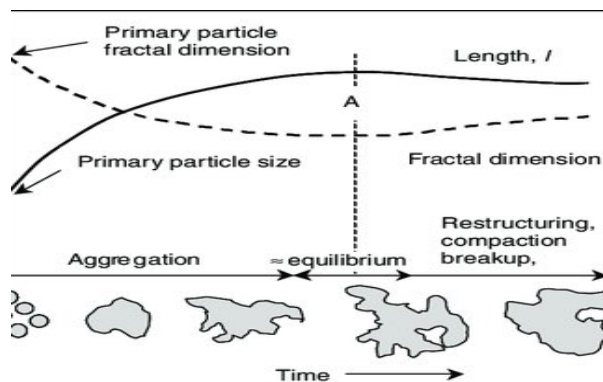
Figure 18: The conceptual picture of agglomerated particles and chain structure particles [32].

2.5.3.3. Effect of shear rate range on suspension viscosity

Based on previous research [33], particle suspensions behave as shear thinning at low shear rates, while particle suspensions demonstrate shear thickening at medium or high shear rates. At higher shear rates, the fluid tends to behave similar to a Newtonian fluid, in which the suspension exhibits a relatively constant viscosity. The variation of suspension viscosity from shear thinning at low-end rheology to shear thickening at high-end rheology, and eventually Newtonian behaviour, could be used to better understand the change of particle arrangements, as depicted in Figure 19 [34].
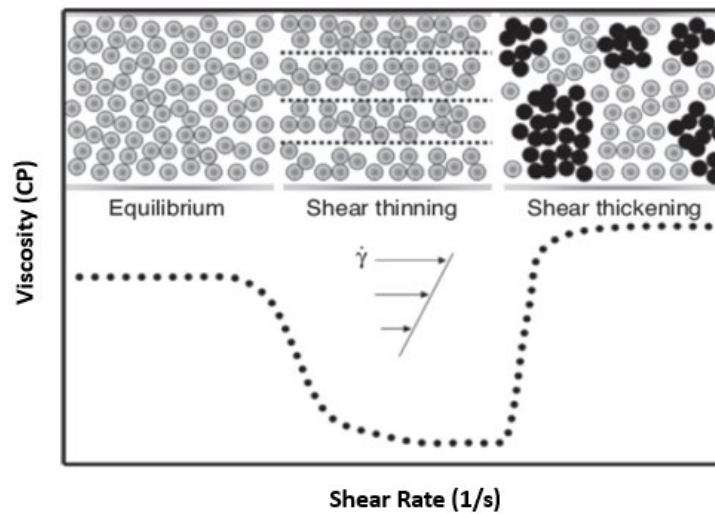
Figure 19: The conceptual picture of flow behaviour of suspensions at different shear rate [34].

2.5.4. Viscosity models of suspensions

The characterization and prediction of flow behaviour for particle suspensions is vital for mud optimization. A better understanding of the viscosity relationship with cutting particles crosses many applications in the drilling industry, as cuttings dispersed in a flowing mud give rise to extra energy dissipation. Several recent research works have addressed and developed equations to predict the relationship between apparent suspension viscosity η_{app}, and the volume concentration of particles $\emptyset$. There are several derivative forms of such equations for most applications, but the Einstein equation [35] is widely considered to be the most useful. This equation [2.9] is a relationship developed for single isolated particles, in which there is a proportional relationship between the suspension viscosity and particle volume concentration, according to,

$$\eta_{app} = \eta_0 \left(1 + 2.5\emptyset\right), \tag{2.9}$$

where η_{app} is apparent suspension viscosity, η_0 is suspending medium fluid viscosity and $\emptyset$ is the volume fraction of the solid particles (assumed to be spherical). The volume fraction is calculated from,

$$\emptyset = \frac{V_p}{V_f + V_p} \ , \tag{2.10}$$

where V_p and V_f denote the volumes of the particle and fluid phases respectively.

The Einstein equation is based on an idealized hard-sphere dispersion model system, as it assumes that there is no any appreciable interaction between the solids, and that all particles are single and isolated. This equation is only applicable for diluted dispersions of spherical particles which volume concentration is less than 1% ($\emptyset < 0.01$) [35].

It can be summarised from the Einstein equation that the viscosity of dispersions mainly depends on the volume concentration of suspended particles and it is a linear function of the particle volume fraction [35]. Although the Einstein equation is limited to rigid and spherical particles, actual experiment conditions can differ considerably from these theoretical assumptions. For higher particle concentration, multi-particle interaction becomes important and it has to be taken accounted. Thus, numerous empirical corrections have been developed to calculate viscosity of suspensions under this circumstance [35].

Krieger-Dougherty [36] suggested a semi-empirical equation, which is applicable for a wide concentration range of suspensions and better fitted to highly concentrated suspension rheology measurements,

$$\eta_r = (1 - \frac{\emptyset}{\emptyset_m})^{-[\eta] \, \emptyset_m} \ , \tag{2.11}$$

where $\emptyset_m$ is the maximum packing fraction or volume fraction of the suspension [29]. The absolute value of the latter is determined by particle packing geometry, which only depends on particle shape and size distribution [37]. It should be mentioned, that particles would realign in the flow direction, which causes more efficient packing rather than random packed structure at rest, so the maximum packing fraction has different value from low shear rate to high shear rate. [η] referred as the 'Einstein coefficient' or 'intrinsic viscosity' and takes the value of 2.5 for spherical particles [38]. However, there is no unique value of intrinsic viscosity as this parameter differs with different suspensions. This particle interaction coefficient increases with the increasing number of fine particles in the suspensions [39].

A similar equation suggested by Quemada et al [40] can also be applied for calculation of relative viscosity over a wider range of concentrations rather than original Einstein equation:

$$\eta_r = (1 - \frac{\emptyset}{\emptyset_m})^{-2} \; , \qquad\qquad\qquad (2.12)$$

However, not one simple model can describe solid-particle relationships perfectly from very dilute to highly concentrated states as particle in a suspending medium can be subject to hydrodynamic interaction, Brownian motion and well as other effects.

The current literature does not provide enough data for particle suspensions from low-end to high-end shear rates. Little comprehensive work and systematic studies have been done for polymer drilling fluids with fine suspended cuttings. As part of the proposed study, investigations will focus on how the cutting particles alter the rheology of polymer drilling fluids and the effect on thixotropic behaviour.

2.6. Polymer synergy

During drilling operation, the drilling fluid is required to have high low-end viscosity. As the drilling fluid moves through the upward section of larger annulus, the fluid velocity decreases, which results in smaller carrying capacity. In order to carry the cuttings to the surface, it is essential for the drilling fluid to exhibit high viscosity at lower shear rate to compensate for the decrease in fluid velocity. Furthermore, in high angle hole drilling, there exists the possibility that the drill string lies on the low side of borehole, as depicted in Figure 20. In this case, the drilling cuttings moving into the high flow area might slide back down to the low side area, which will cause cuttings agglomeration. In order to prevent this happens, increasing the mud low-end rheology helps to reduce this risk, which means the low-end fluid rheology must be kept high enough to effectively clean the low viscosity low side part of the borehole.
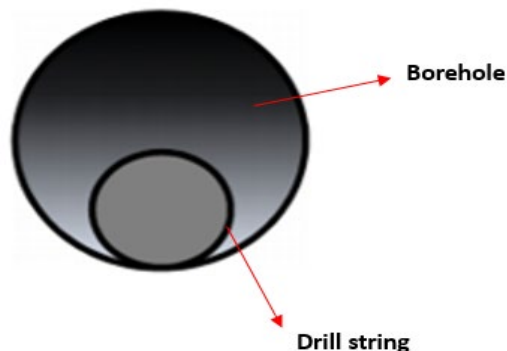
Figure 20: Drilling cuttings agglomeration in high angle well borehole section.

Research on the low-end rheological modifiers and their synergistic optimization is a major area for improvement in the drilling industry. Low-end rheology refers to the rheology at the almost zero constant shear rate. The shear rate of flowing drilling fluid tends to be less than 100 1/s at the wall of the borehole while nearly approaching zero in the centre of annulus. Xanthan Gum is a low-shear-rate rheological booster widely used in the field, as it has high viscosity at low shear rate. The structure of Xanthan Gum and its properties are summarized in Table 5 [41]. Compared with other common gums over a range of shear rates, Xanthan Gum has approximately 15 times the viscosity of Guar Gum or CMC at very low shear rate [41]. In this case, determination of the optimal combination between Xanthan Gum and other gums is very crucial for drilling operation, for a lower cost of drilling mud and production of better rheology from low-end to high-end.

Synergetic interaction refers to the effect of two or more chemicals, together, being greater than the theoretical combination of each polymer. In drilling operation, drilling fluid with extensive shear thinning property is highly desired. High viscosity at low shear rate is desired to control the fluid loss in unconsolidated and fractured formations. Low viscosity at high shear rate is desired for minimising the pressure drop in the coiled tube, drill string, downhole tools and annulus, which in turn increasing the efficiency of drilling pump during operation. Furthermore, having low-viscosity at high shear rates improves solid removal efficiency using hydrocyclone and centrifuge decanters.

Previous research showed that a synergistic interaction occurs between Xanthan Gum and other gums, which brings enhanced viscosity or gelation [42]. The viscosities of polymer blends of Xanthan Gum and Guar Gum with different ratios were measured [42]. The viscosities of the combinations were observed to be higher than that of the single polymers. This phenomenon occurred due to the synergistic rheological interaction between these polymers. One reason for this might be direct interaction between Xanthan Gum chains and Guar Gum chains [43]. The structures of molecules would enhance the entangled networks of polymers and increase inner friction, which in turn increases the viscosity of blended polymer. Moreover, the Xanthan Gum/Guar Gum ratio showed a great influence on the viscosity of blend [42]. Maximum synergy was found for the ratio of Xanthan Gum to Guar Gum (1:1), [Figure 21]. A thorough literature search indicated that the effect of interaction of different rheological boosters on low-end and high-end rheology is not clear enough. The aim of this work is to study the effect of these variables on blend viscosity in detail.

Table 5: Structure and property relationship of Xanthan Gum [43].

Structural features	Properties
Complex aggregates, with weak intermolecular forces	High viscosity at low shear rates (suspension stabilising properties) High viscosity at low concentrations High elastic modulus Pseudoplastic rheology
Rigid helical conformation, hydrogen bonded complexes, anionic charge on side chains	Temperature insensitivity and salt compatibility
Backbone protected by large overlapping side chains	Stability to acids, alkalis and enzymes
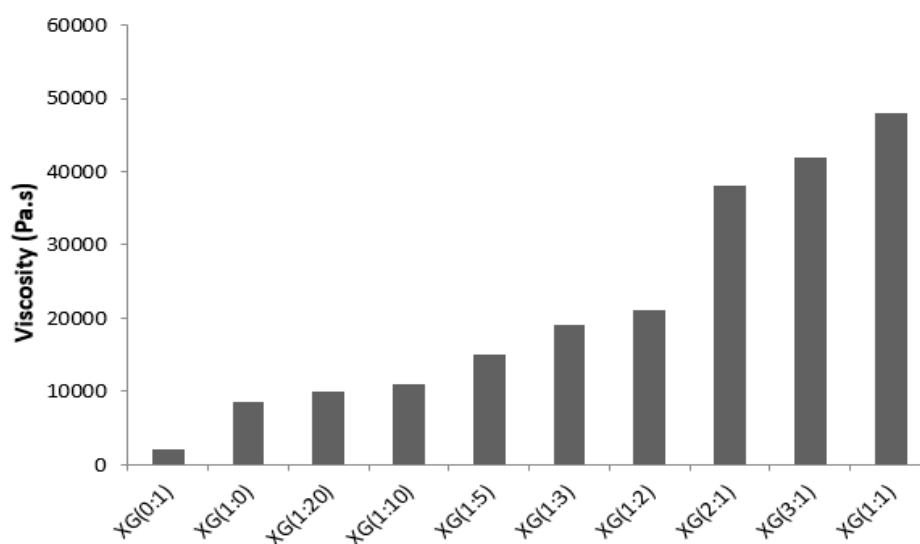
Figure 21: Viscosity synergism between Xanthan Gum and Guar Gum [42].

35

Chapter 3. Methodology

3.1. Introduction

This chapter introduces the methodology for measurement of the rheology, over a wide range of shear rates, for different polymers and bentonite. The methodology for testing different combinations of polymers, leading to a blend that can yield extensive shear thinning behaviour with elevated viscosity at low shear rate, will also be detailed. At last, the experiment to study the effect of solid particles on suspension solutions is illustrated.

3.2. Rheological measurement

3.2.1. Ofite measurement

A 12-speed Ofite 900 viscometer with R1B1 bob and rotor arrangement was used for synergy experiments [Figure 22]. The aim of the experiments was to validate functions of different viscosity boosters and their differences in enhancing low-end rheology. They were dissolved in water at room temperature and stirred at 1000rpm, using an overhead mixer. For the purpose of fluid hydration, the mixing time was maintained at a minimum of 20 minutes and then later measured by Ofite 900 R1B1 viscometer. Then the weight concentrations of additives were adjusted to ensure they had very similar dial readings at an angular velocity of 600 rpm, which corresponded to a shear rate of 1021.24 1/s. This shear rate, and that of 510.69 1/s (corresponding to 300 rpm) are the main shear rates used in petroleum engineering for viscosity measurement [1]. Finally, Haake Mars viscometer was used for step-wise rheological measurement.
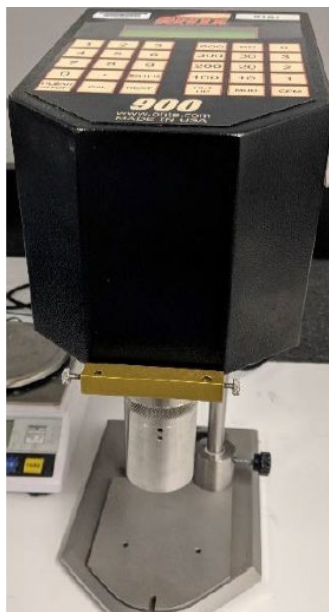
Figure 22: Ofite 900 viscometer with R1B1 geometry.

3.2.2. Haake measurement

3.2.2.1. Haake step-wise test

A specific step-wise shear profile was performed using the Haake Mars viscometer with Z20 DIN sensor geometry, to measure viscosity of a test sample for synergy experiments. According to the instruction manual, 8.2ml of test sample was placed into the cylinder chamber and step-wise shear rates were applied. Various shear rates were applied starting from a low shear rate of 0.1 1/s to a high shear rate of 1900 1/s. At low shear rates, the duration of exposure was 3 minutes, while the duration of exposure for medium and high shear rates was 30 seconds. The corresponding viscosity was obtained with the variation of shear rates. The Haake RheoWin3 software was used to plot shear stress versus shear rate, and viscosity versus shear rate relation of suspensions in real-time during measurement [Figure 23].
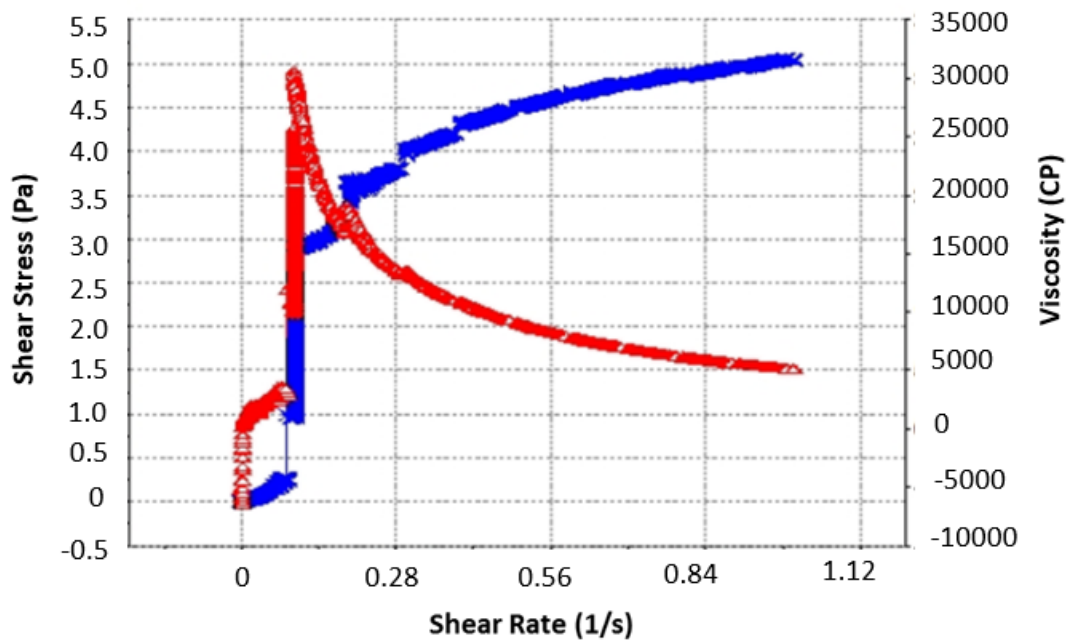
Figure 23: Haake RheoWin 3 interface-real time graph.

The effect of cuttings on suspension was also investigated using the Haake Mars viscometer. High viscosity suspending fluid was used to minimise the particle settlement during the experiments, and different sizes and concentrations of particles were used. The suspensions with particles were sheared before the viscosity measurement. This "pre-shear" condition was applied to ensure suspended particles are randomly oriented and that equilibrium orientation distributions were established. After a period of shearing, the Haake step-wise experiment was conducted [Figure 24]. The experimental temperature was set at 25 ℃.
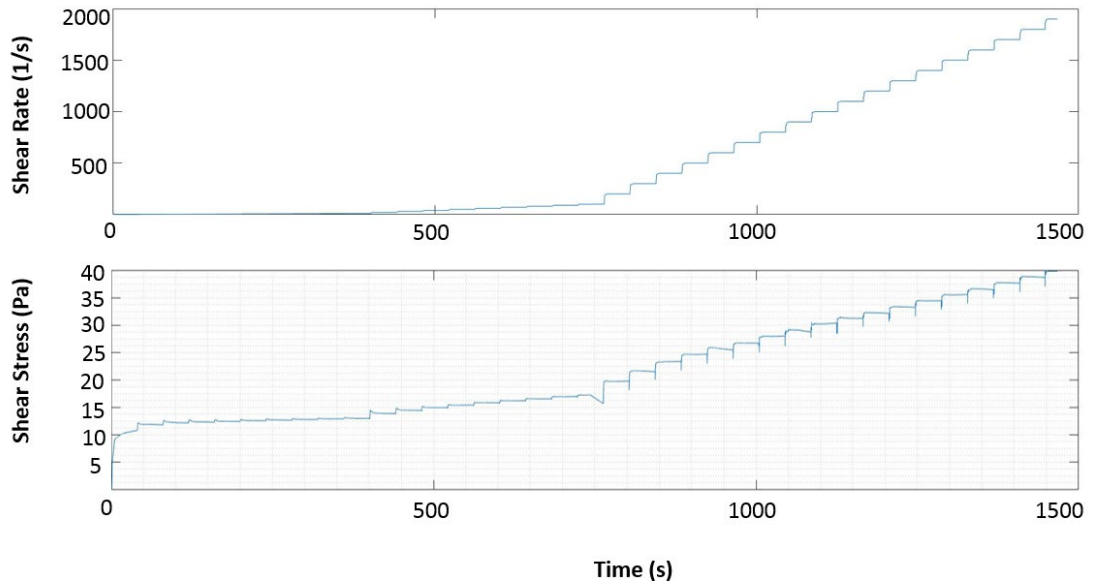
Figure 24: MATLAB analysis of Haake step-wise measurement of one suspension with particles.

3.2.2.2. Haake thixotropic loop test

A thixotropic loop test was conducted under shear-controlled conditions to quantify the thixotropic behaviour of a test sample, as shown in Figure 25. In this test, the test sample was pre-sheared to thoroughly break down any existing structure and allow a rest period to rebuild the structure of the sample. The shear rate was then ramped up from zero shear rate to a maximum of 1900 1/s in 100 seconds and held constant for 80 seconds. It was then ramped smoothly from 1900 1/s back to zero shear rate in 100 seconds.
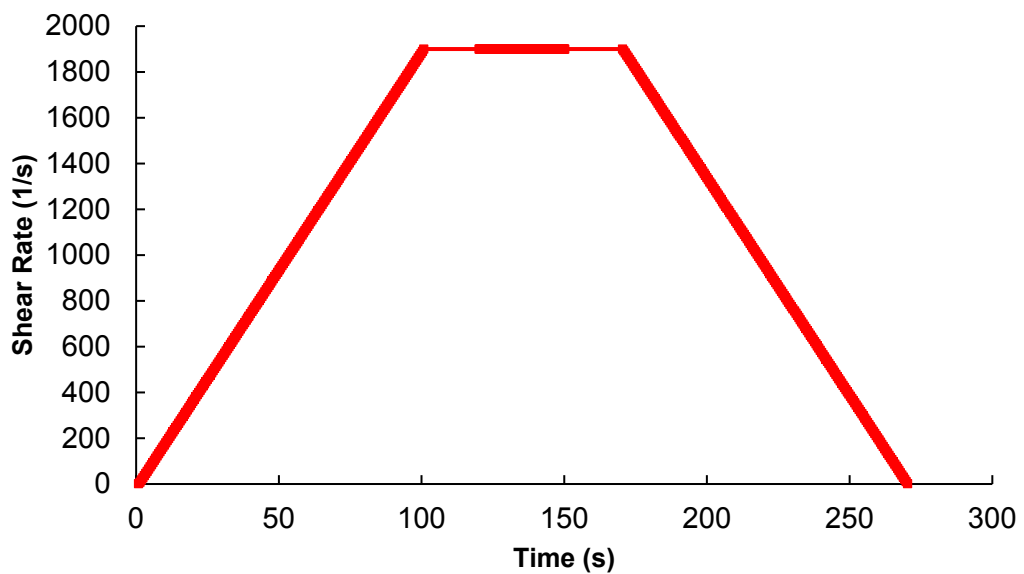
Figure 25: Example of the variation of shear rate with time during a thixotropic loop test of suspension.

38

Figure 26 shows an example of the graphical depiction of the loop test performed with a Haake Mars viscometer for a sample suspension. A hysteresis area can be quantified by measuring the area between ascending and descending curves. A larger hysteresis area refers to higher thixotropic behaviour. For non-thixotropic fluids, the ascending and descending curves are identical, with minimum/zero hysteresis area. The loop test measurement strongly depends on test conditions like shear rate range and shear time, and therefore material can only be compared with the same procedures.
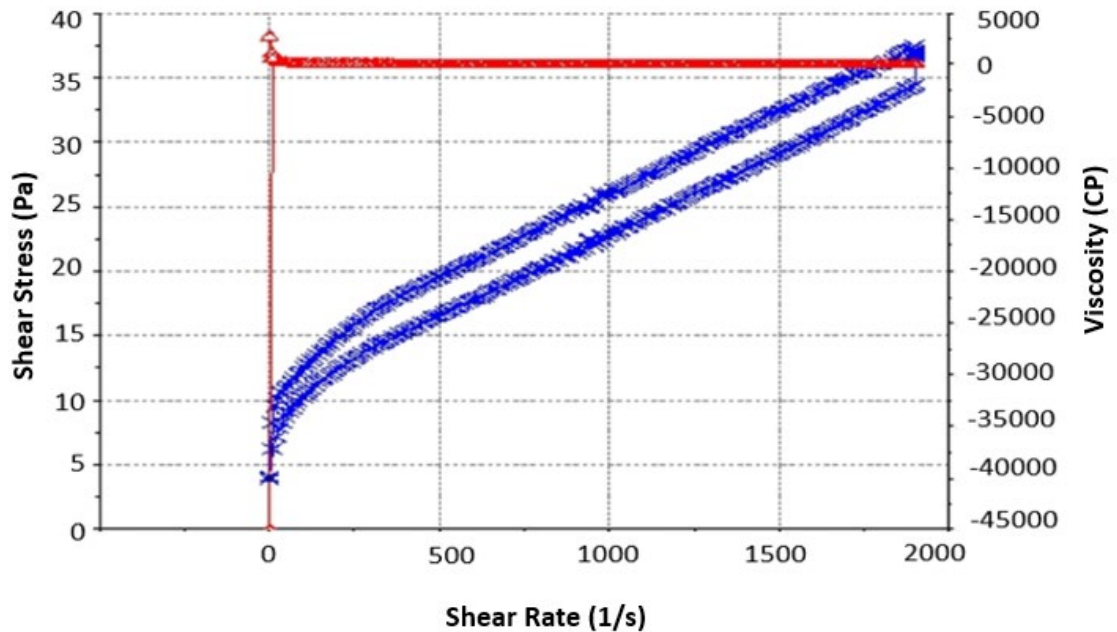
Figure 26: Hysteresis loop test of suspension sample – Haake RheoWin 3 real time graph.

3.2.3. Capillary measurement

A straight pipe viscometer was designed to conduct capillary measurement of the rheology of a flowing fluid. Hydraulic pressure drop across a known length of pipe section was measured at different flow rate using flow meter and pressure sensors. A method of converting hydraulic parameters to rheological parameters are introduced based on pipe viscometer theory.

3.2.3.1. Experiment setup

The pipe viscometers were composed of straight pipes with three different internal diameters. The specification of each pipe is shown Table 6. The total length of each pipe was 6 meters and the entrance length was 2 meters to ensure fully developed flow in the test section. The exit length of the pipe viscometer was 1 meter to minimise any end-effects. [Figure 27] depicts a schematic of the setup.

A differential pressure transmitter, an absolute pressure transmitter and a flow meter were installed on the pipeline to measure the friction drop of fluid flowing through the test section and the volumetric flow rate during experiments.

A detailed description of the apparatus is presented below.

Table 6: Specification of pipe viscometers.

External diameter (inch)	Internal diameter (inch)	Entrance length (m)	Exit length (m)	Typical flow rate (lpm)
0.5	0.43	2	1	4.42-19.47
0.75	0.62	2	1	4.54-25.96
1	0.87	2	1	2.48-25.27
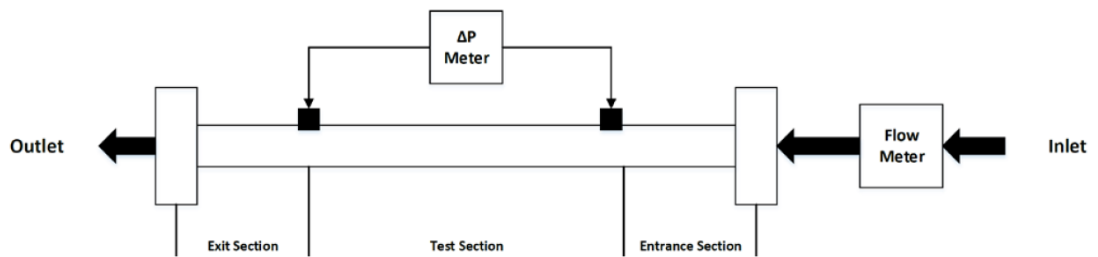
Figure 27: Straight pipe viscometer.

Siemens Sitrans FM Mag 5000 and SITRANS F M TRANSMAG 2 flow meters were both used for flow rate measurements, [Figure 28].The Siemens Sitrans FM Mag 5000 is a microprocessor-based transmitter engineered for high performance. However, the disadvantage encountered with this flowmeter is that it cannot measure flow rate reading correctly below 10 litre per minutes. SITRANS F M TRANSMAG 2 is used instead to measure the flow rate at lower range. It has better accuracy at low flow rate.

Figure 28: SIEMENS flow transmitter FM Mag 5000 and SITRANS F M TRANSMAG 2.

The pressure drop along the pipe viscometer was recorded by MRB20/Keller pressure transmitters [Figure 29]. Two 5 bar MRB20 absolute pressure sensors and a 1 bar Keller differential pressure were used. While the absolute pressure sensor measures the pressure at the point the sensor is connected, the differential pressure sensor records the pressure difference between two points where the absolute sensors are connected. The Keller differential pressure transmitter provides high accuracy differential pressure measurement with ranges from 100mbar to 1bar.The differential pressure can be calculated using either two absolute pressure sensors or directly using the differential pressure sensor. The linearity of sensors was 0.1%, and the data communication was via a 4-20 mA current signal.

Before each experiment, the differential pressure sensor and absolute pressure sensors were calibrated using the hydrostatic height of 6 meters of vertical pipe [Figure 30]. For the differential pressure sensor, the low pressure side was left open to atmospheric pressure to simulate an absolute pressure sensor, for the purpose of a calibration check.

Figure 29:MRB20 absolute pressure transmitter and Keller differential pressure sensor.
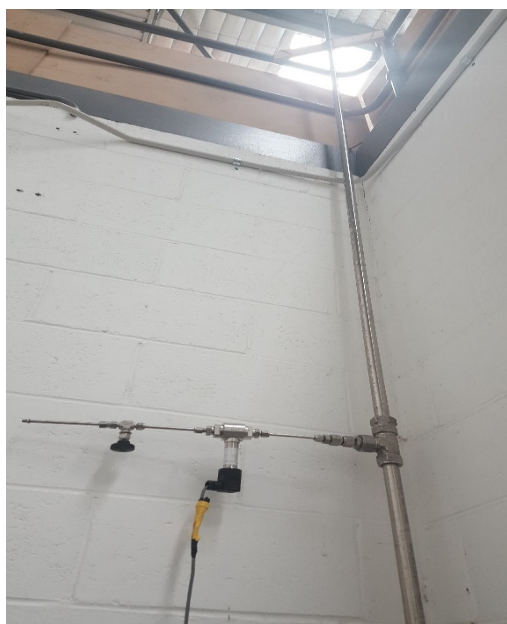
Figure 30: Pressure sensor calibration setup made of 6 meters vertical pipe.

The DAQ SomatXR MX840B-R data acquisition system is used for this experiment, to record and digitise the signals [Figure 31]. Catmaneasy is the software interface used for data acquisition, which provides real-time display of data during the experiment, and enables saving the data in MATLAB format for further processing, [Figure 32]. All recorded data is later processed using a MATLAB code and presented in an Excel spreadsheet.

Figure 31: DAQ SomatXR MX840B-R data acquisition system.
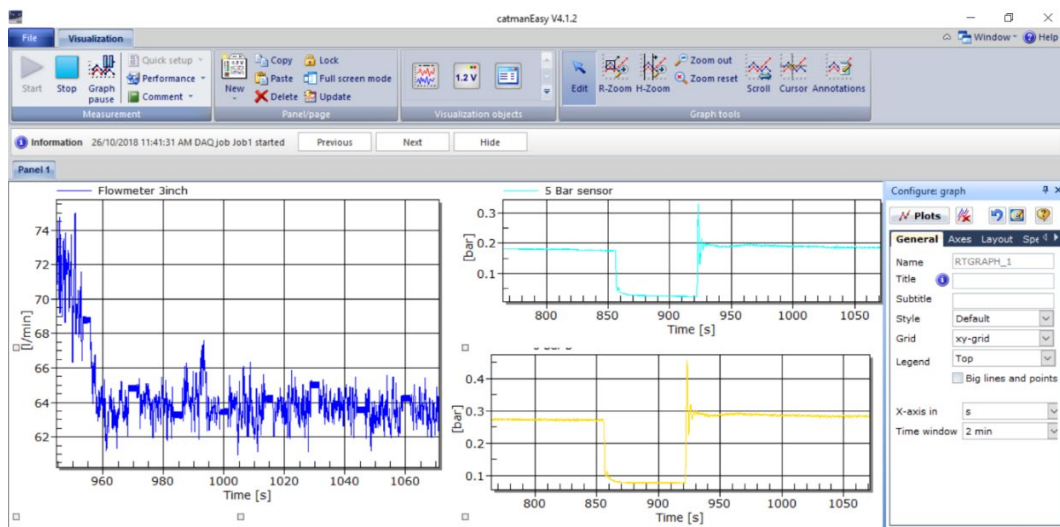
Figure 32: CatmanEasy Interface– real time graph.

3.2.3.2. Bias test

According to experimental procedures, air bubbles along the pipeline were released to minimize the effect air entrainment and bias measurement conducted prior to each experiment.

Figure 33 illustrates the variation of sensor bias of pressure sensors during an experiment. For the bias test, all the valves along the pipe viscometer were closed to ensure that the fluid inside

the pipe is under static conditions. The recording was continued for typically 2 minutes to ensure a stationary signal is obtained for each transducer. The initial pressure readings were recorded as a reference point, which was subtracted from subsequent pressure applied to calculate the actual experimental pressure values at different flow rates. The duration of the experiment for each flow rate was at least 1 minute, to produce a stable signal. The average value for pressure drop and flow rate were calculated.
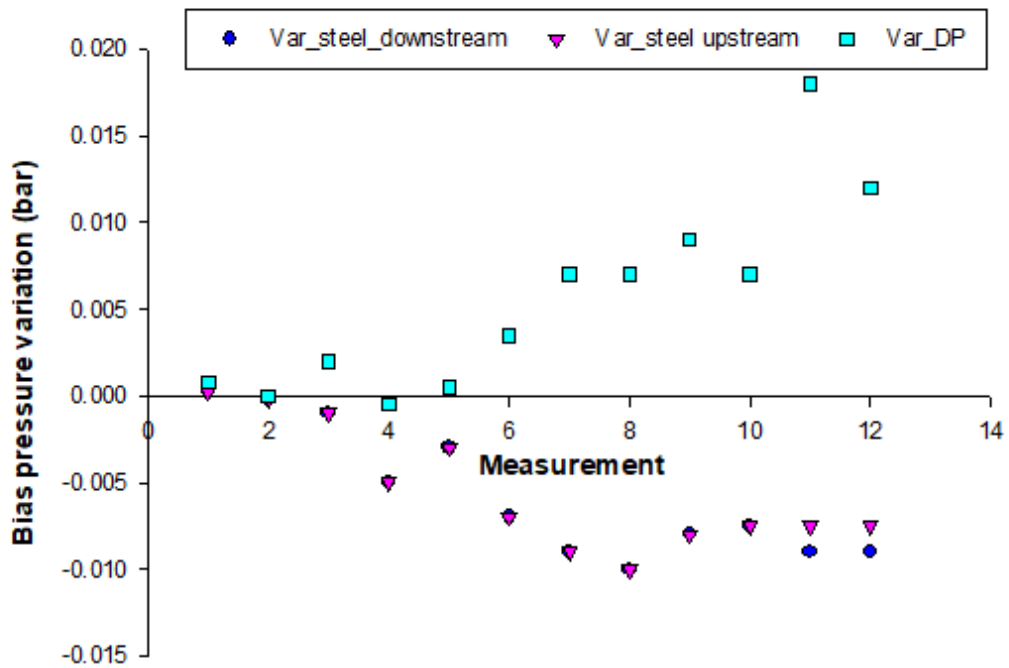
Figure 33: The variation of bias measurement of absolute and differential pressure sensors during an experiment. The bias was measured multiple times during the experiment.

3.2.3.3. Pressure drop prediction

Different rheology models [18] for predicting pressure losses of fluid flowing in a 0.5 inch pipe viscometer were verified by hydraulic experiments. In accordance with different fluid rheological models, this prediction could be computed by applying relevant equations.

Generally, when the flow behaviour of fluid deviates from a simple Newtonian fluid, the friction loss equations become more complex and less accurate [44]. The objective of this part of research is to show the discrepancy of pressure loss calculation using different models. The mathematic formulae to determine the pressure drop of laminal flow in a 0.5 inch straight pipe are summarised in Figure 34 to Figure 36.

Known parameters

- Yield point, τ_y
- Plastic viscosity, μ_p
- Pipe ID
- Density of bentonite, ρ
- Length of test section
- Mean velocity, u

Calculate — Reynolds number, Re

$$Re = \frac{\rho u d_i}{\mu_p}$$

If Re < 2100, laminar; else turbulent

Calculate — Pressure drop per unit length

$$\frac{\Delta p}{L} = \frac{32\mu_p u}{d_i{}^2} + \frac{16\tau_y}{3d_i}$$
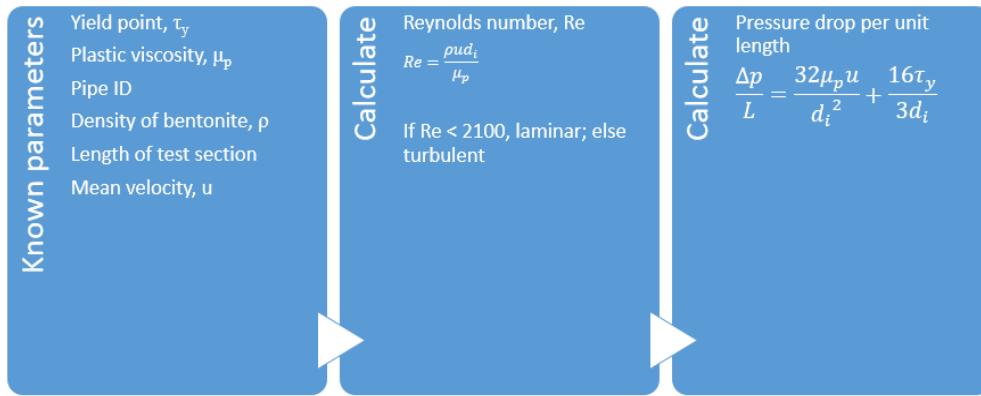
Figure 34: Pressure drop equation of Bingham plastic model fluid, summarised from [18].

Known parameters

- Flow behavior index, n
- Flow consistency index, k
- Density of bentonite, ρ
- Length of test section
- Pipe ID
- Mean velocity

Calculate — Flow consistency index for pipe flow, k'

$$k' = k\left(\frac{3n+1}{4n}\right)$$

Flow characteristics, n'

$$n' = n$$

Calculate — Wall shear stress, τ_w

$$\tau_w = k'\left(\frac{8u}{d_i}\right)^{n'}$$

Wall shear rate, γ_w

$$\gamma_w = \frac{8u}{d_i}\left(\frac{3n'+1}{4n'}\right)$$

Apparent viscosity, μ_{ap}

$$\mu_{ap} = k'\left(\frac{8u}{d_i}\right)^{n'-1}$$

Calculate — Reynolds number, Re

$$Re = \frac{\rho u d_i}{\mu_{ap}}$$

If Re 2100, it is laminar; else turbulent

Friction factor, f (laminar)

$$f = \frac{16}{Re}$$

Pressure drop per unit length

$$\frac{\Delta p}{L} = \frac{2f\rho u^2}{d_i}$$

Figure 35: Pressure drop equation of Power law model fluid, summarised from [18].

Known parameters

- Flow behavior index, n
- Flow consistency index, k
- Yield point, τ_0
- Pipe ID
- Density of bentonite, ρ
- Length of test section
- Mean velocity, u

Iteration — Friction factor (laminar)

$$f = \frac{16}{\psi Re}$$

$$Re = \frac{D^n u^{2-n}\rho}{8^{n-1}k}\left(\frac{4n}{1+3n}\right)^n$$

$$\psi = (1+3n)^n(1-\xi_0)^{1+n}\left[\frac{(1-\xi_0)^2}{(1+3n)} + \frac{2\xi_0(1-\xi_0)}{(1+2n)} + \frac{\xi_0{}^2}{(1+n)}\right]^n$$

$$\xi_0 = \frac{\tau_0}{0.5f\rho u^2}$$

If Re < 2100, laminar; else turbulent

Calculate — Pressure drop per unit length

$$\frac{\Delta p}{L} = \frac{2f\rho u^2}{d_i}$$
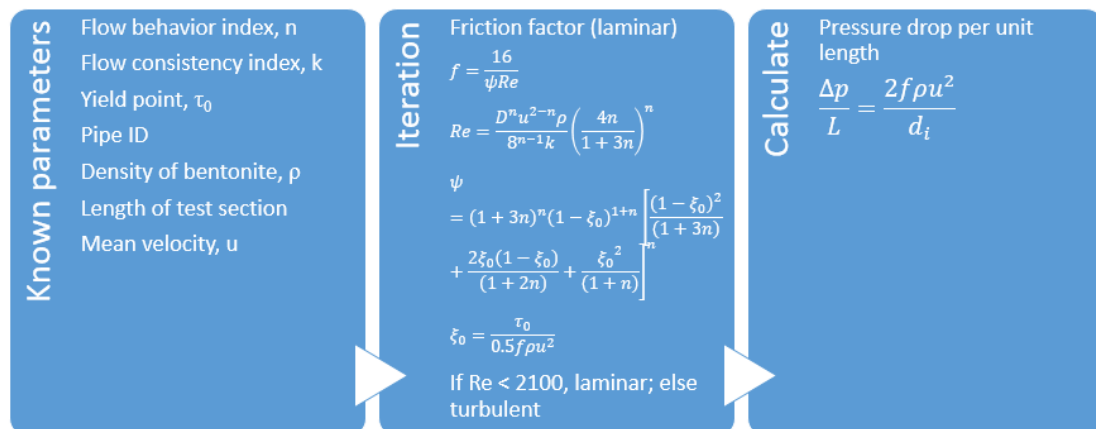
Figure 36: Pressure drop equation of H-B model fluid, summarised from [18].

44

3.3. Test material

3.3.1. Additives

3.3.1.1. Additives for synergy experiments

The viscosifiers, used in synergy experiments are, Guar Gum, Pac-R, Aus-Gel-Xtra , Corewell and Xanthan Gum, which are ideal for viscosity enhancement due to their low cost and resistance to thermal degradation. However, there may be differences in their capability to increase low-end rheology.

Guar Gum is a white powder manufacturing from guar beans, which widely used as a stabilizing, thickening and suspending agent in the drilling industry. The disadvantage of Guar Gum is its sensitivity to high pH. Pac-R is a filtration control additive, which is mostly used in water-based mud. It helps to control filtration rate and provide supplementary viscosity in fresh water, seawater and brine-based fluids. Aus-Gel-Xtra is a modified premium grade Wyoming bentonite which used as a high yielding viscosifier with excellent wellbore cleaning properties. Corewell is a dispersible product which is used to protect exposed formation during drilling operation. Xanthan Gum is a natural white powder, which can dissolve readily in water and thicken the drilling mud.

3.3.1.2. Additives for particle effect experiments

In order to minimise solids settling during the tests and to better characterise the cutting effect on drilling fluid, an aqueous solution of 0.5 wt. % Xanthan Gum was used as suspending fluid. The concentration and type of polymer is particular selected to provide sufficient viscosity to suspend the sand and calcium carbonate particles and to create a nearly stable suspension during experiment. In this research, Xanthan Gum was supplied from Australian Mud Company (AMC) under commercial name of Xanbore^{TM}, [Figure 37].

To prepare 0.5 wt. % fluid, Xanbore^{TM} was completely mixed with water. Xanthan Gum powder was slowly added to distilled water and agitated at 1000 rpm for 20 minutes. Poor dispersion leads to clumping of particles (known as "fish eyes") and reduces chemical functionality.

Figure 37: AMC Xanthan Gum (Xanbore^{TM}) of suspending fluid.

3.3.1.3. Additives for pipe viscometer experiments

An aqueous solution of 6 wt. % bentonite was used for the capillary measurement to study its rheology effect on the friction loss along the straight pipe viscometer. Bentonite is a natural clay mineral most widely used in the water base drilling fluid, and functions as a lubricant and coolant for the drill bit. It helps remove cuttings and prevents blowouts. Bentonite solution was chosen for experiment as it tends to provide a more stable fluid viscosity. Unlike other viscosifier additives such as polymers, it is not affected by bacteria activity or previous shear history. Bentonite fluid was prepared in an industrial tank with capacity of 1000 litres using high-speed agitator, [Figure 38].

Figure 38 : The storage tank with the agitator.

3.3.2. Solid particles

The particle effect experiments were performed using graded sands and Calcium Carbonate particles suspended in Xanthan Gum fluid to form solid-liquid suspensions. Narrow particle size ranges were selected using sieving method – the sieves and the sieve shaker are shown in Figure 39. Three size ranges of sand particles, and one size range of Calcium Carbonate particles were physically sorted using the sieving method. The details of particles are shown in Table 7.

The fine particles weight concentrations in the suspension ranged starting from 1 wt. % to 10 wt. %, to create a diluted to concentrated solid suspensions. As the average densities of fine particles are $2.65\,g/cm^3$, the corresponding particle volume concentrations ranged from 0.3 vol. % to 3 vol. %. Higher angular velocities of the mixer were avoided to minimise formation of air bubbles in the suspension, and to obtain homogeneous monodisperse suspensions. The effect of particle shape was not studied in this research due to the difficulties associated with supplying solid particles with different shapes.

Figure 39: Sieve shaker (left) and sieve meshes (right) for 200 μm, 150 μm, 106 μm, and 75 μm (top to bottom).

Table 7: Size range of solid particles.

Particle	Particle Size (microns)	Solid Concentration (wt. %)	Solid Concentration (vol. %)
Calcium Carbonate	38-75	0.3	1
		0.9	3
		1.5	5
		2.4	8
		3.0	10
Silica Sand	106-200	0.3	1
		0.9	3
		1.5	5
		2.4	8
		3.0	10
	200-250	0.3	1
		0.9	3
		1.5	5
		2.4	8
		3.0	10
	250-300	0.3	1
		0.9	3
		1.5	5
		2.4	8
		3.0	10

Chapter 4. Results and Discussion

Experimental results along with the interpretation are presented below.

4.1. Benchmarking of different rheology measurement techniques

In order to investigate the reliability of the Marsh Funnel as a qualitative measurement of fluid rheology, a particular comparison experiment, also termed 'the benchmark experiment', was designed. The Marsh Funnel and API rotary viscometer were used to determine rheological properties of drilling fluids. Two drilling fluid solutions were made using bentonite and a nature polymer Pac-R. The concentration of the Pac-R was adjusted to produce a similar Marsh Funnel viscosity as the bentonite mud system. The Marsh Funnel viscosity was 81s for the bentonite mud and 81.5s for the polymer mud. The samples were also tested using the Ofite R1B1 viscometer, and the rheology measurements are illustrated in Figure 40.

As observed in the Figure 40, these two fluids might be similar at particular shear rates, but indeed they had distinctive properties, and therefore different responses in drilling. However, if the measurement using the Marsh Funnel was only considered, both fluids were expected to produce similar fluid response (e.g. in the case of pressure drop or cutting transportation).
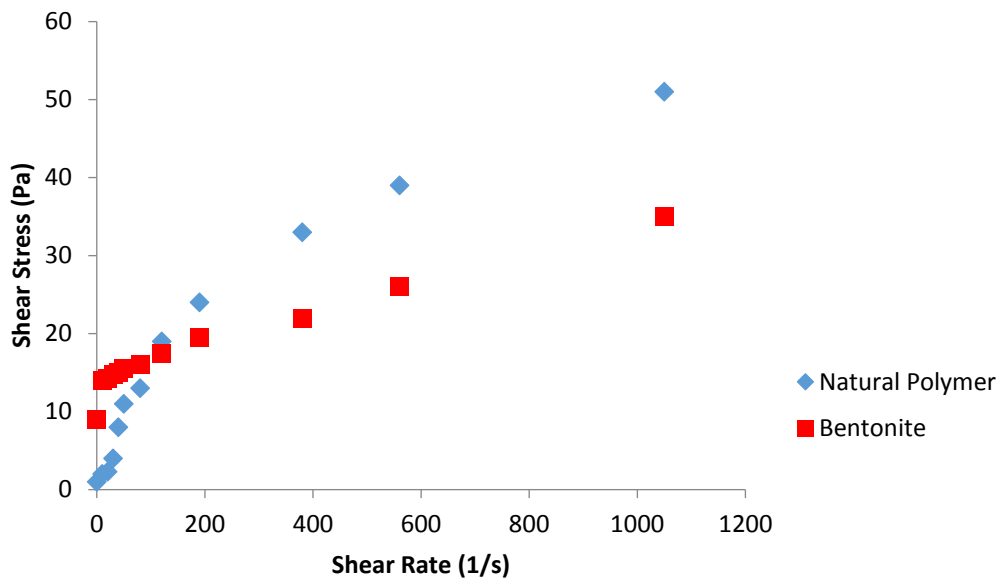
Figure 40: Comparison of fluid viscosity of a polymer and a bentonite solution using Ofite 900 R1B1 rotary viscometer.

Different sensors can be used for a particular rotary viscometer equipment. There is a lack of literature evidence to investigate the effect of sensor type on the rheological measurement. As part of this study, a controlled experiment was devised to evaluate if the measurements from different sensors [Figure 41] are in agreement. In order to evaluate different rotary viscometry

test methods, a 0.3 wt. % Xanthan Gum solution was selected and tested using a Haake Mars rotational viscometer. The concentration and type of polymer were selected in order to achieve high low-end rheology so that any potential inconsistency in measurement due to low values of viscosity would be minimal, and the effect of sensor can be obtained more accurately. Three sensors used in Haake Mars viscometers, namely cylinder sensor Z20DIN, plate-plate sensor PP35Ti and cone-plate sensor C35/4Ti, were used [Table 8].

Figure 41: Haake Mars Z20DIN, PP35Ti and C35/4Ti sensor systems.

Table 8: Specification of Haake Mars sensor systems.

Sensor	Cylinder-Z20DIN	Cone-Plate-C35/4TI	Plate-Plate-PP 35TI
Maximum Shear Rate	1900 1/s	2249 1/s	2749 1/s
Sample Volume	8.20 cm^3	0.80 cm^3	0.80 cm^3
Gap	0.85 mm	0.14 mm	1.00 mm
Angle	0 °	4 °	0 °
Clearance to Bottom	4.20 mm	/	/

Figure 42 showed the measured viscosity from Haake Mars viscometer, using different sensors, by varying the shear rates. It shows that measurements with different sensor geometries are closer to each other at medium and high shear rate ranges. Across the range of shear rates, the cylinder sensor measures up to 1900 1/s while plate-plate sensor can measure up to 2749 1/s and the cone-plate can measure up to 2249 1/s. These three sensor systems meet rheology measurement requirements across a very wide shear range. However, the main disadvantage of the plate-plate and cone-plate sensors is that test fluid can evaporate easily during measurement, and that the sensors are not suitable to measure suspensions with particles. The

cylinder sensor Z20 DIN (bob diameter = 20mm and inner cup diameter =21.7mm, gap 4.20mm) was used for thixotropic loop measurements and rheological measurement of suspension with particles during this research.
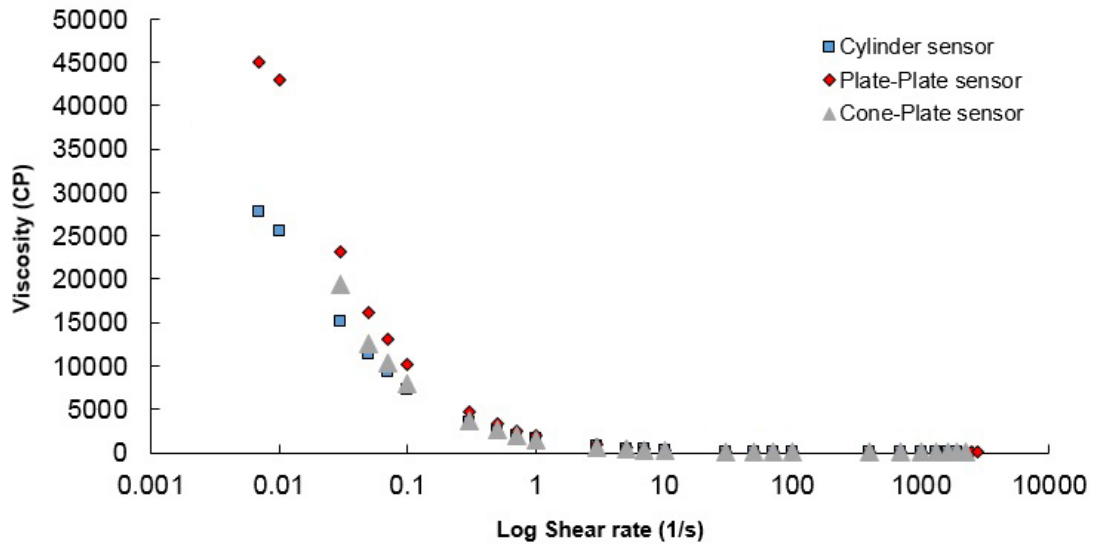
Figure 42: Rheological measurement of 0.3 wt. % Xanthan Gum measuring with different geometries of Haake Mars.

The Ofite R1B1 viscometer is commonly used in petroleum engineering, while the Ofite R1B2 can be used when more accurate measurement of viscosity at low shear rates is required. The measurements of typical viscometer and advanced Haake Mars are in agreement at specific shear rate. To compare these two rheological measurements, a benchmark experiment was conducted with a fluid mixture of 0.18 wt. % Xanthan Gum and 0.02 wt. % Guar Guam, to achieve high viscosity at low shear rate. A log plot of viscosity versus shear rate as shown in Figure 43 suggests that the measurements are similar for different viscometers over the point of 1.7 1/s, however, the typical viscometer Ofite 900 cannot measure very low-end or high-end rheology. Similar comparison experiments were also carried out with other low-end rheology viscosifiers, which suggested the Ofite 900 and Haake Mars are in agreement during measurement over a wide shear range applicable to drilling fluids.
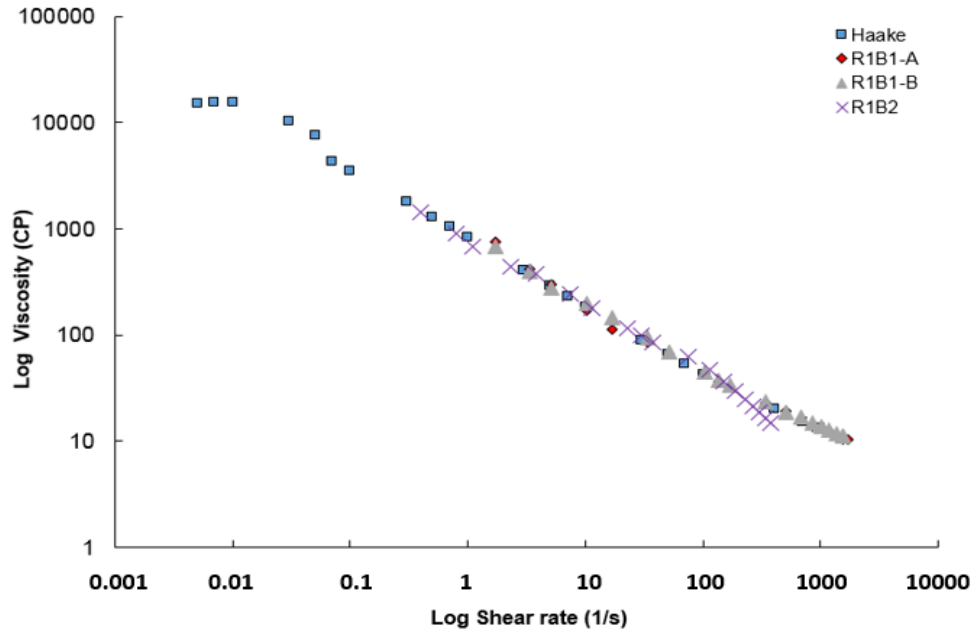
Figure 43: Comparison of rheological measurements with Haake Z20DIN, Ofite R1B1 and R1B2 geometries.

For the rheological measurement of flowing fluid, a straight pipe viscometer is an industrially accepted apparatus. The pressure drop measurements of 6 wt. % bentonite are shown in Figure 44. This measurement was first conducted with 0.5 inch straight pipe viscometer of internal diameter 0.4299 inch. The pressure drop was calculated by comparing the absolute pressure measurements of two 5 bar MRB20 absolute pressure sensors and also directly measured using the 1 bar Keller differential pressure sensor. To determine the rheological parameters and compare with the Ofite 900 viscometer rheological measurements, the wall shear stress and corresponding value of the flow characteristic were calculated. The analysis of the 0.5 inch pipe viscometer data is presented in Table 9.
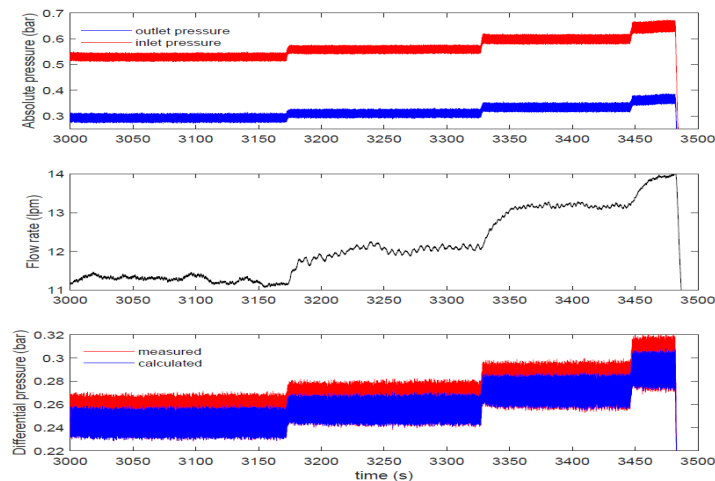
Figure 44: MATLAB interface of pressure drop experiment of 0.5 inch straight pipe viscometer.

Table 9: 0.5 inch straight pipe viscometer data for 6 wt. % bentonite.

Flow Rate Q (Litre/min)	ΔP/L (bar/m) from Keller differential sensor	ΔP/L (bar/m) from MRB20 absolute pressure sensors
4.422	0.052	0.052
4.698	0.054	0.054
5.279	0.050	0.050
5.908	0.056	0.056
6.402	0.058	0.058
6.635	0.056	0.057
7.427	0.060	0.060
7.608	0.063	0.063
8.256	0.067	0.067
8.717	0.068	0.068
9.509	0.072	0.072
10.049	0.075	0.075
10.921	0.079	0.079
11.374	0.081	0.081
12.103	0.084	0.085
13.073	0.090	0.090
14.369	0.096	0.096
15.266	0.102	0.102
15.978	0.116	0.116
16.061	0.115	0.115
16.787	0.144	0.144
17.329	0.161	0.161
17.649	0.170	0.170
18.507	0.186	0.186
18.689	0.191	0.191
19.475	0.204	0.205

The nominal (also often called Newtonian) shear rate can be calculated using the following equation based on dimension of the pipe and flow rate. For example, when Q = 4.422 lpm = $7.385 \times 10^{-5} \text{m}^3/\text{s}$,

$$\dot{\gamma}_w = \frac{8U}{D} = \frac{4Q}{\pi r^3} = \frac{32 \times 7.385 \times 10^{-5}}{\pi \times 0.0109^3} = 578 \text{ 1/s} \qquad (4.1)$$

where $\dot{\gamma}_w$ is the pipe wall shear rate (1/s), U is the mean velocity of bentonite in the pipe (m/s), D is the pipe inner diameter (m), Q is the flow rate (m^3/s) and r is the pipe inner radius (m).

Similarly, the corresponding shear stress at the wall is calculated by

$$\tau_w = \frac{D\Delta P}{4L} = \frac{0.0109}{4} \times 0.052 \times 10^5 = 14.24 \text{ Pa} \qquad (4.2)$$

where τ_w is the shear stress at pipe wall (pa), ΔP is the friction pressure drop (pa/m) and L is the test section length (m).

The calculated rheological results with different flow rate are shown in Table 10,

Table 10: Rheological parameters of 6 wt. % bentonite measured with 0.5 inch straight pipe viscometer.

Flow Rate Q (litre/min)	Pressure Drop (bar/m)	8U/D (1/s)	τ_w (Pa)
4.422	0.052	578	14.24
4.698	0.054	614	14.80
5.279	0.050	690	13.58
5.908	0.056	772	15.33
6.402	0.058	837	15.77
6.635	0.056	867	15.40
7.427	0.060	971	16.47
7.608	0.063	995	17.33
8.256	0.067	1079	18.26
8.717	0.068	1139	18.65
9.509	0.072	1243	19.65
10.049	0.075	1314	20.46
10.921	0.079	1428	21.61
11.374	0.081	1487	22.03
12.103	0.084	1582	23.06
13.073	0.090	1709	24.47
14.369	0.096	1878	26.19
15.266	0.102	1996	27.72
15.978	0.116	2089	31.68
16.061	0.115	2099	31.41
16.787	0.144	2194	39.35
17.329	0.161	2265	43.88
17.649	0.170	2307	46.33
18.507	0.186	2419	50.73
18.689	0.191	2443	52.05
19.475	0.204	2546	55.76

The measurement of fluid rheology is based on the laminar flow regime. Table 10 shows the variation of shear stress at different nominal shear rates, which contains data at both laminar and turbulent regions. The plot of calculated wall shear stress versus 8U/D [Figure 45] shows that the last eight data points appear to be out of laminar flow range. Therefore, they are excluded from the calculations of the rheological parameters.
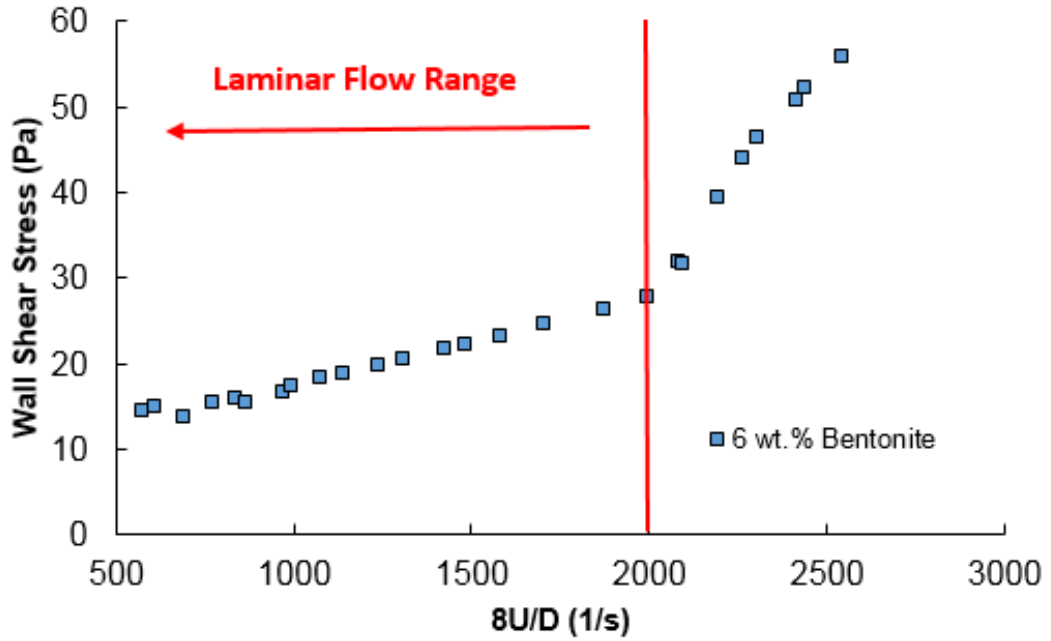
Figure 45: Wall shear stress versus nominal shear rate.

The data points are then presented in a logarithmic plot of wall shear stress versus nominal shear rate to establish a relation between the flow behaviour N and 8U/D . A polynomial trendline is fitted to the data as shown in Figure 46. The flow behaviour $N = 2 \times 0.2715 \ln\left(\frac{8U}{D}\right) - 3.2292$ according to equation (2.4). After obtaining N for different shear rates, the corresponding true wall shear rate $\dot{\gamma}_w$ can be calculated according to equation (2.3), as shown in Table 11. Moreover, the wall shear stress versus nominal shear rate can be plotted and then compared with the Ofite 900 viscometer rheology measurement [Figure 47]. It is important to mention that nominal shear rates are compared with the rotary viscometer measurements, because measurements from the rotary viscometer are recorded at different nominal shear rates.
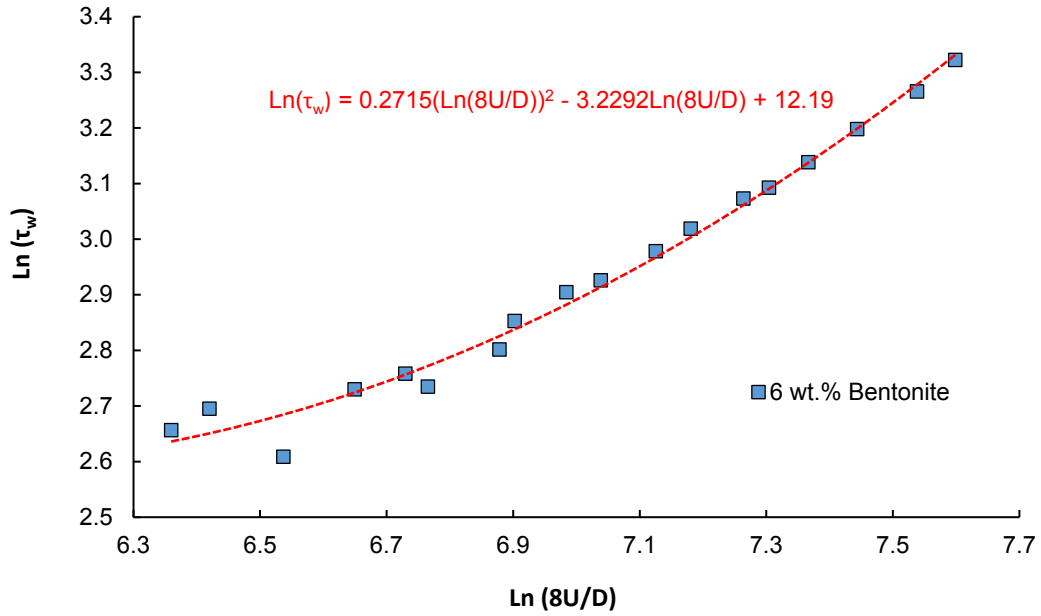
Figure 46: The logarithmic plot of wall shear stress versus nominal shear rate.

Table 11: Calculated rheological parameters of 6 wt. % bentonite measured with 0.5 inch straight pipe viscometer.

Flow Rate Q (litre/min)	Pressure Drop (bar/m)	8U/D (1/s)	τ_w (Pa)	N	$\dot{\gamma}$ (1/s)
4.422	0.052	578	14.24	0.22	1078
4.698	0.054	614	14.80	0.26	1058
5.279	0.050	690	13.58	0.32	1056
5.908	0.056	772	15.33	0.38	1085
6.402	0.058	837	15.77	0.42	1120
6.635	0.056	867	15.40	0.44	1138
7.427	0.060	971	16.47	0.51	1208
7.608	0.063	995	17.33	0.52	1225
8.256	0.067	1079	18.26	0.56	1289
8.717	0.068	1139	18.65	0.59	1335
9.509	0.072	1243	19.65	0.64	1418
10.049	0.075	1314	20.46	0.67	1475
10.921	0.079	1428	21.61	0.72	1570
11.374	0.081	1487	22.03	0.74	1619
12.103	0.084	1582	23.06	0.77	1700
13.073	0.090	1709	24.47	0.81	1807
14.369	0.096	1878	26.19	0.86	1952
15.266	0.102	1996	27.72	0.90	2053
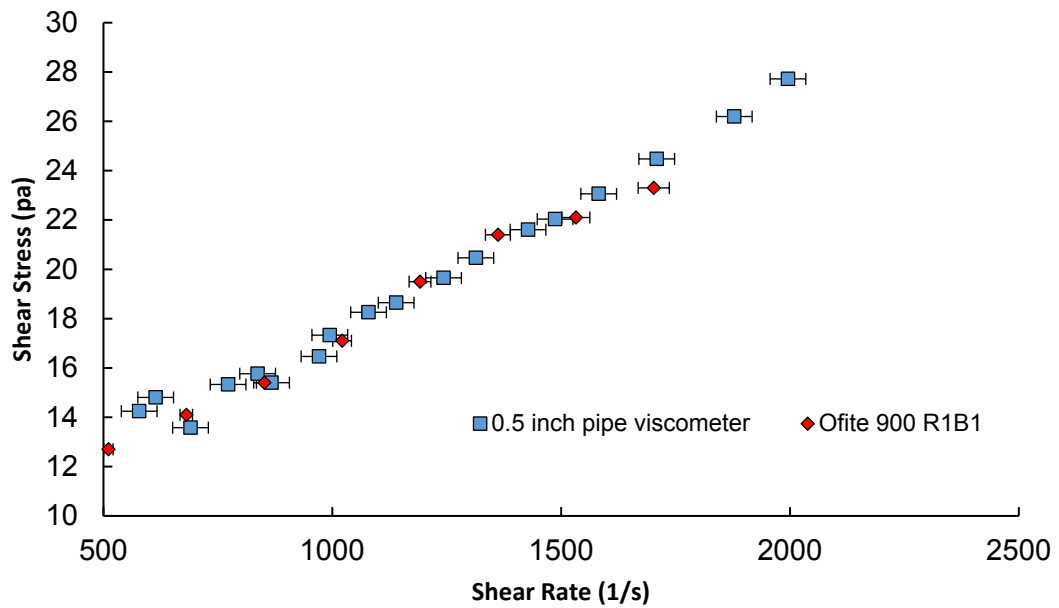
Figure 47: Comparison of 6 wt. % bentonite rheological measurements with 0.5 inch straight pipe viscometer and Ofite 900 viscometer.

In the experiments conducted using the 0.75 inch straight pipe viscometer, the pressure drop measured by the differential pressure sensor and absolute pressure sensors were different. The corresponding N value was different at same flow rate, [Table 12] and [Table 13], which resulted in different wall shear stress at the same nominal shear rate, [Figure 48] and [Figure 49]. An average value of pressure drop calculated, [Table 14] and corresponding plotting of wall shear stress and nominal shear rate obtained.

Table 12: Calculated rheological parameters of 6 wt. % bentonite measured with 0.75 inch straight pipe viscometer (using differential sensor Keller).

Flow Rate Q (litre/min)	Pressure Drop (bar/m)	8U/D (1/s)	τ_w (Pa)	N	$\dot{\gamma}$ (1/s)
4.544	0.018	198	7.19	0.42	265
5.058	0.019	220	7.48	0.43	294
5.407	0.020	236	7.72	0.43	313
5.803	0.020	253	7.90	0.43	335
6.412	0.021	279	8.27	0.44	369
6.761	0.022	295	8.61	0.44	388
7.036	0.023	307	8.89	0.44	404
7.867	0.023	343	9.23	0.45	449
8.576	0.024	374	9.53	0.45	488
9.136	0.025	398	9.83	0.45	519
9.787	0.026	427	10.04	0.45	555
10.277	0.026	448	10.22	0.46	581
11.309	0.027	493	10.70	0.46	638

12.064	0.028	526	11.13	0.46	679
12.087	0.028	527	11.13	0.46	680
13.474	0.030	587	11.63	0.47	755
14.965	0.031	652	12.25	0.47	836
15.693	0.031	684	12.37	0.47	875
16.568	0.033	722	12.82	0.47	922
17.960	0.034	783	13.29	0.48	997
19.239	0.035	838	13.73	0.48	1065
20.780	0.036	906	14.33	0.48	1148
21.687	0.037	945	14.75	0.48	1196
22.781	0.039	993	15.18	0.49	1255
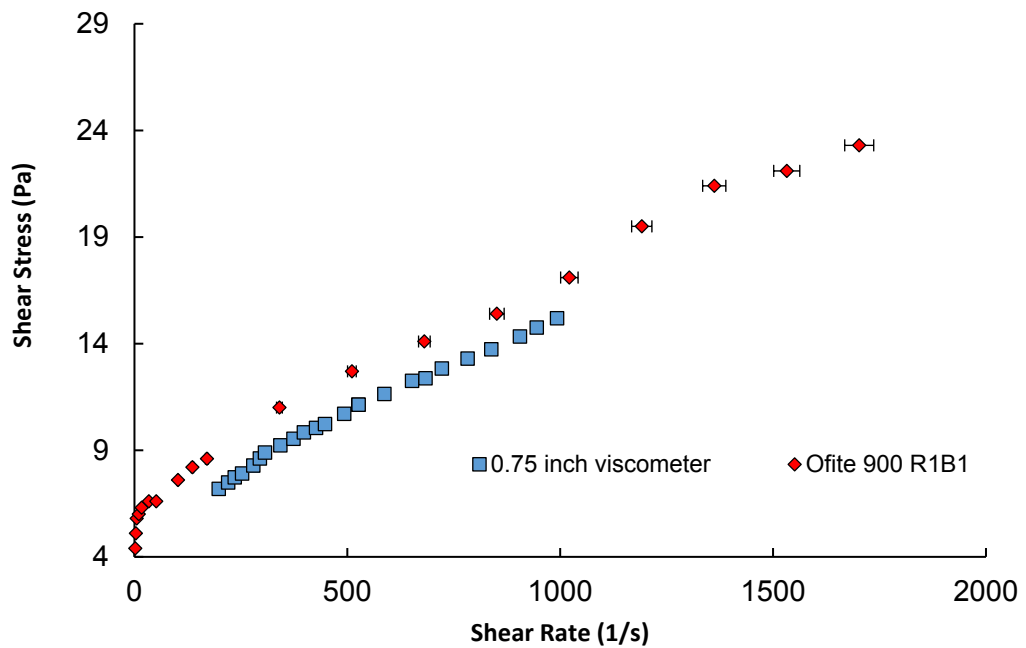
Figure 48: Comparison of 6 wt. % bentonite rheological measurement with 0.75 inch pipe viscometer (using differential sensor Keller) and Ofite viscometer.

Table 13: Calculated rheological parameters of 6 wt. % bentonite measured with 0.75 inch straight pipe viscometer (using absolute sensors MRB20).

Flow Rate Q (litre/min)	Pressure Drop (bar/m)	8U/D (1/s)	τ_w (Pa)	N	$\dot{\gamma}$ (1/s)
4.544	0.029	198	11.51	0.27	333
5.058	0.030	220	11.81	0.28	365
5.407	0.031	236	12.16	0.28	387
5.803	0.031	253	12.34	0.28	412
6.412	0.032	279	12.71	0.29	450
6.761	0.033	295	13.07	0.29	471

7.036	0.034	307	13.25	0.30	488
7.867	0.035	343	13.58	0.30	539
8.576	0.035	374	13.88	0.31	582
9.136	0.036	398	14.22	0.31	616
9.787	0.037	427	14.40	0.32	655
10.277	0.037	448	14.60	0.32	684
11.309	0.039	493	15.16	0.33	745
12.064	0.039	526	15.55	0.33	790
12.087	0.040	527	15.55	0.33	79
13.474	0.041	587	16.05	0.34	873
14.965	0.042	652	16.68	0.35	960
15.693	0.043	684	16.78	0.35	1002
16.568	0.044	722	17.21	0.35	1053
17.960	0.045	783	17.70	0.36	1133
19.239	0.046	838	18.19	0.36	1207
20.780	0.048	906	18.72	0.37	1295
21.687	0.049	945	19.13	0.37	1346
22.781	0.050	993	19.57	0.37	1409
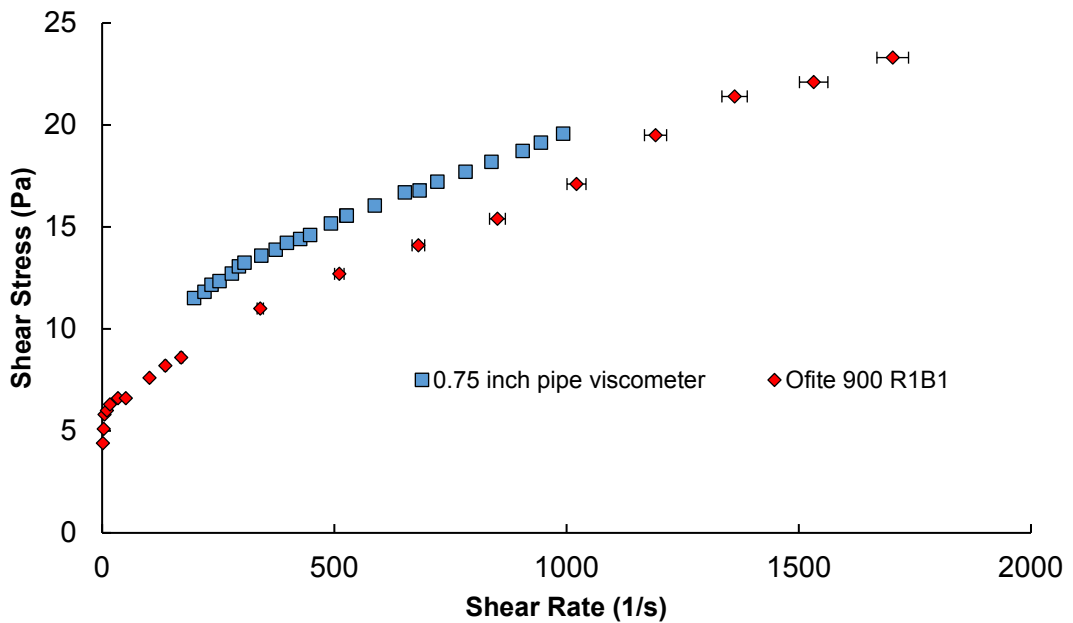
Figure 49: Comparison of 6 wt. % bentonite rheological measurement with 0.75 inch pipe viscometer (using absolute sensors MRB20) and Ofite viscometer.

Table 14: Calculated rheological parameters of 6 wt. % bentonite measured with 0.75 inch straight pipe viscometer (using average pressure drop measured by absolute and differential sensors).

Flow Rate Q (litre/min)	Pressure Drop (bar/m)	8U/D (1/s)	τ_w (Pa)	N	$\dot{\gamma}$ (1/s)
4.544	0.024	198	9.35	0.33	299
5.058	0.025	220	9.65	0.34	330
5.407	0.025	236	9.94	0.34	350

5.803	0.026	253	10.12	0.34	374
6.412	0.027	279	10.49	0.35	410
6.761	0.028	295	10.84	0.35	430
7.036	0.028	307	11.07	0.35	446
7.867	0.029	343	11.41	0.36	494
8.576	0.030	374	11.71	0.37	535
9.136	0.031	398	12.02	0.37	568
9.787	0.031	427	12.22	0.37	605
10.277	0.032	448	12.41	0.38	633
11.309	0.033	493	12.93	0.38	692
12.064	0.034	526	13.34	0.39	734
12.087	0.034	527	13.34	0.39	736
13.474	0.035	587	13.84	0.39	814
14.965	0.037	652	14.47	0.40	898
15.693	0.037	684	14.57	0.40	938
16.568	0.038	722	15.02	0.41	987
17.960	0.039	783	15.50	0.41	1064
19.239	0.041	838	15.96	0.41	1135
20.780	0.042	906	16.53	0.42	1220
21.687	0.043	945	16.94	0.42	1270
22.781	0.044	993	17.38	0.42	1330

Figure 50 shows the rheological measurement of a 6 wt. % bentonite solution using the 0.5 inch, the 0.75 inch straight pipe viscometers and the Ofite 900 viscometer. It can be seen that the calculated shear stress of the 0.5 inch and 0.75 inch pipe viscometers at different shear rate are quite similar to rotary measurement readings. It is observed that the 0.5 inch capillary viscometer can measure the rheology of test fluids at high-end shear rate greater than 2000 1/s compared with the Ofite viscometer.
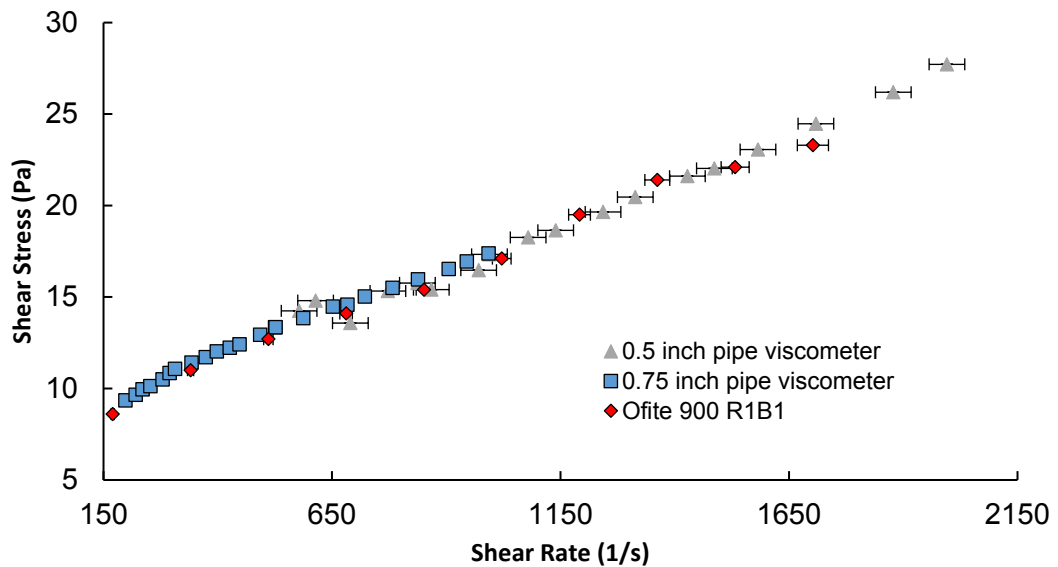
Figure 50: Comparison of 6 wt. % bentonite rheological measurement with 0.5 inch, 0.75 inch pipe viscometer and Ofite 900 viscometer.

Figure 51, similarly, shows the rheological measurement of a 6 wt. % bentonite solution to compare a 1 inch straight pipe viscometer to the Ofite 900. It illustrates that the measurements between the two viscometers are different This is attributed to small values of pressure drop within the test section of the 1 inch pipe, which leads to inaccurate measurement of shear stress.
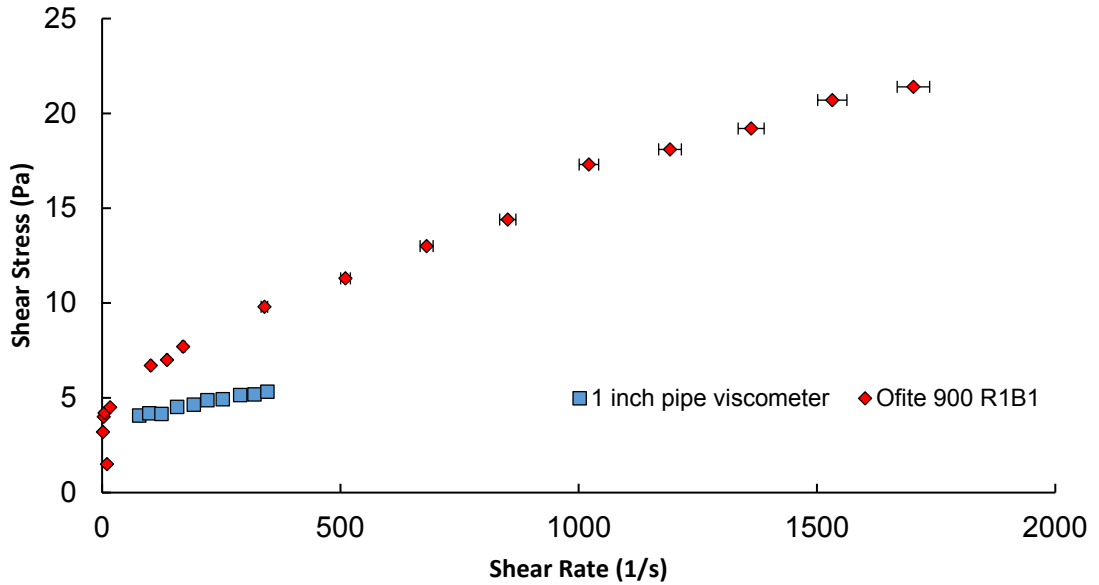
Figure 51: Comparison of 6 wt. % bentonite rheological measurement with 1 inch pipe viscometer and Ofite 900 viscometer.

A hydraulic experiment was conducted to predict the friction loss of bentonite flowing along the 0.5 inch straight pipe. The rheological data and density of 6 wt. % bentonite were measured by the Ofite 900 viscometer and mud balance under controlled temperature for the pressure drop prediction. The full rheology measurement of the test sample is presented in [Figure 52]. The density of test fluid is 1060kg/m^3. Three rheological models are chosen for the regression of 6 wt. % bentonite full measurement including the Bingham Plastic, Power-Law and H-B models from [Table 2]. The corresponding rheological parameters are calculated and shown in [Table 15]. Extensive model evaluation from Figure 34 to 36 was conducted to predict the pressure drop of bentonite flowing along the 0.5 inch straight pipe viscometer, as detailed in [Table 16]. The experimental flow rates of laminar flow condition began from 4.422 lpm to 15.266 lpm, as shown in the plot of pressure drop versus flow rate, in [Figure 53].
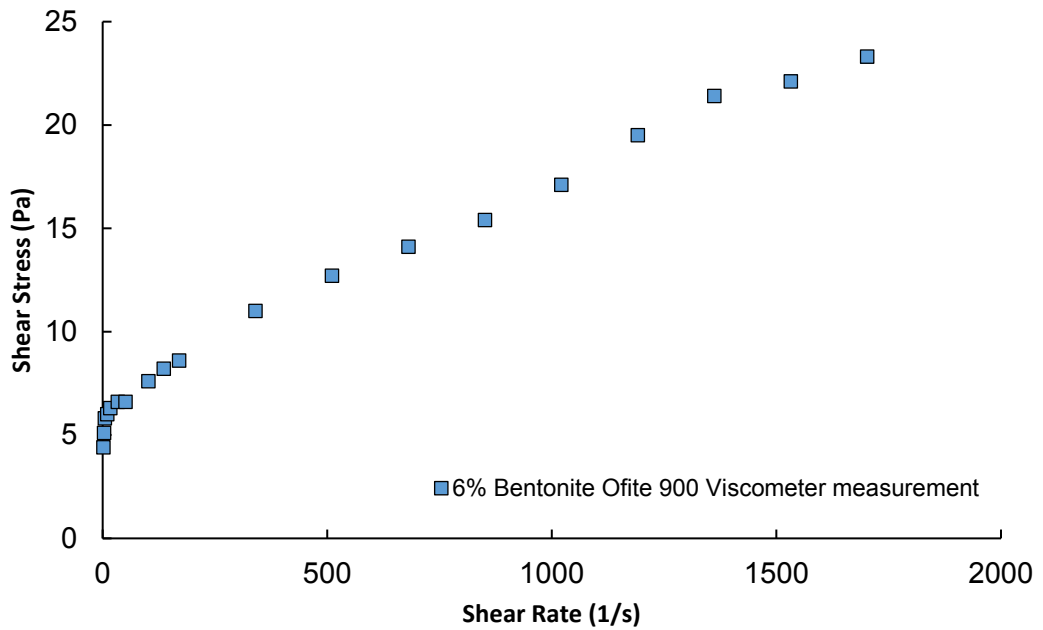
Figure 52: Full rheological measurement of 6 wt. % bentonite using Ofite 900 viscometer.

Table 15: Rheological constants of 6 wt. % bentonite for 0.5 inch pipe viscometer.

Pipe Viscometer	Bingham Plastic	Power Law	Herschel-Bulkley
0.5 inch	$\tau = 6.16$ Pa $\mu_p = 0.0108$ Pa	K=3.3205 N=0.2303	$\tau = 4.355$ Pa K=3.3205 N=0.2303

Table 16: Calculation of pressure drop of 6 wt. % bentonite in laminar flow condition measuring with 0.5 inch pipe viscometer.

Flow Rate Q (litre/min)	Measured DP (bar/m)	Predicted DP (bar/m)		
		Bingham Plastic	Power Law	Herschel - Bulkley
4.422	0.052	0.053	0.097	0.059
4.698	0.054	0.054	0.098	0.061
5.279	0.050	0.057	0.101	0.064
5.908	0.056	0.061	0.103	0.067
6.402	0.058	0.063	0.105	0.069
6.635	0.056	0.064	0.106	0.071
7.427	0.060	0.068	0.109	0.074
7.608	0.063	0.069	0.109	0.075
8.256	0.067	0.073	0.112	0.078
8.717	0.068	0.075	0.113	0.080
9.509	0.072	0.079	0.115	0.083

10.049	0.075	0.082	0.117	0.085
10.921	0.079	0.087	0.119	0.088
11.374	0.081	0.089	0.120	0.090
12.103	0.084	0.093	0.122	0.093
13.073	0.090	0.098	0.124	0.096
14.369	0.096	0.104	0.127	0.100
15.266	0.102	0.109	0.128	0.103
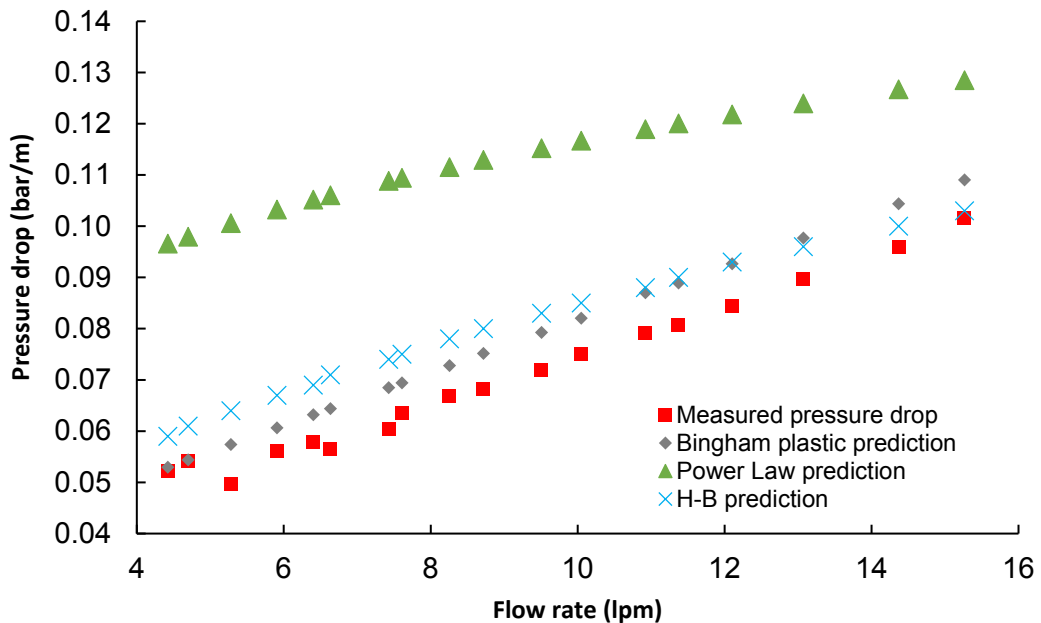
Figure 53: Pressure loss predictions of three different rheological models.

It can be seen from Figure 53 that the Power Law model prediction produces a poor estimation of pressure drop at different flow rates. The friction loss prediction of 6 wt. % bentonite using the Bingham plastic and Herschel-Bulkley models are considerably closer to the measured pressure drop. It should be noted that the conventional approach of pressure drop prediction is based on the rheological constants. The particular choice of the rheological constants of rheological models when data fitting, could affect the determination of friction loss of the test fluid flowing in hydraulic circuits. It is noteworthy that rheological parameters at different ranges of shear rate also result in different rheological constants. To increase the accuracy of pressure drop prediction, the rheological model parameters are required to be determined over the shear rate range in which the pressure drop is determined.

It is also possible to use pipe viscometer data to calculate the pressure drop directly. This can be performed using the relationship between shear stress and shear rate, as given in equations (2.5) and (2.7). For a given flow rate, the nominal shear rate can be determined, and

corresponding shear stress can be obtained from the rheology measurement. The corresponding shear stress is then used to calculate the pressure drop based on the dimension of the conduit.

4.2. Synergetic interaction

Figure 54 shows a log-log plot of viscosity versus shear rate for four different viscosifiers. It shows that all viscosifiers exhibit shear thinning behaviour. At high shear rate, all viscosifiers show similar values for viscosity. The results show that the mixture with 0.2 wt. % Xanthan Gum and 0.2 wt. % Corewell gives highest viscosity for shear rates less than 1 1/s. However, its viscosity drops sharply with the increasing of shear rate, which has been evidenced by the major role of Xanthan Gum as a low-end rheology viscosifier. Poor low-end rheological measurements of Guar Guam and Pac-R were obtained, with decreasing viscosities with increasing shear rate.
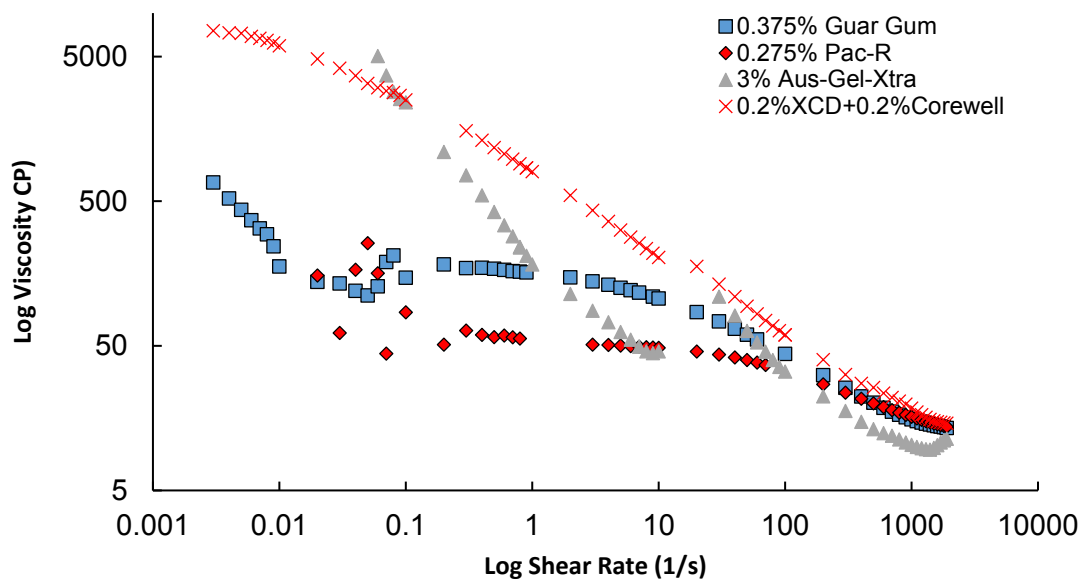
Figure 54: Rheological measurement of viscosifiers from 0 1/s to 1900 1/s.

4.2.1. Development of Ctrol^{TM} and CTrolX^{TM}

The study of synergetic properties between mixed viscosifers was of great interest for this research. Different combinations of additives were used for experiments to develop the preventative drilling fluid Ctrol^{TM} and the remedial drilling fluid CTrolX^{TM} for field application. These two products were developed with the support of this thesis, and are commercialised as two trademarks. Both additives are produced at commercial scale and tested in number of drilling operations in Australia and US.

As commercialisation and intellectual property restriction, generic names of chemical additives were used.

Several sets of experiments were performed to find the optimum concentration of each polymer to yield maximum shear thinning behaviour, for Ctrol^{TM} and CTrolX^{TM}. Figure 55 shows the viscosity versus shear rate, measured using the Haake Mars viscometer, for each formulation. It can be seen from Figure 55, that the changing of weight concentration (from Concentration 1 to 2) of CTrolX^{TM} results in different low-shear-rate viscosity. Additive 2 has no effect to enhance the low-end rheology while Additive 4 can improve the low-shear-rate viscosity to some extent with different weight concentration. T6 reflects the optimal combinations for CTrolX^{TM} which exhibits high viscosity at low shear rate.
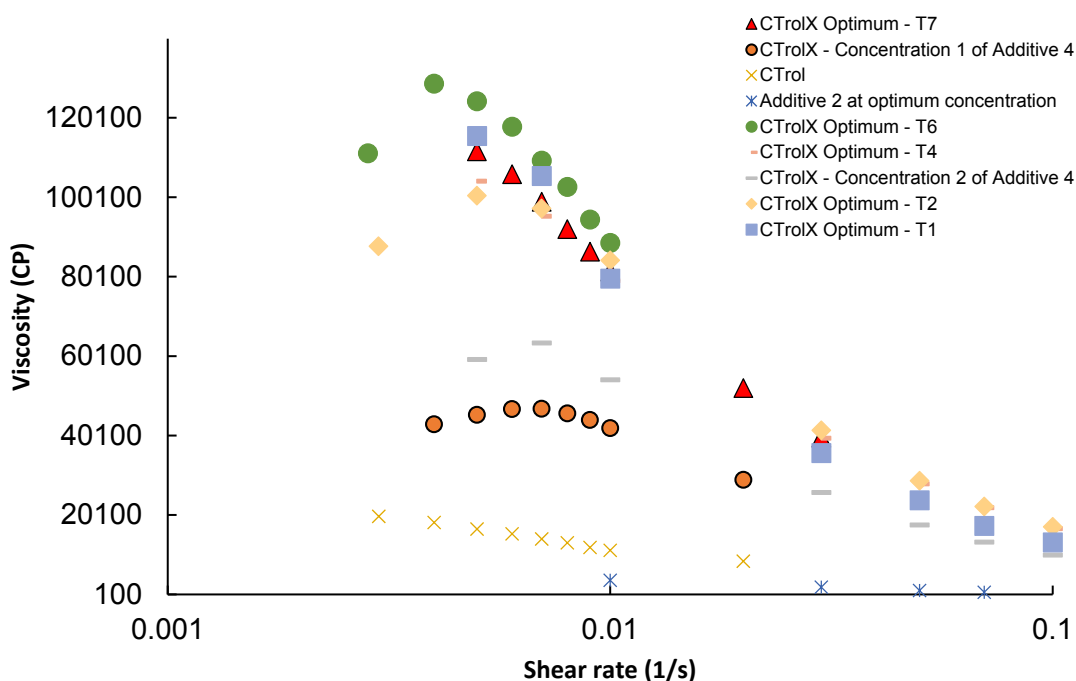
Figure 55: Results of changing weight concentrations of additives for development of CTrolX^{TM}.

Since the Haake rheological measurement is sensitive to the shear rate below 0.01 1/s, experiments were performed a number of times to ensure repeatability of results, Figure 56. The graph shows that Ctrol^{TM} has very high low-end viscosity at shear rate below 0.01 1/s and decreases sharply with the increasing of shear rate.
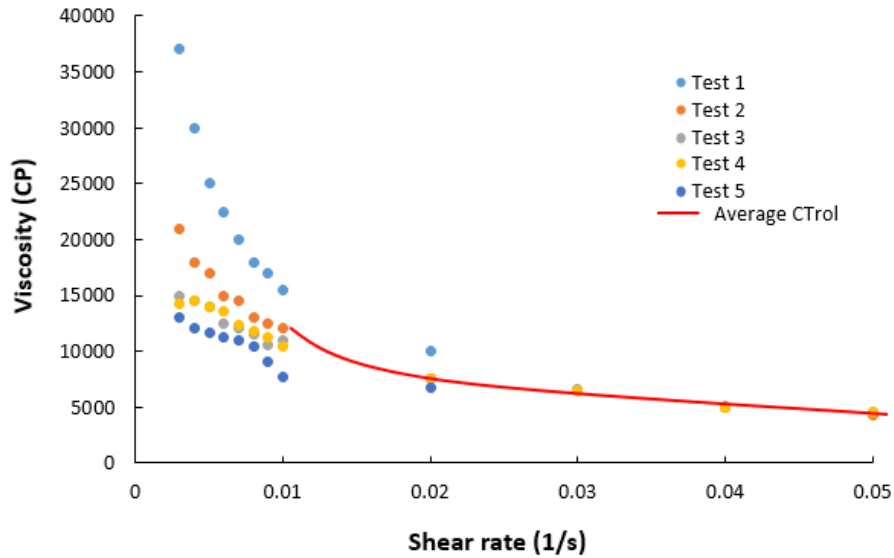
Figure 56: Repeatability of Ctrol™ measurements.

4.2.2. Field application of Ctrol™ and CTrolX™

These experiments are performed by Drilling Mechanics Group researchers for benchmarking Ctrol™ with other commercial fluids and also using Ctrol™ in the field for two Coiled Tubing drilling operations using RoXplorer drilling rig in Victoria Australia [Figure 57].

In the coiled tube drilling trial, the RoXplorer was a revolutionary drill rig for mineral exploration that utilises continuous steel coil. The downhole mud motor systems of RoXplorer, made of a positive displacement motor and a downhole hammer, were connected to 500 meters of coiled tube. The downhole motors received hydraulic energy from the drilling mud to deliver rotary and reciprocating movements to the percussive bit. This coiled tubing drilling allowed for continuous drilling and pumping and increased the rate of penetration, making drilling faster, cheaper and safer than conventional drilling.

Figure 57: Coiled tube drilling system, RoXplorer, used in the drilling trials in Australia - courtesy DET CRC.

The benchmark experiments in the field were performed to compare the efficiency of Ctrol[TM] and CtrolX[TM] with two commercial drilling fluid systems. After each experiment, water was circulated to return fluid loss level to the initial value before testing the new drilling fluid. Figure 58 shows the fluid loss variation with flow rate, for Ctrol[TM], CtrolX[TM] and two commercial polymers. Figure 59 shows flow return after Ctrol[TM] invasion into unconsolidated formations. It can be seen from these figures that Ctrol[TM] and CtrolX[TM] established significant flow return comparing with two other commercial drilling fluid systems.
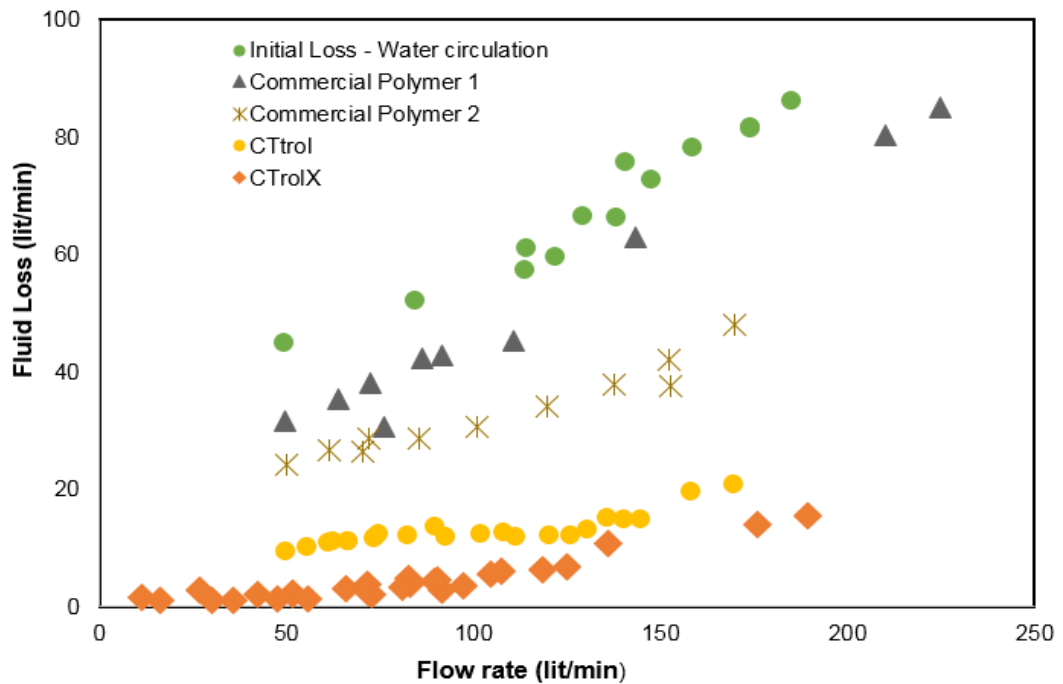

Figure 58: The benchmark of Ctrol[TM] and CTrolX[TM] in the field (Mostofi and Samani 2017).
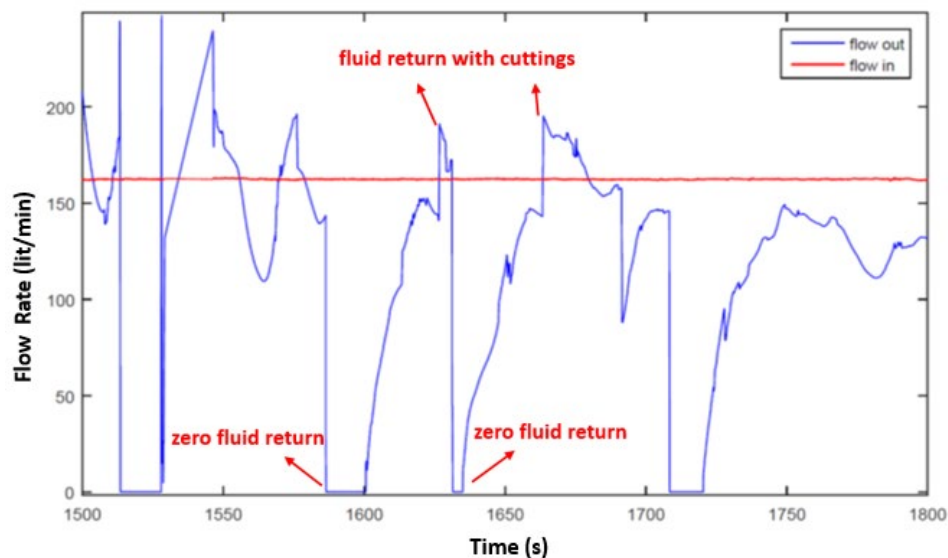

Figure 59: Establishing return after Ctrol[TM] invasion into unconsolidated formations. The data collected from the RoXplorer field trial in Victoria. (Mostofi and Samani 2018).

4.3. Particle effect on rheology

In the following section, the effects of solids concentration and size on the viscosity of suspensions are presented. The experiments were designed to investigate the effect of solid particles on polymer viscosity at different shear rates and also the change in thixotropic property.

As previous literature suggested that the cuttings settling velocity in suspension decreases significantly with increasing of the particle volume concentration whilst increasing with increase in particle size [45], thus, a Haake step-wise experiment was designed to verify this using the Haake viscomter with a suspension of 0.5 wt. % Xanthan Gum with 0.3 vol. % silica sand, at a size range of 250-300 micron. The shear rate was ramped up from zero shear rate to 1900 1/s and then ramped down from 1900 1/s to zero shear rate. Figure 60 shows the plot of shear rate versus time for ramp-up and ramp-down. The measured viscosity at shear rates of 100 1/s and 1000 1/s for ramp-up and ramp-down are denoted on the Figure 60 as points A, D and points B, C respectively. It can been seen that the difference in viscosity at each shear rate, between ramp-up and ramp-down are minimum. This suggests no significant effect of sedimentation on the experiment of viscosity.
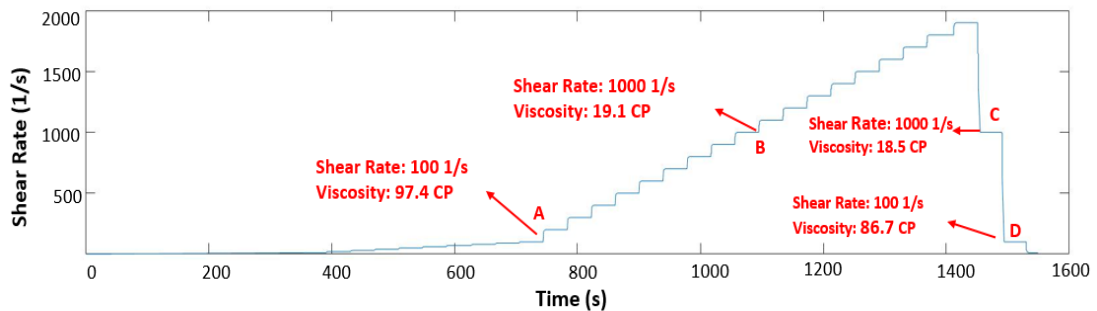
Figure 60: Haake step-wise measurement of suspension with 0.3 vol. % sand at size range of 250-300 micron.

The effect of solid volume concentration on the rheology of suspensions are shown in Figure 61 to Figure 64. Here, suspensions of silica sand of different size distributions (106-200,200-250 and 250-300 μm) and volume concentrations (0.3-3.0%), and 38-75 μm Calcium Carbonate particles with different volume concentrations (0.3-3.0%) were used to measure viscosity versus shear rate, using the Haake Mars Z20DIN viscometer and the blank fluid 0.5wt. % Xanthan Gum.
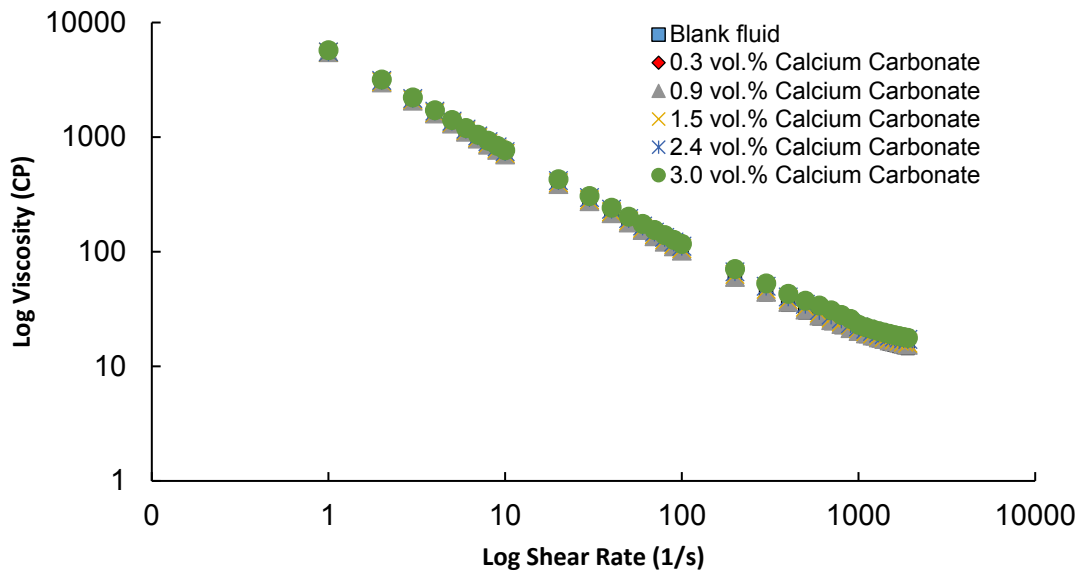
Figure 61: Comparison of viscosity of suspension with 38-75 micron CaCO$_3$ at different volume concentration.
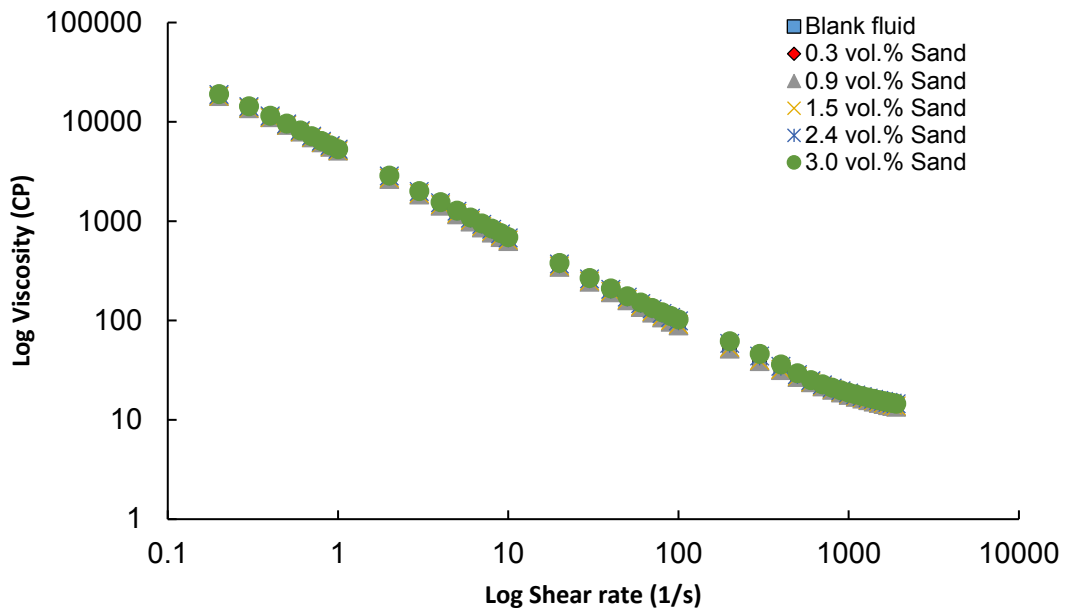
Figure 62: Comparison of viscosity of suspension with 106-200 micron silica sand at different volume concentration.
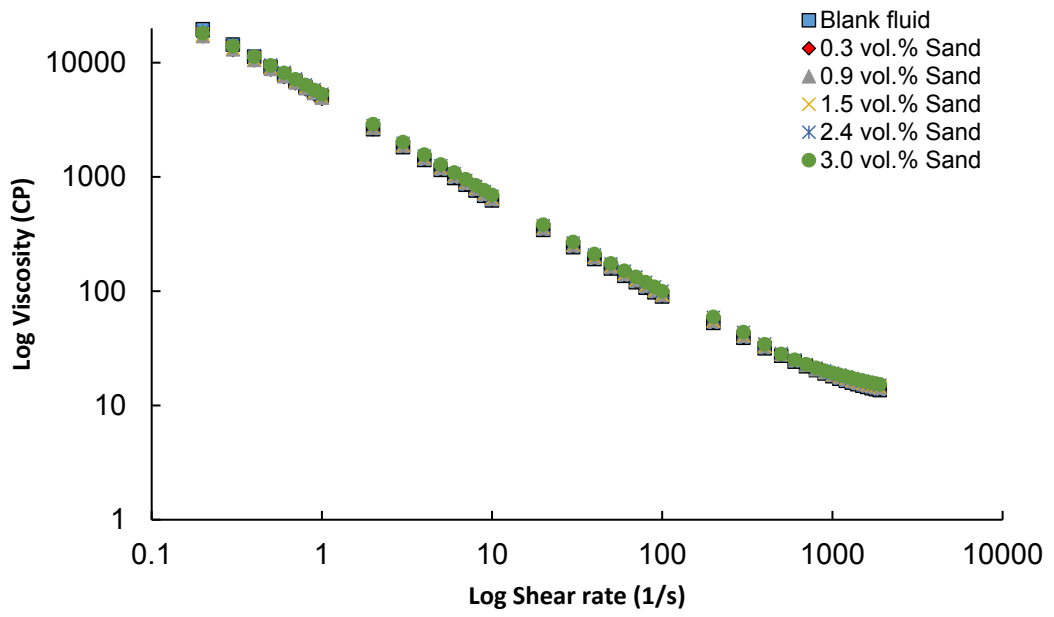
Figure 63: Comparison of viscosity of suspension with 200-250 micron silica sand at different volume concentration.
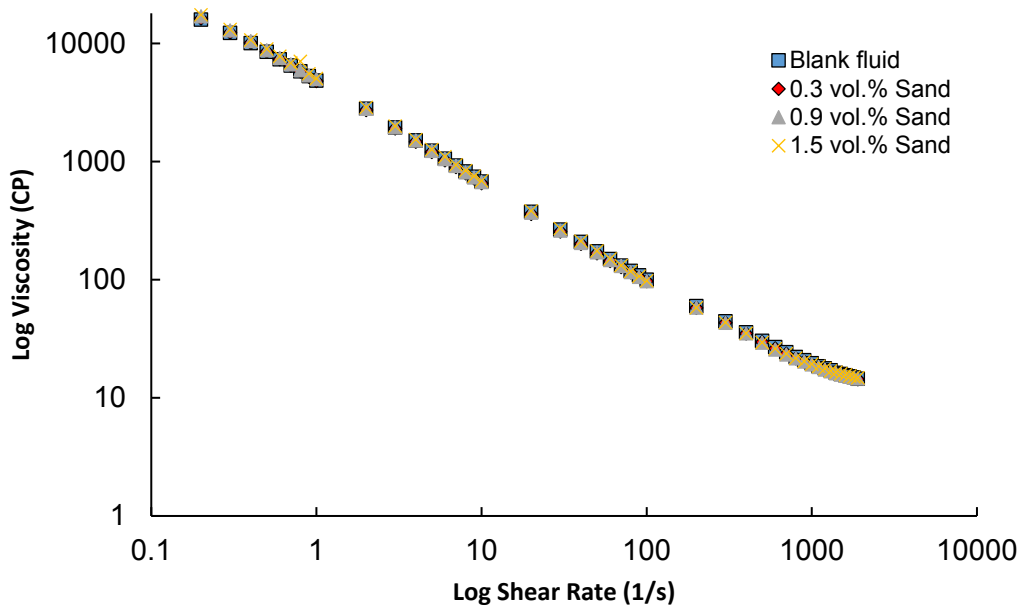
Figure 64: Comparison of viscosity of suspension with 250-300 micron silica sand at different volume concentration.

The data in Figure 61 - Figure 64 suggests that there is a minimum change in the viscosity of suspensions solutions as compared with the blank solution, for the suspensions used in the experiments. To better characterise the effect of solid particles on the fluid rheology, the relative viscosity η_r is obtained for each suspension solution, defined as:

$$\eta_r = \frac{\eta_s}{\eta_b} \tag{4.3}$$

where η_s is the suspension viscosity and η_b is the blank fluid viscosity, which is the viscosity of the suspending fluid without solid particles. The effect of solid particles on the fluid can be reflected in the magnitude of relative viscosity.
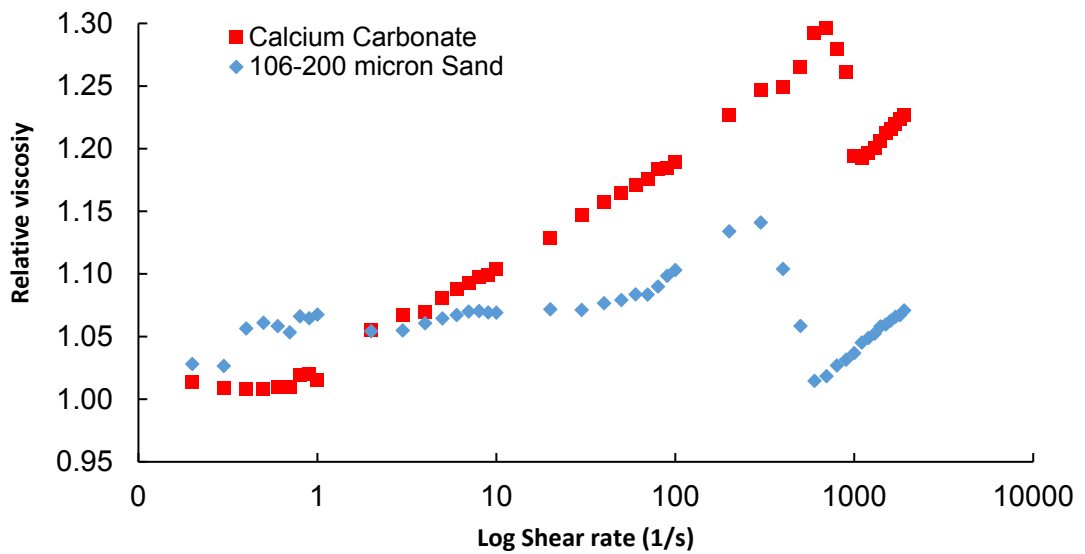

Figure 65: Relative viscosity of suspensions with 3.0 vol. % particles at shear rate from 0 to 1900 1/s.

Figure 65 shows that the relative viscosity seems to be smaller at lower shear rates, and increases gradually with shear rate. As shown in the graph, the relative viscosity of Calcium Carbonate solution at low shear rate as low as 1.01, and increases gradually reaching a maximal relative viscosity of 1.3 at approximately 700 1/s shear rate. A similar trend can be observed for the suspension with silica sand. One possible explanation for this trend is that particles can form aggregates at low shear condition, and therefore shear will produce less interaction between aggregated cuttings. However, the established network breaks at medium or high shear rates (greater than 700 1/s), and the interaction of particles increases rapidly, and as a result the suspension viscosity increases.

4.3.1. Effect of solid particle size

As the experimental results above suggest that the size distribution of particles will affect the viscosity of suspension solutions, the relative viscosity versus shear rate was plotted for different volume concentration suspensions [Figure 66 and Figure 67]. Here the results of suspensions with 0.3 vol. % [Figure 66] and 1.5 vol. % [Figure 67] of sand and Calcium Carbonate are considered. The figures show that Calcium Carbonate, which has the smallest particle size distribution of 38-75 μm, has higher relative viscosity at medium to high shear rates starting from 10 1/s for 0.3 vol. % solution and 30 1/s for 1.5 vol. % solution.

In the region of low shear rate (below 1 1/s), the effect of size of particles on the suspension viscosity is noticeable but the measurements do not show a particular trend. For example the highest relative viscosity is exhibited by 250-300 micron sand size at volume fraction of 0.3 vol. % [Figure 66] while 106-200 micron sand has higher relative viscosity at volume fraction of 1.5 vol. % [Figure 67].

For the medium to high shear range, while the small particle size solution (38-75 micron calcium carbonate) exhibits higher relative viscosity, the other two sand solutions do not follow a specific trend. The 200-250 micron size has higher relative viscosity than 250-300 micron size at 0.3 vol. % volume concentration [Figure 66], however, it exhibits a lower relative viscosity compared with 106-200 micron sand at 1.5 vol. % volume concentration [Figure 67]. This inconsistency could be potentially attributed to the fact that the sizes of silica sand used in the experiments are relatively close, and therefore, the effect of size could not be captured from these experiments.

Further experiments can be performed to understand the effect of size on suspension using much wider size range of solid particles. In this case, it would be required to use a different viscosity measurement technique, as the Haake sensor dimensions limits the range of solid particles that can be tested.
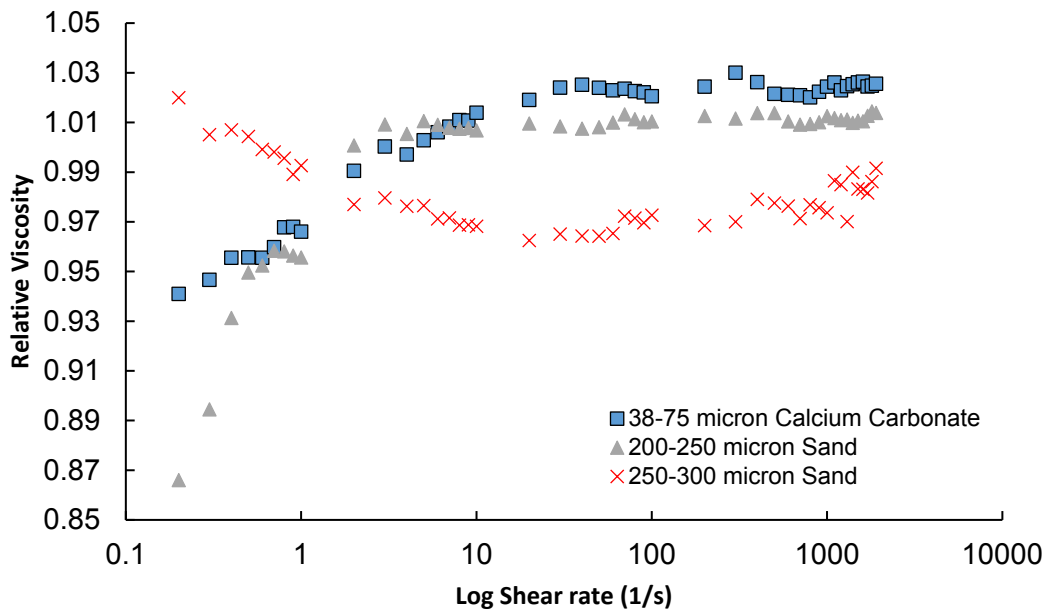
Figure 66: Relative viscosity of suspensions with 0.3 vol. % particles at shear rate from 0 to 2000 1/s.
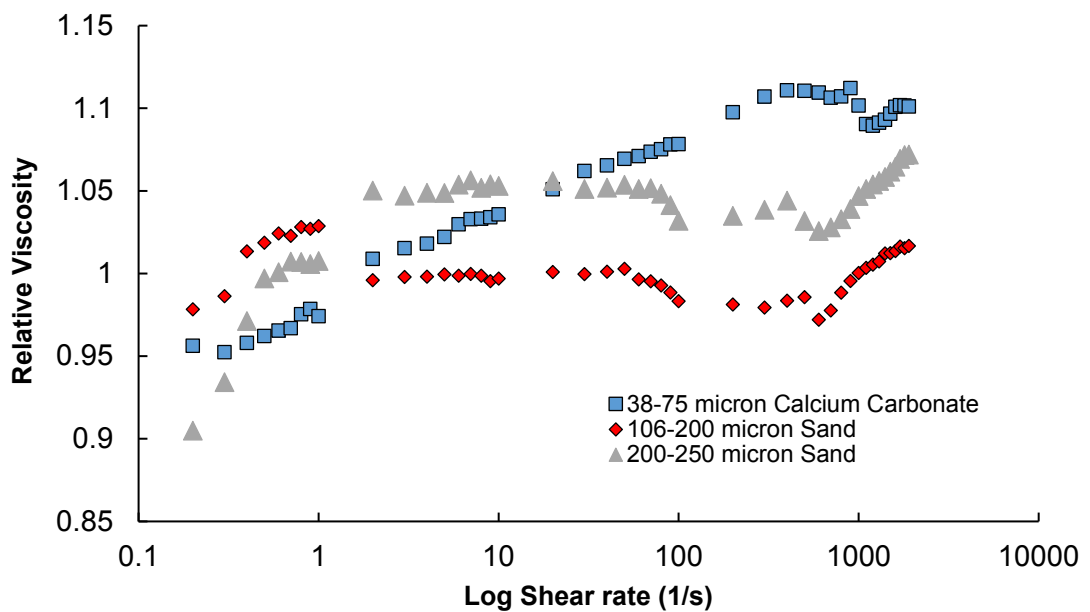
Figure 67: Relative viscosity of suspensions with 1.5 vol. % particles at shear rate from 0 to 2000 1/s.

The extent of thixotropic behaviour was studied using loop tests, and comparing the relationship of shear stress and shear rate in upward and downward shear rate curves. One way to quantify the extent of the thixotropic behaviour is to calculate the area confined in the loop curve. Figure 68 is a plot of shear stress versus shear rate for a 0.5 wt. % Xanthan Gum suspension fluid containing 2.4 vol. % 250-300 μm silica sand particles, and Figure 69 is for

106-200 μm silica sand particles. The hysteresis area restricted between the ascending and descending curves reflects the thixotropic behaviour of the suspension fluid. A polynomial curve fit was applied to calculate loop area. For the calculation of this hysteresis area, Figure 68 shows the area under the ascending curve is 30229Pa/s while the area under descending curve is 29276Pa/s, yielding a hysteresis area of 953Pa/s.
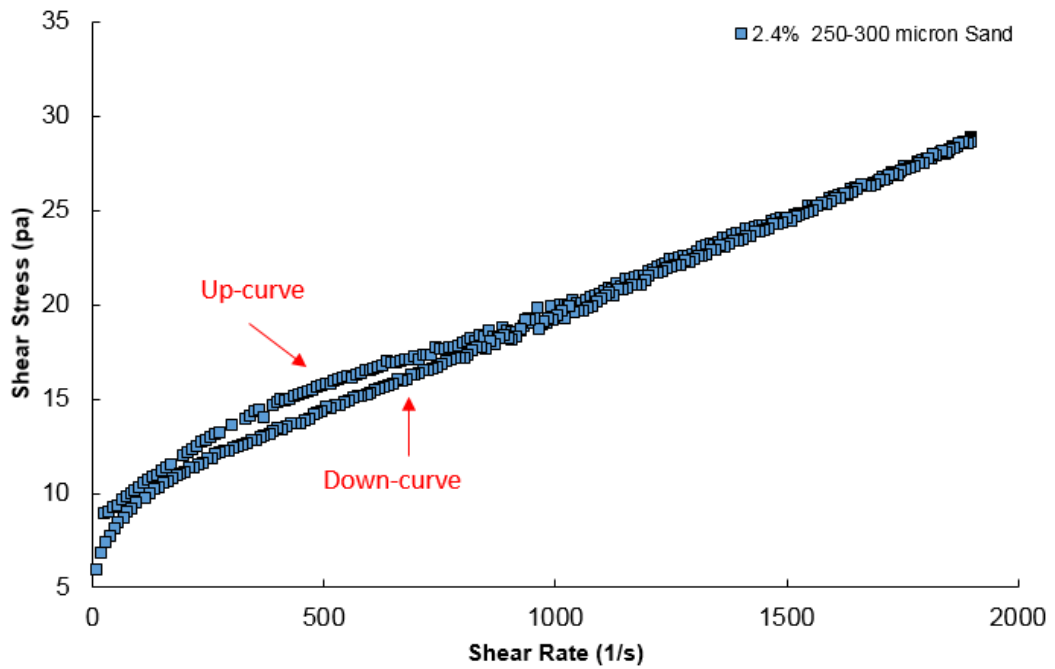
Figure 68: Thixotropic loop test of suspension with 2.4 vol. % 250-300 micron silica sand.
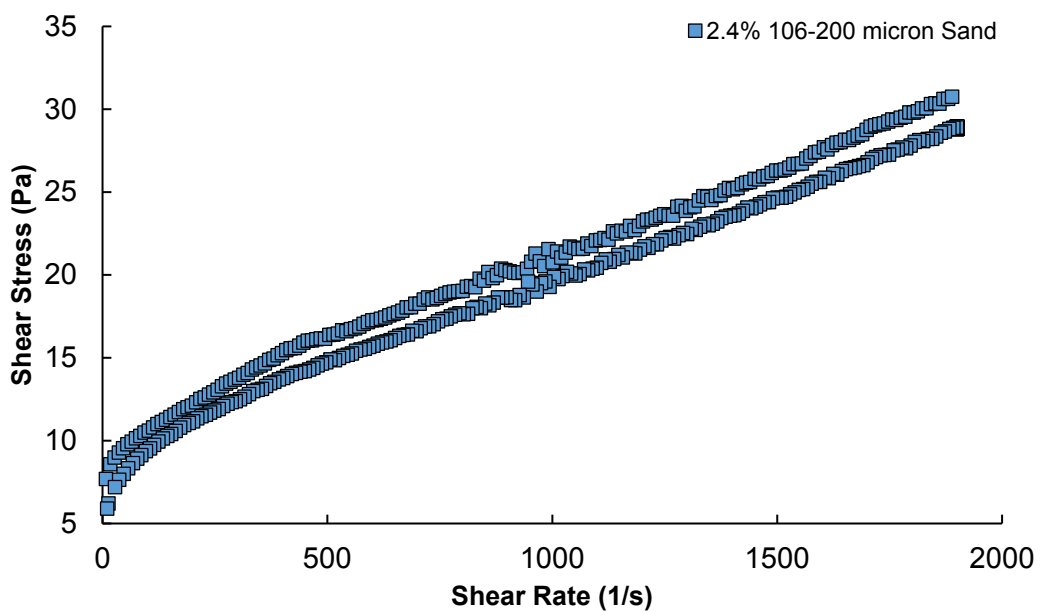
Figure 69: Thixotropic loop of suspension with 2.4 vol. % 106-200 micron silica sand.

The calculated area of loop tests with 2.4 vol. % of different particle sizes are shown in Table 17.

Table 17: Thixotropic loop tests of 2.4 vol. % of CaCO₃ and silica sand suspensions with different particles sizes.

Particle	Particle Size (microns)	Solids Concentration (vol. %)	Hysteresis Area Value
Calcium Carbonate	38-75		14
Silica Sand	106-200	2.4	2666
	200-250		367
	250-300		953

Based on Table 17, and the loop area shown in Figure 68 and Figure 69, it can be concluded that the presence of cutting increases thixotropic behaviour, however, the extent is not correlated with the size of particles. It is worth mentioning that more consistent results could be obtained by repeating the experiments using different measurement gap-times.

4.3.2. Effect of solid particle concentration

In order to better demonstrate the effect of solid concentrations, the viscosity of suspensions with Calcium Carbonate and silica sand are considered. The plot of relative viscosity at different concentrations of particles is plotted for shear rates of 0 to 1 1/s and 100 to 1900 1/s .The relation between solid volume concentration and relative viscosity is shown in Figure 70 to Figure 73. The experimental data in the figure suggests that the relative viscosity increases with increase in volume concentration of solid particles.

Figure 70 to Figure 73 show the relation between the volume concentrations of Calcium Carbonate/fine sand particles and the relative viscosity of suspensions from low-end to high end rheology. For suspensions with the same particle size, the relative viscosity of suspensions increases with increasing particle volume concentrations at the same shear rate. This trend is more obvious for particles with volume concentrations greater than 2.4 vol. % at low-end rheology (shear rate less than 1 1/s). One possible explanation is that the increase in particle concentration enhances particle-particle interactions. The inner particle force of fine cuttings dominates at low shear rates which giving a large increase in viscosity. Furthermore, from medium to high shear rate starting from 100 1/s, the gradient of curve is almost constant, indicating that the relative viscosities of different calcium carbonate suspensions have no significant change with the increasing shear rates in this range.
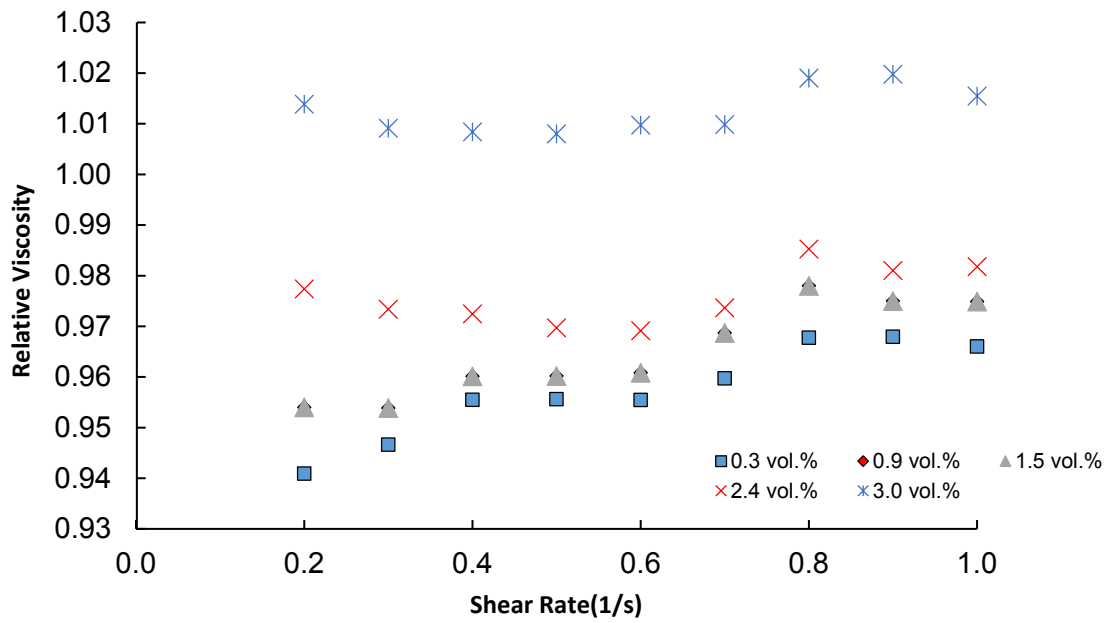
Figure 70: Relative viscosity of CaCO$_3$ suspensions with different volume concentration at shear rate from 0 to 1 1/s.
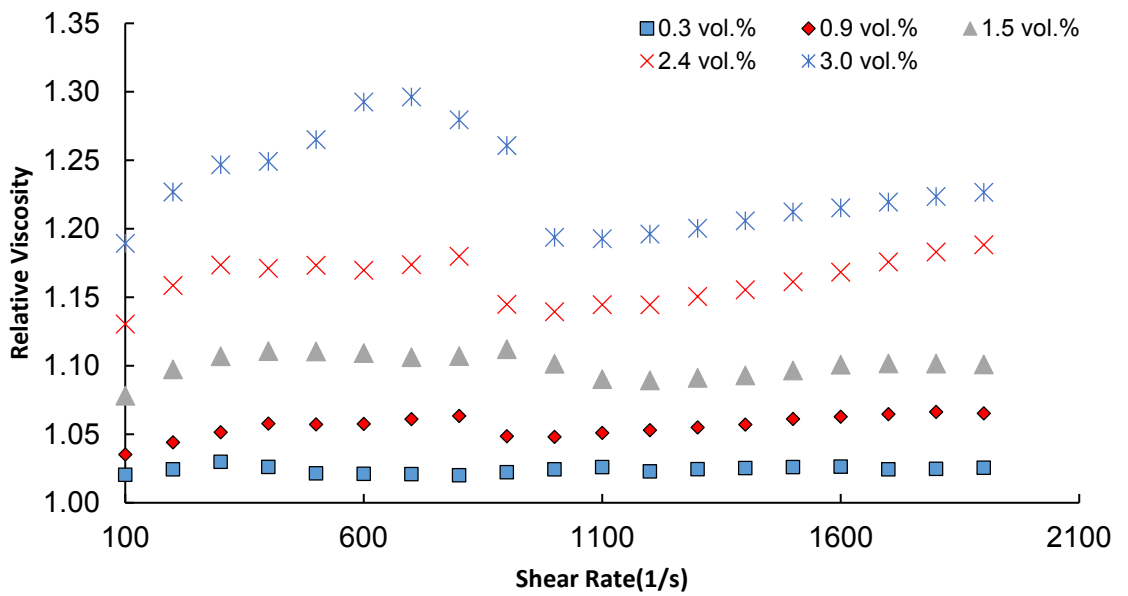
Figure 71: Relative viscosity of CaCO$_3$ suspensions with different volume concentration at shear rate from 100 to 1900 1/s.
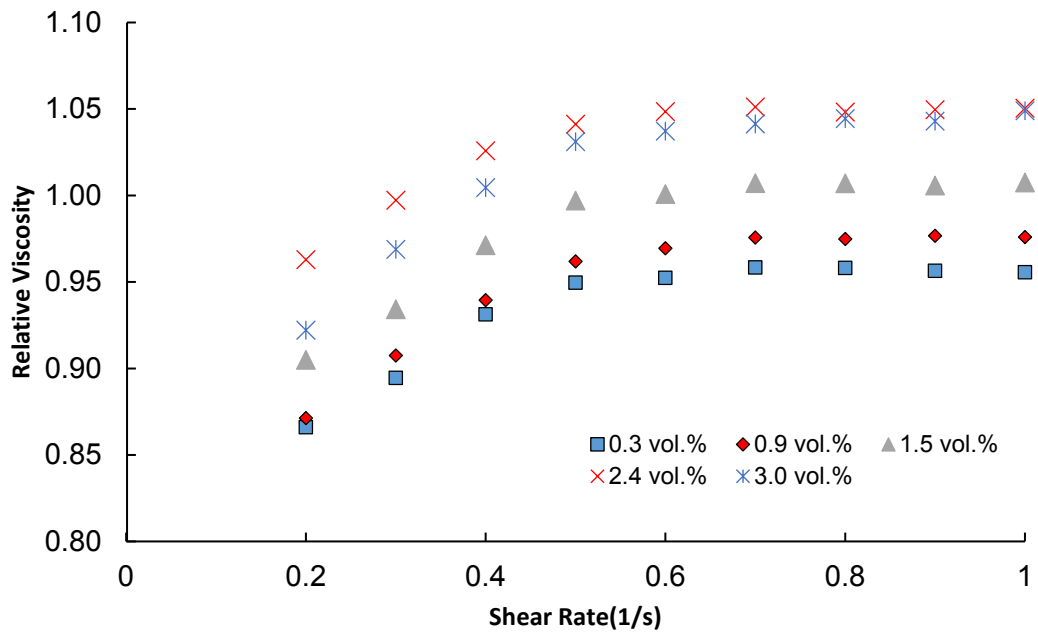
Figure 72: Relative viscosity of 200-250 micron sand suspensions with different volume concentration at shear rate from 0 to 1 1/s.
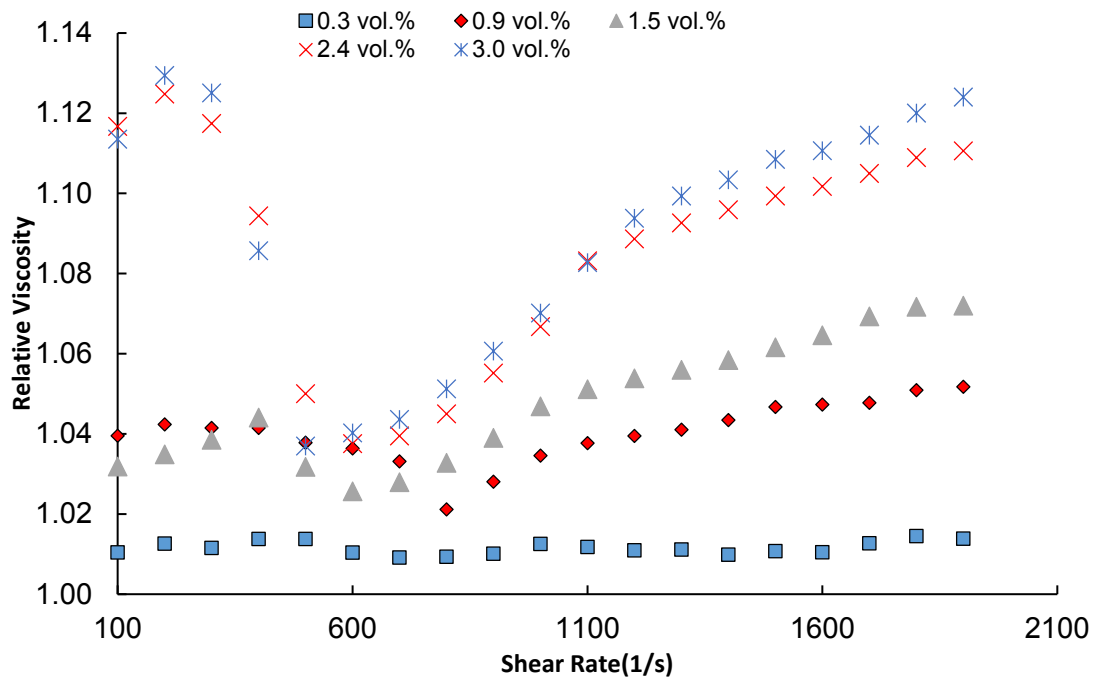
Figure 73: Relative viscosity of 200-250 micron sand suspensions with different volume concentration at shear rate from 100 to 1900 1/s.

In Figure 74, the variation of relative viscosity with different concentration at specific shear rate is illustrated. The data suggests that the relative viscosity increases with increasing volume concentration of solid particles.
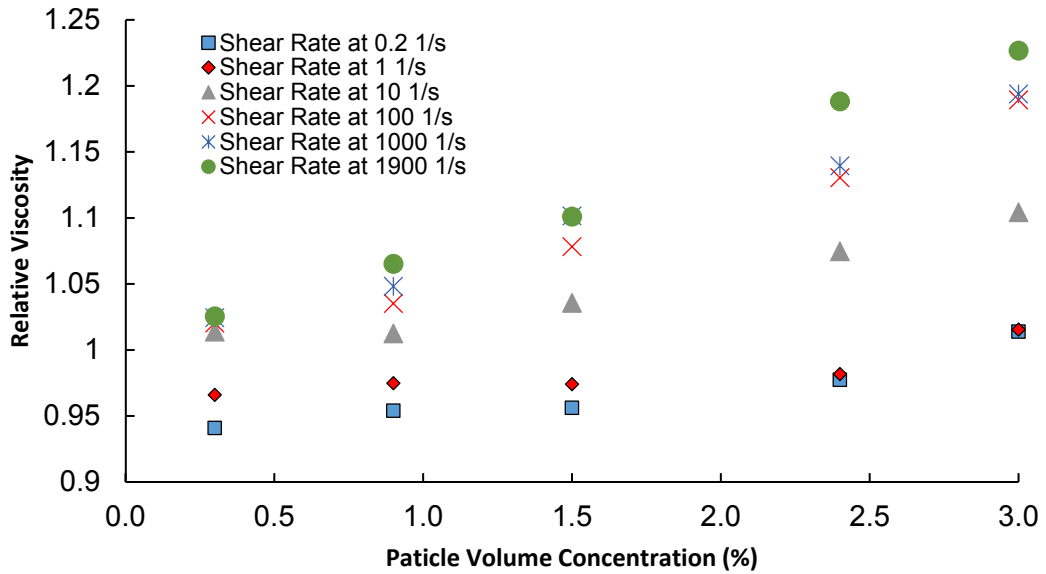
Figure 74: Relative viscosity of 38-75 micron CaCO₃ with different volume concentration at specific shear rate.

To investigate the effect of concentration of solid particles on the extent of the thixotropic behaviour, the loop tests of suspensions with Calcium Carbonate and silica sand of dispersed and agglomerative conditions were performed. [Figure 75] and [Figure 76] show plots of shear stress versus shear rate for the loop tests performed on 0.9 vol.% and 1.5 vol.% respectively.
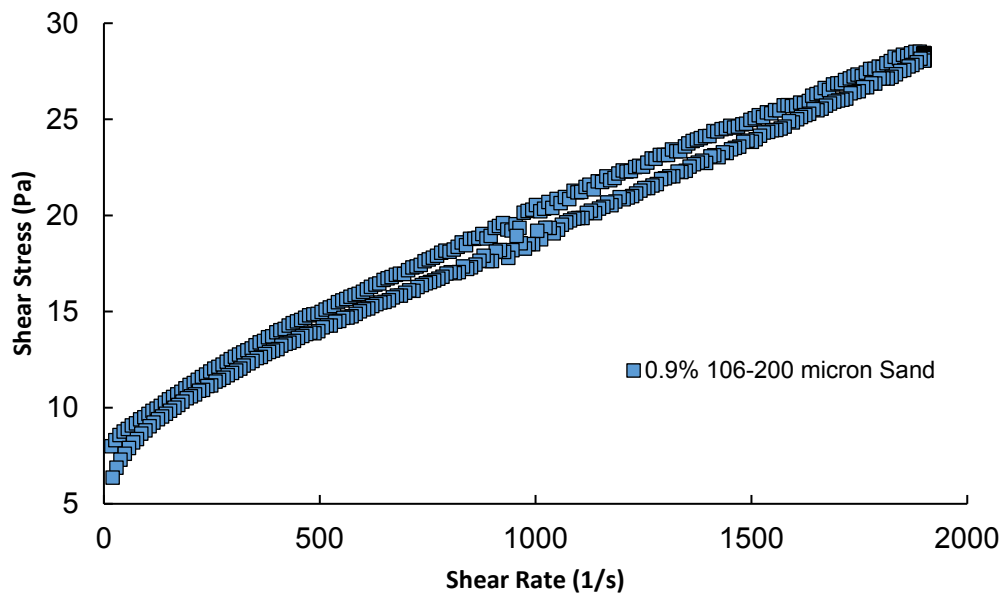
Figure 75: Thixotropic loop of suspension with 0.9 vol. % 106-200 micron silica sand.
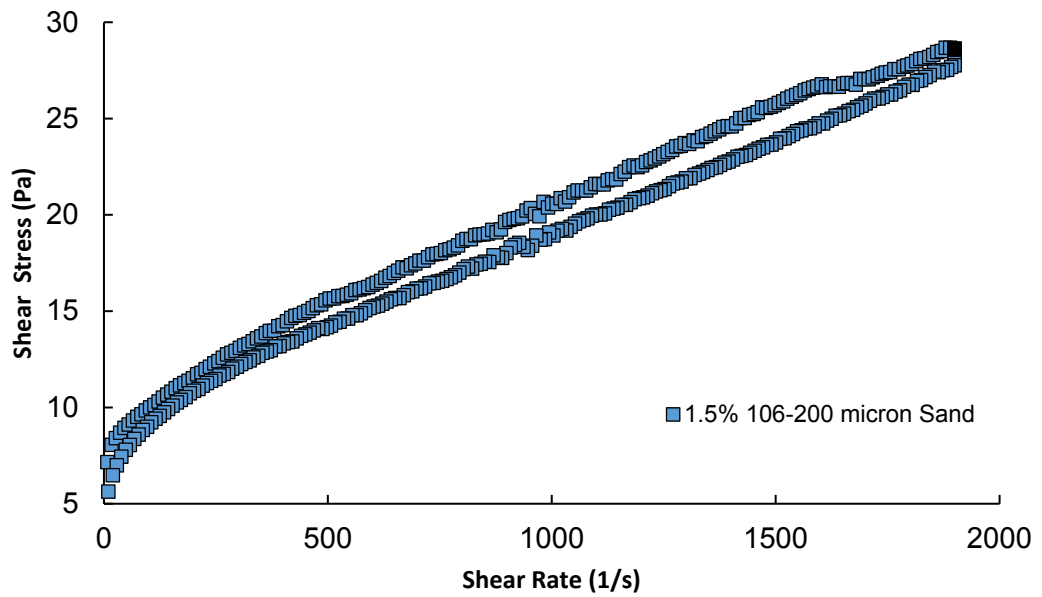
Figure 76: Thixotropic loop of suspension with 1.5 vol. % 106-200 micron silica sand.

The experimental results in Table 18 suggest that, for agglomerative particle suspensions, the thixotropic capability of suspensions is greater with the increasing of particle volume concentration, as demonstrated by the increasing hysteresis area with increasing solids concentration.

Table 18: Thixotropic loop tests of suspensions with silica sand particle of different volume concentrations.

Particle	Particle Size (microns)	Solid Concentration (vol. %)	Hysteresis Area Value
Silica Sand	106-200	0.9	982
		1.5	4367
		3.0	5043
	200-250	0.3	611
		1.5	2006
	250-300	0.3	775
		1.5	969

It can be concluded from the experiment results that the volume fraction of particles in suspension significantly affects the viscosity of mono-dispersed suspensions with fine particles. The effect of particle size is minimal during medium and high shear rate regions, for the fluids under investigation. Furthermore, the suspension viscosity also depends on the imposed range of shear rate.

It is noteworthy that the impact of solid suspensions on the suspension rheology can be also affected by the viscosity of suspending liquid. For example, the extent of the effect could be potentially different if the suspending fluid has a different viscosity. For practical applications, lower viscosities are more relevant for drilling operation, however, the settlement of the particles during drilling operation is an issue that requires further investigation, and therefore, different measurement techniques should be incorporated. In future research, the pipe viscometer will be used to investigate the rheology of suspensions.

Chapter 5. Conclusion

This thesis was focused on the rheology of drilling fluids. The work began with a review of different measurement techniques, followed by benchmarking the fluid rheology obtained from different viscosifiers (drilling fluid additives). The interaction between different polymers was studied experimentally, which led to the development of two drilling fluid systems, Ctrol^{TM} and CTrolX^{TM}, for preventative and remedial drilling fluid loss respectively. Finally, the effect of drill cuttings on the fluid rheology studied at a wide range of shear rates. A summary of key findings are presented below.

5.1. Effective methods of drilling fluid viscosity measurement

There are different measurement techniques developed and standardised within drilling engineering to measure and represent the viscosity of drilling fluid. These methods are reported as part of API standards, and are extensively used within the drilling industry as best practices to design, measure and monitor the drilling fluid in the lab and in the field. These methods are compared and benchmarked with other measurement techniques, which are more commonly used in other engineering disciplines.

Different measurement techniques were compared in this thesis. This comparison entailed measurement techniques using the Marsh Funnel (flow through constriction), different rotary viscosity measurement equipment (different tools and sensors), and pipe viscometer (capillary). The results showed that pipe viscometer (different pipe dimensions) and different rotary viscometers (Haake and Ofite with five different sensor arrangements) have agreement in terms of viscosity measurements at measured shear rates. However, the measurement of fluid viscosity using the Marsh Funnel demonstrated that is not a reliable tool to quantify fluid viscosity even at qualitative level – two fluids with the same Marsh Funnel viscosity exhibited very different fluid rheology measured using rotary viscometers.

The thesis also reviewed the effectiveness of industry practice of measuring and quantifying fluid viscosity at only two shear rates of 510 1/s and 1020 1/s. The results of benchmark experiments obtained from solutions made using common drilling fluid polymers with similar measurements at high shear rate (1020 1/s), showed that there are significant difference in fluid rheology: while the high-end rheology of these solutions were almost the same, the low-end rheology at low shear rates were up to two orders of magnitudes different. The benchmark results therefore suggest that the response/behaviour of the fluid in processes depending on low shear rate (e.g. fluid loss control and sedimentation of cuttings within tanks) will be significantly different for these fluids, while the conventional fluid viscosity measurements considers these fluids as comparable solutions.

5.2. Ctrol^{TM} and CTrolX^{TM} drilling fluids

This research work facilitated the development of two drilling fluid systems for fluid loss control, namely Ctrol^{TM} and CTrolX^{TM}. Particularly, the body of experimental work related to characterising the low-end rheology of different polymer combinations were performed as part of this thesis. As a part of the research, this thesis also provided laboratory support to researchers on site (Dr Masood Mostofi and Frank Samani) during the implementation and field testing of these products. Both products are registered and patented under trademark names of Ctrol^{TM} and CTrolX^{TM}.

Ctrol^{TM} is a preventative drilling fluid, which is used under normal drilling operation. The fluid is designed on the basis of rheological synergies between different natural and synthetic polymers, which can deliver extensive shear thinning property. Ctrol^{TM} exhibits small viscosities at high shear rates, providing effective hole cleaning, drag deduction and sample (cutting) delivery to surface (with minimum level of cutting spreading). At low shear rates, Ctrol^{TM} has significantly higher viscosity, which makes the drilling fluid an effective solution for fluid loss control in unconsolidated grounds and also natural fractures with small apertures.

CTrolX^{TM} is a remedial drilling fluid, which is deployed after drilling natural fractured formations or after inducing hydraulic fractures to control the fluid loss. CTrolX^{TM} is injected/circulated when the drilling process is on hold. In this thesis, the low-end rheology of different polymer and bentonite combinations were tested to derive a recipe with maximum viscosities at low shear rates (at the range of 0.001-0.1 1/s).

5.3. Effect of fine particles on mono-dispersed suspension rheology

In the final part of this research, the effect of solid fine particles on the polymer rheology was investigated. The experimental conditions in terms of solid size and concentration were selected to represent drilling conditions in the field.

The test protocol was developed to minimise any possibility of cuttings settlement during the experiments. The experiments were performed at low to high shear rates, ranging from 0 1/s to 1900 1/s. A suspending fluid with high viscosity was used to suspend the cuttings and minimise the settlement of cuttings during the experiments. The results were interpreted based on relative viscosity at each shear rate derived from the ratio of suspension fluid viscosity over the suspending fluid viscosity. The thixotropic property of suspension was measured using a profile of loop test.

The results showed that shear rate and cutting concentration are two key factors affecting relative viscosity, and the suspension viscosity is not much affected by the sizes tested in this research. The effect of cuttings on suspension viscosity was minimum at low shear rates, while

the relative viscosity increases continuous with shear rate. Figure 77 illustrates a conceptual variation of relative viscosity with particle concentration and shear rate. The results confirm that the relative viscosity is controlled by the concentration of solid particles, and the effect is higher at higher shear rates.

The thixotropic behaviour of fluids is affected by the presence of cuttings. Even at high polymer concentration, the suspending fluid exhibited a minimum thixotropic behaviour measured from hysteresis in the loop experiments. The suspension fluids showed a thixotropic behaviour, where the area between the ramp up and ramp down of shear rate increases with cutting concentration. The data also shows that the extent of thixotropic behaviour is not correlated with the size of particles. These trends are conceptually demonstrated in Figure 78.
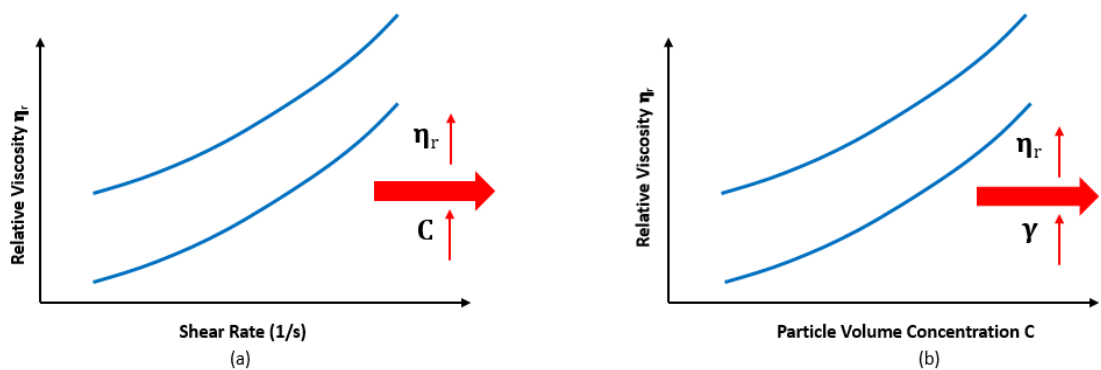

Figure 77: (a) variation of relative viscosity with particle concentration, (b) variation of relative viscosity with shear rate.
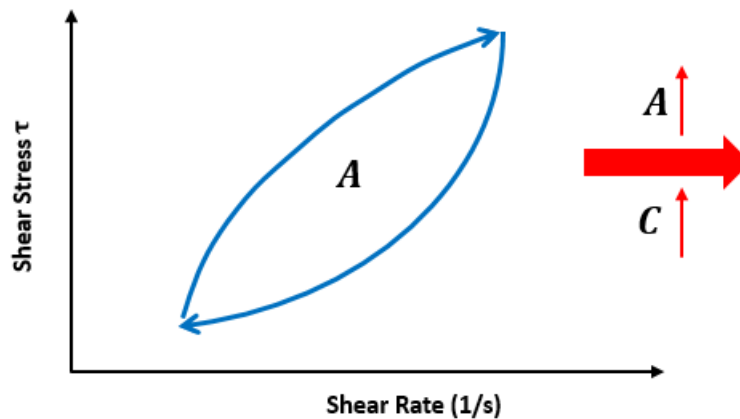

Figure 78: Variation of thixotropic loop area with particle concentration.

5.4. Recommendations for future work

There are areas that we believe further work can be performed which are not covered here due to the current limitation in available equipment, time and in expanding the focus of this work.

The mechanisms of interactions between polymers can be further studied. In this work, a pure experimental and trial and error approach was implemented to derive the optimum composition of Ctrol^{TM} and CTrolX^{TM}. The work benefited from literature specifying possible combinations and mechanisms that can result in the synergies between different polymers, however, the mixed solutions were only quantified in terms of resultant viscosity. The limitations were mainly due to lack of equipment and also possible complex interactions of the polymer mixture. Indeed, further work can be performed in future research to better understand the variation of the interaction of the polymer systems.

The effect of cuttings on drilling fluid rheology can be further studied at a larger range of cutting size, lower viscosity of suspending solution and under dynamic conditions of the wellbore. Due to equipment limitations (dimensions of the Haake concentric sensor), the range of cutting size was limited, which can be in part the reason that a particular trend related to the effect of cuttings on the suspension relative viscosity was not observed. Furthermore, extremely high viscosity was used for the suspending fluid to ensure that the particles would not settle during the experiment. Indeed, it is possible that more pronounced effects related to the solid particles could be observed if a thinner suspending fluid would have been used. These experiments can be performed in future using a pipe viscometer, in which the dynamic condition of the pipe in vertical arrangement will be sufficient to suspend and transport the cuttings. The other benefit of conducting the experiments using the pipe viscometer is that the measurements will be under the same dynamic conditions of the wellbore where the drilling fluid transports the cuttings to surface. As part of this research, a pipe viscometer was developed in the laboratories; however, the complementary experiments to evaluate the effect of cuttings using a pipe viscometer, under thermal and pressure control were not performed due to time constrains, and planning is underway to conduct these experiments as part of doctoral studies after completion of this research work.

References

[1]   Bourgoyne Jr, A.T., et al., Applied drilling engineering. Volume 2. 1986.

[2]   Bloys, B., et al., Designing and managing drilling fluid. Oilfield Review, 1994. 6(2): p. 33- 43.

[3]   Pitt, M., The Marsh funnel and drilling fluid viscosity: a new equation for field use. SPE Drilling & Completion, 2000. 15(01): p. 3-6.

[4]   Walker, T.O., Additive for reducing fluid loss or filtration rate for aqueous drilling fluid containing both high salinity and high soluble calcium. 1976, Google Patents.

[5]   Fontana, P., L. Watkins, and P. Aronstam, Drilling system and method for controlling equivalent circulating density during drilling of wellbores. 2007, Google Patents.

[6]   Chen, G., et al., A study of wellbore stability in shales including poroelastic, chemical, and thermal effects. Journal of Petroleum Science and Engineering, 2003. 38(3-4): p. 167-176.

[7]   Barnes, H.A., J.F. Hutton, and K. Walters, An introduction to rheology. 1989: Elsevier.

[8]   Barnes, H.A., Thixotropy—a review. Journal of Non-Newtonian fluid mechanics, 1997. 70(1-2): p. 1-33.

[9]   Chhabra, R.P. and J.F. Richardson, Non-Newtonian flow and applied rheology: engineering applications. 2011: Butterworth-Heinemann.

[10]   Hemphill, T., W. Campos, and A. Pilehvari, Yield-power law model more accurately predicts mud rheology. Oil and Gas Journal;(United States), 1993. 91(34).

[11]   Huang, X. and M.H. Garcia, A Herschel–Bulkley model for mud flow down a slope. Journal of fluid mechanics, 1998. 374: p. 305-333.

[12]   Garakani, A.K., et al., Comparison between different models for rheological characterization of activated sludge. Iranian journal of environmental health science & engineering, 2011. 8(3): p. 255.

[13]   Roussel, N. and R. Le Roy, The Marsh cone: a test or a rheological apparatus? Cement and concrete research, 2005. 35(5): p. 823-830.

[14]   Kumar, A. and R.K. Gupta, Fundamentals of polymer engineering, revised and expanded. 2003: CRC Press.

[15]   API, R., 13D.(2010). Standard procedure for rheology and hydraulics of oil-well fluids. Recommended practice Sixed Edition, May. American Petroleum Institute.

[16]   Accessory, A.B.V., Brookfield Engineering Laboratories. Inc., Stoughton, Massachusetts, date unknown.

[17]   Kang, Y.J., S.Y. Yoon, and S. Yang. Viscosity measurement using hydrodynamic divergencing chamber and digital counting in microfluidic channels. in 2010 IEEE 23rd International Conference on Micro Electro Mechanical Systems (MEMS). 2010. IEEE.

[18]   Munson, B.R., et al., Fundamentals of fluid mechanics. 2014: John Wiley & Sons.

[19] Collins, M. and W. Schowalter, Behavior of non-Newtonian fluids in the entry region of a pipe. AIChE journal, 1963. 9(6): p. 804-809.

[20] Barker, B. Massecuite consistency measurement using a pipeline viscometer. in Proc S Afr Sug Technol Ass. 2008.

[21] Vajargah, A.K. and E. van Oort, Determination of drilling fluid rheology under downhole conditions by using real-time distributed pressure data. Journal of Natural Gas Science and Engineering, 2015. 24: p. 400-411.

[22] Rommetveit, R. and K. Bjorkevoll. Temperature and pressure effects on drilling fluid rheology and ECD in very deep wells. in SPE/IADC Middle East Drilling Technology Conference. 1997. Society of Petroleum Engineers.

[23] Ford, J., et al. Experimental investigation of drilled cuttings transport in inclined boreholes. in SPE Annual Technical Conference and Exhibition. 1990. Society of Petroleum Engineers.

[24] Shauly, A., A. Wachs, and A. Nir, Shear-induced particle migration in a polydisperse concentrated suspension. Journal of Rheology, 1998. 42(6): p. 1329-1348.

[25] Fadairo, A., D. Orodu, and O. Falode. Investigating the carrying capacity and the effect of drilling cutting on rheological properties of jatropha oil based mud. in SPE Nigeria annual international conference and exhibition. 2013. Society of Petroleum Engineers.

[26] Mahto, V. and V. Sharma, Rheological study of a water based oil well drilling fluid. Journal of Petroleum Science and Engineering, 2004. 45(1-2): p. 123-128.

[27] Bergström, L., Shear thinning and shear thickening of concentrated ceramic suspensions. Colloids and Surfaces A: Physicochemical and Engineering Aspects, 1998. 133(1-2): p. 151-155.

[28] Coussot, P., Mudflow rheology and dynamics. 2017: Routledge.

[29] Peker, S.M. and S.S. Helvaci, Solid-liquid two phase flow. 2011: Elsevier.

[30] Watanabe, Y., A. Kawamoto, and K. Matsuda, Particle size distributions in functionally graded materials fabricated by the centrifugal solid-particle method. Composites science and Technology, 2002. 62(6): p. 881-888.

[31] Mangesana, N., et al., The effect of particle sizes and solids concentration on the rheology of silica sand based suspensions. Journal of the Southern African Institute of Mining and Metallurgy, 2008. 108(4): p. 237-243.

[32] Mueller, S., E. Llewellin, and H. Mader, The rheology of suspensions of solid particles. Proceedings of the Royal Society A: Mathematical, Physical and Engineering Sciences, 2009. 466(2116): p. 1201-1228.

[33] Cheng, X., et al., Imaging the microscopic structure of shear thinning and thickening colloidal suspensions. Science, 2011. 333(6047): p. 1276-1279.

[34] Papenhuijzen, J., The role of particle interactions in the rheology of dispersed systems. Rheologica Acta, 1972. 11(1): p. 73-88.

[35] Mooney, M., The viscosity of a concentrated suspension of spherical particles. Journal of colloid science, 1951. 6(2): p. 162-170.

[36] Wildemuth, C. and M. Williams, Viscosity of suspensions modeled with a shear-dependent maximum packing fraction. Rheologica acta, 1984. 23(6): p. 627-635.

[37] Quemada, D., Rheology of concentrated disperse systems and minimum energy dissipation principle. Rheologica Acta, 1977. 16(1): p. 82-94.

[38] Gonzalez-Gutierrez, J., et al., Models to predict the viscosity of metal injection molding feedstock materials as function of their formulation. Metals, 2016. 6(6): p. 129.

[39] Asakura, S. and F. Oosawa, Interaction between particles suspended in solutions of macromolecules. Journal of polymer science, 1958. 33(126): p. 183-192.

[40] Berli, C.L., D. Quemada, and A. Parker, Modelling the viscosity of depletion flocculated emulsions. Colloids and Surfaces A: Physicochemical and Engineering Aspects, 2002. 203(1-3): p. 11-20.

[41] Sworn, G., Xanthan gum, in Handbook of hydrocolloids. 2009, Elsevier. p. 186-203.

[42] Tako, M. and S. Nakamura, Synergistic interaction between xanthan and guar gum. Carbohydrate Research, 1985. 138(2): p. 207-213.

[43] Algin-Yapar, E., Nasal inserts for drug delivery: an overview. Tropical Journal of Pharmaceutical Research, 2014. 13(3): p. 459-467.

[44] Subramanian, R. and J. Azar. Experimental study on friction pressure drop for nonnewtonian drilling fluids in pipe and annular flow. in International Oil and Gas Conference and Exhibition in China. 2000. Society of Petroleum Engineers.

[45] Junin, R. and K.W. Meng, SLURRY TRANSPORT AND PARTICLE SETTLING IN ANNULUS IN CUTTINGS REINJECTION PROCESS.

Appendices

Additives Data Sheet

Appendix A - AMC GUAR GUM

PRODUCT DATA SHEET

AMC GUAR GUM™
VISCOSIFIERS

AMC
DRILLING OPTIMISATION

Description

AMC GUAR GUM™ is a modified natural polymer specifically used to create a low solids, biodegradable drilling fluid for use in water wells.

Application

AMC GUAR GUM™ provides excellent viscosity, breaks down naturally and avoids mudding of water aquifers which frequently occurs when using bentonite as a mud additive.

To extend the life expectancy of a AMC GUAR GUM™ fluid, biocide should be added to prevent fermentation.

To accelerate the development of a well, sodium hypochlorite solution can be added. The addition of 10L of sodium hypochlorite per 1000L of AMC GUAR GUM™ fluid followed by surging, will assist in optimum well production.

Advantages

· Effective in low concentrations

· Can be used in most makeup waters

· Environmentally acceptable.

Typical Physical Properties

Appearance: White to yellow powder
Specific gravity: 1.1 – 1.3

Recommended Treatment

APPLICATION	kg / m³	lb / bbl
Normal conditions	3 – 4	1 – 1.4
Unconsolidated formations, coarse gravels	5 – 8	1.8 – 2.8

Please Note: Several factors will dictate the most appropriate concentration rate. Please contact your nearest AMC representative for optimum results.

Appendix B - AMC PAC-R

AMC PAC R™
VISCOSIFIERS

AMC
DRILLING OPTIMISATION

Description

AMC PAC R™ is a high molecular weight polyanionic cellulose polymer that is an extremely effective viscosifier with minor filtration control properties in fresh, hard and saline waters.

Application

AMC PAC R™ is multifunctional, viscosifier that promotes better hole cleaning, while forming a protective colloid which inhibits the hydration of water sensitive formations and promotes borehole stability through filtration control. AMC PAC R™ will enhance the lubricating properties of the fluid and can be added to foam to improve cuttings transportation. AMC PAC R™ can be added to enhance a bentonite based fluid system and is compatible with most polymers and lubricants. Addition rates can be adjusted to suit specific applications.

Advantages

- Economical
- Effective in low concentrations
- Increases viscosity
- Improved filtrate control
- Improves borehole stability
- Environmentally acceptable
- Extends life of foam or stiff foam in air drilling.

Typical Physical Properties

Appearance:	Fine white, free flowing powder
pH (1% aqueous solution):	7.0 - 8.0
Specific gravity:	1.5 – 1.6

Recommended Treatment

APPLICATION	KG / M³	LB / BBL
To reduce torque and improve core recovery	1.0 – 3.0	0.35 – 1.0
To provide encapsulation and stabilise clays and shale	2.0 – 5.0	0.7 – 1.75
To improve the quality of the filter cake	1.5 – 2.5	0.5 – 0.88
To improve the properties of a bentonite based drilling fluid	0.5 – 2.5	0.18 – 0.88

AMC PAC R™ can be slowly introduced into mechanical agitation, through water discharge or through a mud hopper.

Please Note: Several factors will dictate the most appropriate concentration rate. Please contact your nearest AMC representative for optimum results.

Appendix C - AMC GEL XTRA

AMC GEL XTRA™
VISCOSIFIERS

AMC
DRILLING OPTIMISATION

Description

AMC GEL XTRA™ is a modified premium grade Wyoming sodium bentonite formulated to ensure ease of mixing with superior mud making qualities in fresh water. AMC GEL XTRA™ is designed for use in mineral exploration, water well and directional drilling operations.

Application

AMC GEL XTRA™ is recommended as an 'ultra' high yielding viscosifier for building a mud system with excellent hole cleaning properties and low filtrate values in fresh to brackish water. The product makes an economical drilling fluid which has specific application in water wells with permeable sections or poorly consolidated caving formations.

Typical Physical Properties

Appearance:	Grey to tan powder
Moisture:	8 – 10%
Specific gravity:	2.45 – 2.55
pH (4% solution):	9.0 – 10.0

Recommended Treatment

APPLICATION	KG / M³	LB / BBL
Normal drilling conditions	15 – 30	5 – 10.5
Unconsolidated formations	35 – 45	12 – 16
Lost circulation and caving formations	40 – 60	14 – 21
Make-up for stiff foam systems	15 – 30	5 – 10.5

Please Note: Several factors will dictate the most appropriate concentration rate. Please contact your nearest AMC representative for optimum results.

Advantages

- Yields rapidly in fresh water to give ultra high viscosity

- Economical

- Enhances fluid loss characteristics

- Assist in bore hole stabilisation

- Helps eliminate loss circulation conditions

- Environmentally acceptable

- NSF/ANSI Standard 60 endorsed has been registered with the USA National Sanitation Foundation (NSF) for use in potable water well construction.

Appendix D - COREWELL

SECTION 9 PHYSICAL AND CHEMICAL PROPERTIES

Information on basic physical and chemical properties

Appearance	Off white granular crystals; soluble in water.		

Physical state	Divided Solid	**Relative density (Water = 1)**	Not Available
Odour	Not Available	**Partition coefficient n-octanol / water**	Not Available
Odour threshold	Not Available	**Auto-ignition temperature (°C)**	Not Applicable
pH (as supplied)	9.0	**Decomposition temperature**	Not Available
Melting point / freezing point (°C)	Not Available	**Viscosity (cSt)**	Not Applicable
Initial boiling point and boiling range (°C)	Not Applicable	**Molecular weight (g/mol)**	Not Applicable
Flash point (°C)	>400	**Taste**	Not Available
Evaporation rate	Not Applicable	**Explosive properties**	Not Available
Flammability	Not Applicable	**Oxidising properties**	Not Available
Upper Explosive Limit (%)	Not Applicable	**Surface Tension (dyn/cm or mN/m)**	Not Applicable
Lower Explosive Limit (%)	Not Applicable	**Volatile Component (%vol)**	Not Available
Vapour pressure (kPa)	Not Applicable	**Gas group**	Not Available
Solubility in water (g/L)	Miscible	**pH as a solution (1%)**	Not Available
Vapour density (Air = 1)	Not Applicable	**VOC g/L**	Not Available

Appendix E – AMC XAN BORE

PRODUCT DATA SHEET

AMC XAN BORE™
VISCOSIFIERS

AMC DRILLING OPTIMISATION

Description

AMC XAN BORE™ is a premium quality biopolymer powder designed to provide maximum solids suspension and hole cleaning in vertical wells as well as horizontal directional drilling applications. AMC XAN BORE™ is a distinctive product, able to produce a thixotropic shear thinning fluid. AMC XAN BORE™ also acts as a very effective mud filtrate viscosifier.

Application

AMC XAN BORE™ can be added to a pre-hydrated bentonite based fluid or can be used as a single viscosifying additive in fresh, brackish or saturated salt water.

AMC XAN BORE™ fluids are highly shear thinning which improves bit cleaning significantly. The fluid will revert to higher viscosities at low shear rates. This unique property provides many benefits in HDD bores by providing excellent carrying capacity of coarse cuttings, sand and gravel.

In HDD drilling, improved hole cleaning and cuttings transport allows for quicker and easier back reams and pull backs on longer bores.

In CBM drilling, the highly thiotropic mud filtrate of AMC XAN BORE™ minimises damage to coal seams and cleats.

Typical Physical Properties

Appearance:	Cream coloured powder
pH (1% solution):	6.0 – 8.0
Specific gravity:	0.6 – 0.7

Recommended Treatment

1 – 3 kg / m³ (0.35 – 1.0 lb / bbl) of water through a mud hopper or a high shear mixer.

Advantages

- Passes the Standards Australia Test AS4351 for biodegradability

- Has quick break properties to assist in waste disposal

- Suitable for use in hard, soft and salt water environments.